Bern University
of Applied Sciences

Quality assurance of timber structures

Research report

Bettina Franke
Steffen Franke
Marcus Schiere
Andreas Müller

Schweizerische Eidgenossenschaft
Confédération suisse
Confederazione Svizzera
Confederaziun svizra

▶ Institute for Timber Construction, Structures and Architecture

Quality assurance of timber structures

Qualitätssicherung von Holztragwerken

Research report

Authors	Bettina Franke, Steffen Franke, Marcus Schiere, Andreas Müller
Project Leader	Prof. Dr. Steffen Franke
Head of the Institute	Prof. Andreas Müller

Bern University of Applied Sciences
Institute for Timber Constructions, Structures and Architecture

The test results in this report relate exclusively to the subjects tested. Information about measurement uncertainty will be provided on request.

Zusammenfassung

Die Kombination von moderner Architektur mit dem nachwachsenden Rohstoff Holz führt zu beeindruckenden und anspruchsvollen Holztragwerken mit hohen Bedürfnissen an die Planung, Produktion, Logistik, Inbetriebnahme und Nutzung. Die Ansprüche an neuzeitliche Holztragwerke steigen stetig im Hinblick auf Design, Optik, schlanke Querschnitte und grosse Spannweiten. Gleichzeitig ist die Qualitätssicherung während der Errichtung und Nutzungsphase entscheidend. Die realitätsnahe Abschätzung der Gefahren für das Holztragwerk während der Bau- und Nutzungsphase wie auch die Holzfeuchteverteilung in den Holztragelementen, das Risiko der Rissbildung und die Sicherung der Formstabilität der Querschnitte ist hierbei wichtig.

Das Forschungsvorhaben konzentriert sich auf Einwirkungen aus dem lokalen Klima, der resultierenden Holzfeuchteverteilung, Formstabilität, Eigenspannungen und möglichen Rissen im Tragquerschnitt. Ziel ist es, mit neuen Forschungsergebnissen konkrete Empfehlungen für die Ausführung von Holztragwerken zu geben. Die Übertragung von entwickelten numerischen Modellen und Methoden in abgesicherte Empfehlungen für die Bemessung und Planung in der Praxis stehen im Vordergrund.

Die verwendeten und erarbeiteten Grundlagen für das Projekt bilden die Klimadaten der Schweiz, Messdaten aus Langzeitmessungen zum Nutzungsklima und dem Holzfeuchtegehalt in Tragquerschnitten, das entwickelte numerische Modell zur Abbildung der Feuchtediffusion, der Dimensionsänderung und der resultierenden internen Spannungen. Ergänzend wurden in kleinen Laborserien benötigte Materialparameter bestimmt.

Die innerhalb der Langzeitmessung erhaltenen Klimadaten und Holzfeuchtewerte wurden nach der Nutzung klassifiziert und für die Praxis entsprechend aufbereitet. Parallel wurden auch veröffentlichte Messdaten anderer Forschungsinstitute berücksichtigt. Neu stehen nun neben den allgemeinen Angaben in der SIA 265:2012 konkrete Anforderungsprofile für vielfältige Gebäudekategorien und auch Brückentragwerke zur Verfügung. Für Brückentragwerke sind noch spezielle Einflüsse, die immer noch zu Verwirrungen und offenen Fragen führten, betrachtet und bewertet worden. Die Anwendung eines Monitoringsystems zur Qualitätssicherung wird beschrieben.

Ein numerisches Modell wurde erstellt, validiert und für Parameterstudien zur Beurteilung der Querschnittsgrösse oder des Einflusses des Errichtungszeitraumes angewandt. Anhand der tatsächlich auftretenden Klimasituationen in z. B. Eishallen, Reithallen und Brückentragwerken, wurden die im Querschnitt auftretenden Dimensionsänderungen und Spannungen berechnet und bewertet.

Für die Planung der Errichtung eines Holztragwerkes werden abschliessend Hinweise zu auftretenden Feuchtebeanspruchungen und deren Auswirkungen gegeben. Die erreichten Ergebnisse geben dem planenden Ingenieur und auch Behörden, zusätzlich zu den in der SIA 265:2012 verankerten Werten, neue Richtgrössen für die Abschätzung der zu erwartenden Holzfeuchte innerhalb eines Tragwerkes im speziellen auch deren Verteilung über die Querschnittsbreite während der Errichtung und Nutzung.

Keywords: Holzfeuchte, Verteilung der Holzfeuchte, Feuchteinduzierte Spannungen, Monitoring, Qualitätssicherung, Feuchtesimulation, Gebäudeklimas

Abstract

The combination of modern architecture with the renewable raw material wood leads to impressive and demanding timber structures with high requirements for planning, production, logistics, commissioning and use. The demands placed on modern wooden structures are constantly increasing in terms of design, appearance, slender cross sections and large spans. Meanwhile, quality assurance during the construction and operational phase is crucial. The realistic estimation of the risks for the timber structure during the construction and operation phase as well as the distribution of wood moisture content in the timber load bearing elements, the risk of cracking and the shape stability of the cross sections are important.

The research project focuses on impacts of the local climate, the resulting wood moisture distribution, dimensional stability, moisture induced stresses and possible cracks in the cross-sections. The aim is to provide recommendations for the erection of wooden structures with new research results. The focus lies on the transfer of results from the developed numerical models and methods to secure recommendations for design and planning in practice.

The used and developed basics of the project are the climate data of Switzerland, measurements of climate and moisture content in load bearing cross-sections obtained from long-term monitoring campaigns, and the developed numerical model to calculate the moisture diffusion, the dimensional change and the resulting moisture induced stresses. In addition, required material parameters were determined in small laboratory series that improve and support measurements made during the monitoring campaigns.

The climatic data and wood moisture content values obtained within the long-term measurement were classified according to the building type and visualized accordingly for the practicing engineers. Published data from other research institutes were also included into the analyses where possible. In addition to the general information on moisture content as listed in the SIA 265:2012, useable climate profiles are now available for a variety of building types and for bridges, too. Specific questions concerning bridges that still led to discussion and unanswered questions were considered and evaluated. The application of a quality assurance monitoring method and system is described.

The created numerical model was validated and used in parameter studies to assess the effects of cross-section size or the impact of the construction period. realistic climate profiles found in ice rinks, riding halls and bridges were used to calculate dimensional changes and moisture induced stresses.

Recommendations are given on the seasonal fluctuations of humidity and its effects on the timber structures. This could support engineers during the planning and building phase. In addition to the expected fluctuations listed in the SIA 265:2012, obtained results give the planning engineer and authorities new benchmarks for the estimation of the expected wood moisture content within a supporting structure. Of interest could be the distribution across the section width during erection and operation.

Keywords: Moisture content, moisture gradient, moisture induced stresses, monitoring campaigns, quality assurance, moisture content simulation, building environments

Acknowledgements

The following papers are outcomes of the research work carried out in the project.

Schiere M., Franke S., Franke B., Müller A. (2017) Numerical sensitivity study of moisture induced stress levels in glulam cross-sections, CompWood, Vienna, Austria

Müller A., Franke B., Schiere M., Franke S. (2017) Advantages of moisture content monitoring in timber bridges, International Conference on Timber Bridges, Skelefftea, Sweden

Franke S., Franke B., Schiere M., Müller A. (2017) Timber bridges – Load carrying behaviour according to climate changes, IABSE Symposium, Vancouver, Canada

Franke B. (2017) Holzfeuchte smart kalkuliert für moderne Tragquerschnitte, S-WIN-Kurs 2017, Weinfelden, Switzerland

Schiere M., Franke B., Franke S. (2018) Antworten zur Tragfähigkeit infolge dynamischer Klimawechsel, S-WIN Tagung Von der Forschung zur Praxis, Biel/Bienne, Switzerland

Franke B., Schiere M., Franke S. (2018) Stress developments in large timber cross-sections in relation to geometry and encountered climate, WCTE 2018, Seoul, Republic of Korea

Schiere M., Franke B., Franke S. (2018) Comparison between local versus regional climate using monitoring data of timber structures, WCTE 2018, Seoul, Republic of Korea

Franke B., Franke S., Schiere M., Müller A. (2018) Moisture content and moisture-induced stresses of large glulam members: laboratory tests, in-situ measurements and modelling, Nordic Wood Forum, Växjö, Sweden

Table of Content

Appendix A   Monitoring objects

1 Introduction

1.1 Influence of moisture content on structures

The demands on load bearing performance of modern load bearing timber structures increases to meet requirements on design, span, and material. Timber structures span large distances in halls, are used in bridges, shell structures, and multi-story structures. Alongside, quality of the structure during the erection of the structure should also be guaranteed. The performed research concentrated on the influence of moisture on the load bearing performance of timber. This concerned the response of moisture content fluctuations in timber elements, but also on moisture induced stresses that develop due to moisture gradients. The aim is to develop practical recommendations for engineers concerning these aspects.

The moisture content fluctuations and distributions in relation to the induced stress distributions over the cross-sections have been investigated on a wide variety of sizes and materials. It is however difficult to maintain the overview on research performed on small specimens like in Frandsen et al. (2007) and on large cross-sections such as by Jönsson (2004) or Franke et al. (2016). They do however provide insight into topics that could help engineers in planning and design tasks such as:

- The variations of moisture content per season and building operation,
- Risk of crack generation inside cross-sections and on surfaces of cross-sections, and
- Moisture content distributions over cross-sections and the assignment of service class as mentioned in the SIA 265:2012 or EN 1995-1-1:2004.

Softwood is currently the most common material to build with. However, hardwoods are increasingly used and engineered wood products such as beech veneer find new applications. Experience with these newer materials is however limited but enjoy great interest for newer high load bearing applications. Aspects like shape stability during building erection, maintaining production quality during transport, or response to events such as building maintenance or simply behaviour during annual operation are matters that interest the timber construction industry.

Moisture as a cause of structural failure was quantified by a study in which damage in existing buildings in southern Germany were assessed. Moisture accounted for half of the observed structural damage: too wet, too dry, or varying moisture conditions (Frese and Blass, 2011). The latter accounted for approximately one sixth of the damage in need of repair (Dietsch and Winter, 2018). About 90% of the encountered damage was found in glued laminated timber. The rest of the damage concerned wrong assumption of loads or erroneous calculation of load bearing capacities for instance. Moisture content variations have been suggested as possible cause for total collapse in Frühwald et al. (2007).

That service classes were wrongly assigned during design has been proven by structures that had to be closed temporarily due to reached limits in the structural load bearing capacity in combination with high moisture contents (Basellandschaftliche Zeitung, 2012 and Sigrist, 2013). Roof structures were not able to carry design snow loads anymore. Downtime of public or private buildings financially impacts communities and companies. These often invested in timber structures and need additional funds and efforts to repair, modify, or reinforce load-bearing elements.

1.2 Goal and objectives of the project

The goal of the project is to gather available international knowledge and research results, add own experimental data to this, and produce recommendations for engineers involved in the design, production and planning of future timber structures. The type of results that can be found in the research are:

- Simple solutions to estimate the wood moisture contents in (new) timber structures,
- Recommendations for planning of the erection processes (section wise building, protective measures, etc.,
- Possible reductions in load bearing capacity due to moisture content variations,
- Optimised layup of glued laminated timber,
- Outlook on the use of material in standard climates and in extreme climates, and
- Indication of how numerical programs can be used in the future to plan structures concerning climatic influences.

The focus is on practical solutions:

- Simplified moisture content distributions to derive moisture gradients,
- Derivation of shape stability of cross-sections following from moisture content fluctuations,
- Consolidation of 1D- and 2D-Finite Element models to simulate moisture content fluctuations and moisture induced stresses,
- Sensitivity of calculated results to variations in material parameters,
- Obtaining material parameters for simulations and monitoring, especially for beech veneer,
- Summarising typical climate scenarios for building erection periods, normal building operation,
- Numerical simulations to investigate consequences for load bearing capacities of timber members in varying climate

The research also eventually helps to focus future scientific questions regarding the use of coatings and which areas of application are interesting or deserve special attention, reinforcements perpendicular to the grain and what long-term effects could be expected and help to investigate if size of cross-sections is unlimited or if a certain maximum dimension should be maintained.

Along with the investigations mentioned, a top-up was obtained to continue existing work of quality assurance of timber bridges. The extra work can be found to answer questions on:

- Special considerations concerning local climate and environment around bridges and the influence on moisture content in the structure,
- Effects of adding or omitting protective measures or coatings on structural elements to protect them from impact of weather,
- Optimization of monitoring methods for large cross-sections typical for bridges,
- Summary of recommendations for practicing engineers and planners.

2 Monitoring Methods

2.1 General

The most accurate method to measure moisture content is through the oven-dry method. Gravimetric methods are used where the weight of a wood sample is measured before and after it is dried. The difference is then expressed as a mass percentage (M%). The method is however not practical in monitoring applications and alternative, less accurate methods are applied that measure wood's physical properties like resistance, dielectric properties, decolouration, etc. One of the most common methods is the electrical resistance measurement, Figure 1 (left). A second method known as the sorption method (Dietsch et al. 2014) or the bore hole method (Li et al. 2018) is based on the hygroscopic properties of wood, see Figure 1 (right). In this method, the relative humidity and temperature are measured in a small cavity in the timber. The sorption isotherms are used to determine the relative humidity. The electrical resistance method is discussed in this section and the sorption method will be discussed in Section 2.2.8.

Despite the larger inaccuracies in comparison to the oven dry method, the electrical resistance method has proven to be extremely practical in long term monitoring campaigns. Extensive comparisons between methods to measure moisture content in monitoring applications and equipment are available in Hermann (2009), Berger (2014), Gamper et al. (2014), and Dietsch et al. (2015). Details about behaviour of electrical properties of timber are found for instance in Skaar (1988). The author also lists uncertainties within this method being material density, calibration, pin type, electrode distance, etc.

In monitoring applications, it is often more important to know whether timber is very dry, wet, or soaked. Leakage of bridge decks has for instance been detected timely before wood-decay processes advanced too much (Franke et al. 2015). In monitoring in different large span structures, moisture content variations at different depths in load bearing elements could be measured caused by ambient climate variations in Gamper et al. (2014). Similar was done with agricultural buildings in Yiang et al. (2017). The electrical resistance methods were also used in measurements to monitor moisture content variations in timber elements exposed to weather (Niklewski et al, 2017). New methods and measurements setups are still developed to monitor moisture content variations. Brischke et al. (2008) embedded cables into substitute dowels to monitor moisture content in a bridge. Björngrim (2017) monitors moisture content by placing three screws of different lengths into the load bearing elements to monitor developments in two different depths from the surface. Sensors are also embedded into wood-based materials during production (Li et al. 2018) so no need to be installed afterwards.

2.2 Monitoring moisture content through electrical resistance method

2.2.1 Principle of electrical resistance measurement method

The electrical resistance method is based on the principle that the physical properties of wood change as the moisture content of wood changes too. Measuring dielectric properties of wood also change as moisture content changes and it is considered the second electric moisture content measurement (Skaar, 1998). The principle is that the resistance between two electrodes that are not placed too far apart is measured. Different distances between electrodes in literature are found such as 20 mm or 40 mm (Li et al, 2018) and 30 mm (Gamper et al., 2014). The electrodes can be cables (Birschke et al., 2008), screws (Franke et al., 2016), plates (Li et al., 2018), or partially insulated nails (Gamper et al. 2014). The diameter of these electrodes is generally found around 4 mm or 5 mm. The used equipment and the corresponding electrodes are discussed later in Section 2.2.7.
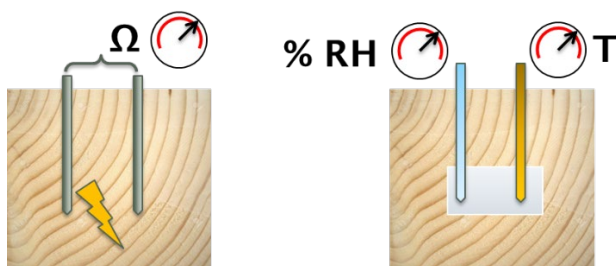

Figure 1: Illustration of moisture content measurement using the resistance method (left) and sorption or bore hole method (right)
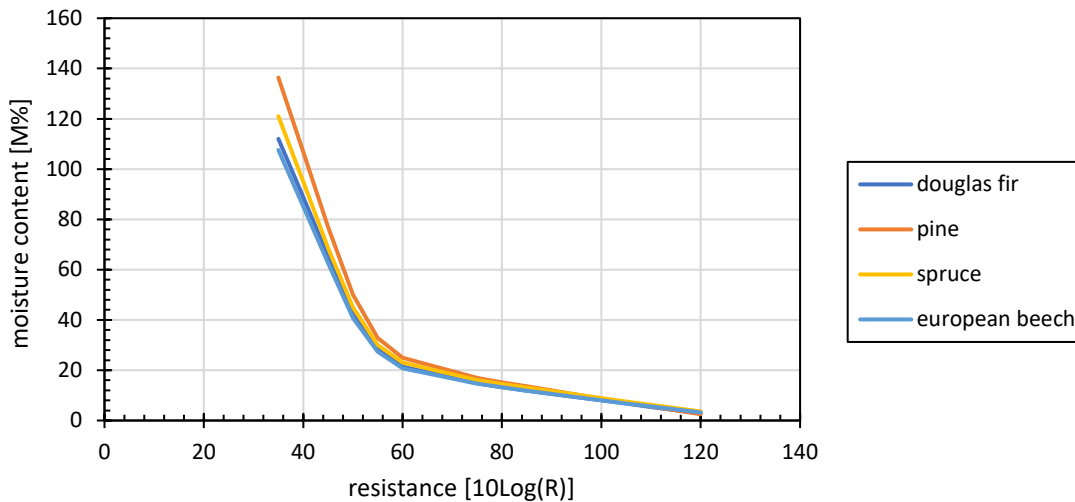
Figure 2: Illustration of resistance curves from electrical resistance to wood moisture content.

The resistance measured is schematically interpreted as three resistances connected in series (Li et al., 2018 and Niklewski, 2018). The middle one for the resistance of the timber, and the two outer ones for the contact resistances between the two electrodes and the wood. The range of resistances measured goes from a couple of 100 kΩ at 30 M% moisture content to 100 GΩ at 6 M% moisture content. It is especially the latter value of resistance that poses a challenge to measure as very small currents need to be detected.

2.2.2   Conversion from electrical resistance to moisture content

To convert the measured electrical resistance to moisture content, two steps are needed and a third one is optional.

1. A curve or equation is first needed to convert electrical resistance to moisture content.
2. Compensation for temperature as the electrical resistance is affected by temperature of the material.
3. Optionally, a calibration can be carried out in which the moisture content of the wood where the electrical resistance was measured is calculated using the oven dry method. This can be done to compensate for errors due to contact surface between wood and electrode or measurement equipment.

An example of electrical resistance curves for different timber species is found in Figure 2. This figure shows how the electrical properties have been measured on a wide range of moisture contents, for different wood species. The curves were measured using the Gigamodul by Scanntronik Mugrauer GmbH. The horizontal axis represents the tenfold of the logarithmic of resistance (logarithmic base of 10).

2.2.3   Temperature corrections

Along with the electrical resistance, it is recommended to measure material temperature as well. This is done to correct for an increase of the resistance as temperature drops, or reduction as the temperature increases. A rule of thumb is that a correction of 1 M% should be made per 10 ˚C, mentioned both by Skaar (1988) and Gerber (2004). Care is to be taken when using the electrical resistance method when temperatures below zero are expected. Uncertainties in the temperature correction increase and are therefore not very reliable as mentioned by Björngrim et al. (2017). Uncertainties can still be acceptable around -5 ºC but unreliable below -10 ºC (Fortino et al., 2016). This is explained by the conduction of electricity in water being provided by free moving ions. In ice, these are locked into crystals. However, Rode and Clorius (2004) amongst others mention that water in wood always remains in a liquid from, even below zero.

2.2.4 Measurement in salty and chemical environments

Salt positively affects the conduction of electricity in wood (Hermann, 2008). Salt storage buildings, e.g. for roads, are often built in wood, steel corrodes too easily. Such effects can also be imagined in road bridges in countries or regions where salt is used to prevent ice developing on the road deck in winter. Once a leakage occurs in a road deck and salt seeps through with the water, measurements will be affected by this too. Moisture content measurements could however be possible in materials that are not easily impregnated like Spruce.

2.2.5 Effect of glue lines

Cured adhesive in glulam is expected to act as an insulator and increase the resistance measured between two pins. Glue lines delay moisture transport (Hassani, 2015). Wenker and Welling (2017) mention that glue line had little to no effect on the measurement of electrical resistance in Beech LVL. Measurements in laboratories of the Bern University of Applied Sciences did show a difference of 2 M% to 3 M% at an average moisture content of 12 M%, explained later in Chapter 6. Tschuck and Schmid (2012) found that Resorcin Formaldehyde and Melamine Formaldehyde do not affect the measurement of moisture content in glued structures to a measurable quantity. Polyurethane adhesives do affect measurement of moisture content causing errors up to 5 M% at a wood moisture content of 20 M%. The higher the moisture content, the larger the error in measurement of wood moisture content is. Comparisons were only made in the hygroscopic range.

2.2.6 Numerical study of effect of electrode distance

Li et al. (2018) assumes a linear relationship between measured resistance and electrode distance, hence doubling the electrode distance doubles the electrical resistance. The sensitivity to either parameter can in that case be calculated through a simple numerical example using Equation (1) (Skaar, 1988):

$$\log(R) = A - B\log(\text{M\%}) \tag{1}$$

A summary of the calculations given below is also given in Table 1. Li et al. (2018) determined values A = 17.482 and B = 8.3126 for 3 mm diameter screws inserted 40 mm apart. If the pin distance is set to 20 mm, the electrical resistance would logically only be half. At 12 M% the electrical resistance is 324 MΩ. Placing the electrodes at half of this distance results in a resistance of 162 MΩ. Calculating wood moisture content based on the 40 mm distance would give 13.8 M% which represents 15 % error. An error of 10 % in the electrode distance (4 mm) results in an 0.5 M% moisture content error. Curiously, Hermann (2008) did not find such a large difference in moisture content as suggested with the calculation above. Doubling the electrode distance from 30 mm to 60 mm at a wood moisture content of 15 M% minimally increased the resistance and only resulted in a moisture content decrease of 0.15 %. Hence, something barely measurable. Skaar (1988) however argues that this also has to do with the relation between the pin diameter and the distance between these.

Continuing the linear resistance approach by Li et al. (2008) above the fiber saturation point, inaccuracies are however much larger. In the same configuration A and B were determined as 10.477 and 3.0536 respectively. An error in the pin distance of 10% results in an error of 1.7 M% and reducing electrode distance from 40 mm to 20 mm results in a difference of 12.7 M%.

Björngrim et al. (2017) measures moisture content with screws up to 600 mm deep into the structures while maintaining an accuracy of 1.5 M%. It seems wise, like Hermann (2008) suggests, that FEM calculations are to be performed to improve insight in the future. However, this would require resistance properties measured at different temperatures and moisture contents, which then need to be translated into parameters that can be used to calculate the electric field between two electrodes.

Table 1: Uncertainties in resistances calculated with published parameters or mentioned by different authors

Source	Electrode distance / error	Moisture content/error
Li et al. (2018)	40 mm / 20 mm	12 M% / 1.8 M%
Li et al. (2018)	40 mm / 36 mm	12 M% / 0.5 M%
Hermann (2008)	30 mm / 60 mm	15 M% / 0.15 M%
Li et al. (2018)	40 mm / 20 mm	40 M% / 12.7 M%
Li et al. (2018)	40 mm / 36 mm	40 M% / 1.7 M%

2.2.7 Technical equipment used to measure electrical resistance

Electrical resistance is in most cases measured using Gigamodul equipment supplied by Scanntronik. This equipment allows measuring electrical resistance between eight electrode pairs, and each sensor is measured separately so that electrical fields do not interfere when these electrode pairs are placed in each other's vicinity.

The equipment and the conversion curves are discussed for three different types of equipment:

- Gigamodul produced by Scanntronik Mugrauer GmbH. The electrical resistance can also be measured using the Materialfox sold by the same company, but this has a smaller range in measurable moisture contents.
- The handheld Gann Hydromette M 4050
- Omnisense Wireless sensors

The most commonly applied equipment throughout the monitoring campaigns is the Gigamodul. It can measure moisture content of wood from 6 M% upwards. The Materialfox measures this from 12 M% upwards. However, uncertainties in the high hygro-sorptive range have been mentioned by both Gamper et al. (2014) and Tschuk and Schmid (2012). The calibration curves provided by the software that is delivered along with the equipment underestimates moisture contents above 20 M% up to 2 M% and 5 M%, respectively. The used electrode pairs are partially insulated, stainless steel, hammer electrodes. Instead of hammering these electrodes into the wood though. They are predrilled 4 mm on the insulated part and predrilled only 3 mm on the section where contact with the wood is important, i.e. electrode tip which is 6 mm long. The electrodes are shown in Figure 3 (left). The conversion from electrical resistance to moisture content is seen in Figure 3 (right).

During inspections, the handheld Gann Hydromette M 4050 with pointed hammer electrodes is used to measure wood moisture content with a different equipment to have reference moisture content as measured with the Scanntronik equipment. The second reason to do this is to provide the optional calibration or offset mentioned in Section 2.2.2 when needed. The electrodes and conversion parameters are shown in Figure 3 (right).

Whereas the moisture contents were generally measured using the equipment supplied by Scanntronik Mugrauer GmbH, moisture contents in the training facility of the ice hockey club of Davos (CH) were measured with the wireless sensors supplied by Omnisense®. Eight loggers powered by batteries were connected wireless with one gateway and could log and transmit both electrical resistance from about 6 M% upwards and two inputs for climate. Measured values are viewed online (paid service) and downloaded from a website to allow post processing afterwards. Moisture content is calculated directly and is valid for Douglas fir. Conversion for Norway spruce needs to be done afterwards. The electrodes suggested by Omnisense were screws. The electrodes and conversion parameters are shown in Figure 3.
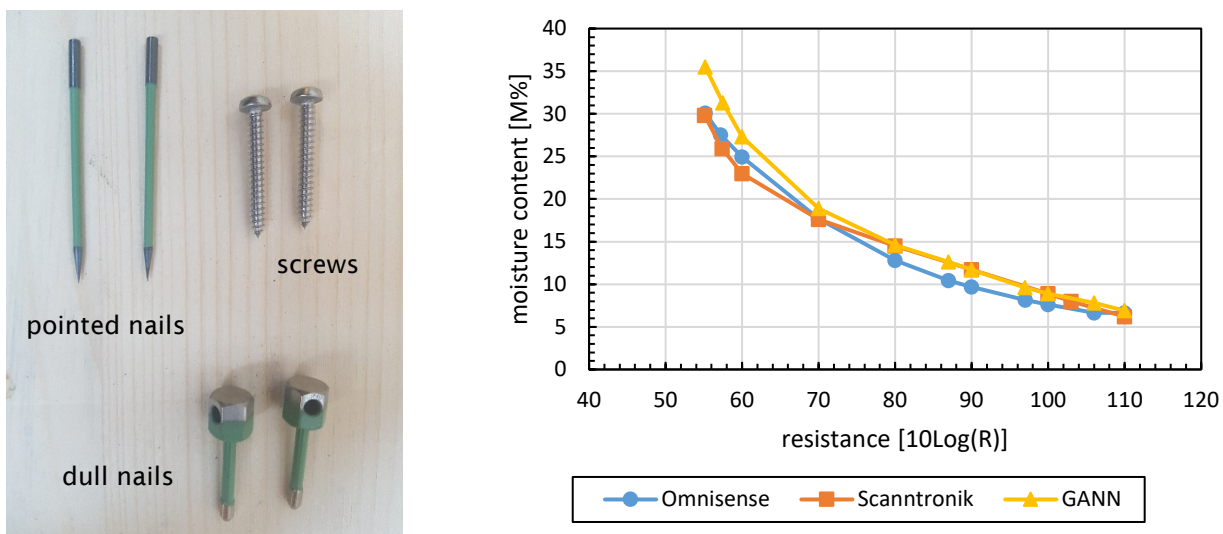

Figure 3: Electrodes used in the different equipment (right) and the conversion curves from electrical resistance to moisture content (left)

Since the Omnisense equipment does not output electrical resistance, but moisture content of douglas fir instead, the output was checked using resistances ranging from 330 kΩ to 100 GΩ. The douglas fir values were converted to Norway spruce afterwards. The same resistances were also used to measure the conversion of resistance to moisture content provided by the Gann Hydromette M 4050 used during inspections. All reference temperatures are 26 ˚C (approximately for the Omnisense equipment). The right diagram of Figure 3 shows the comparison of all these curves. The possible underestimation of the high moisture contents mentioned by both Gamper et al. (2014) and Tschuk and Schmid (2012), is reflected in the diagram. The Omnisense equipment continuously underestimates the moisture content with respect to the Gann Hydromette M 4050. The Gann Hydromette M 4050 and Scanntronik conversion curves do overlap in the low moisture content ranges. The underestimation of the wood moisture content by the Omnisense equipment mentioned by Niklewski (2018) is also reflected in Figure 3.

2.2.8 Development of calibration curves for beech veneer

Conversion curves from resistance to moisture content can also be set up using laboratory experiments, like performed by Björngrim et al. (2017) and Li et al. (2018). This can be done for instance when:

- conventional measurement setups cannot be used due to e.g. size of the specimen or location of the measurement,
- different equipment, electrodes, materials are used, or
- no proper curves are available for the material, for instance in old timber beams in structures of cultural heritage.

More examples can be imagined and listed. Setting up own calibration curves is however time intensive.

These curves were determined in the laboratories of the Bern University of Applied Sciences. Wenker and Welling (2017) mentioned that using resistance curves for European beech could be used as nothing better was available yet. Five beech veneer elements were supplied by Pollmeier Massivholz GmbH & Co.KG from which samples of 8 cm x 8 cm x 4 cm were used to determine the resistance measured between two electrodes. Instead of using one single set of samples and expose them continuously to different relative humidity and temperature, a more statistical approach was pursued. Samples, up to eight per climate, were preconditioned in four different climates for about two months each to be sure that equilibrium moisture contents were achieved. The four different climates at 20 ˚C were established as follows:

- 33 %RH developed over a solution of potassium chloride
- 50 %RH available in the furniture testing laboratory/climate chamber
- 65 %RH available in the materials testing laboratory
- 83 %RH developed over a solution of calium chloride

The samples were prepared such that resistance transverse to the grain and resistance along the grain could be measured. Several measurement setups were developed. The standard measurement setup is
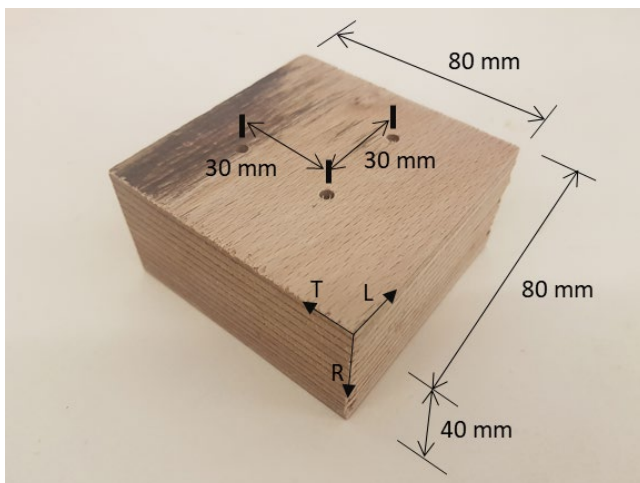

Figure 4: Standard setup to determine calibration curves converting resistance into wood moisture content

observed in Figure 4. Electrodes, dull nail-type electrodes seen in Figure 3, were placed at 30 mm from each other, in transverse and longitudinal direction. They were predrilled such that they would measure resistance in the midplane. In softwood the diameter of the predrilled hole is 3.0 mm when the dull nail-type electrodes are used. In this case, the holes were predrilled at a diameter of 3.5 mm. The electrodes were placed perpendicular to the veneer layer (LT). Since the veneers have a thickness of approximately 3 mm each and the uncoated part of the electrodes was 6 mm, resistance is always measured over at least two separate veneers. The setup shown in Figure 4 is called setup A.

Apart from this, three other setups were used:

- Measurement of resistance across to the glue lines, setup B. The electrodes were placed perpendicular to the LR-plane, at an angle of 45° to the glue line to ensure the electrodes were surrounded by enough material as recommended in Skaar (1998).
- Measurement of resistance parallel to the glue lines, setup C. The electrodes were inserted from the LR plane right into the glue line so that the resistance was measured over two separate veneers.
- Two measurements of resistance transverse to the grain, setup D. This measurement focused on the diameter of the predrilled hole being either 3.0 mm or 3.5 mm. The smaller diameter means that the electrodes need to be driven in with more force.

Whereas tests under setup A were performed in different climates, setup B, C, and D were performed only at a temperature of 20 °C and a relative humidity of 65 %RH.

After the samples were taken from their preconditioned climate, the holes for the electrodes were pre-drilled, the electrodes were inserted, and the weight of the samples was recorded. The electrode pairs were then connected to the Scanntronik Gigamodul and the resistance was logged every half hour. The initial temperature in the climate chamber was 20 °C and was maintained for several days. The samples were weighted every couple of days. After an equilibrium was achieved, the temperature was decreased to 10 °C. Stable relative humidities at lower temperatures could not be established by the climate chamber. In total, samples stayed in the climate chamber at least a week, longer if equilibrium in weight had not been achieved yet. After equilibrium in resistance and moisture content had been achieved at 10 °C, electrodes were removed, weighed once more and the oven-dried.

Equation (1) proposed by Skaar (1988) was used to fit through the measured relation between resistance and moisture content. For measurements transverse to the grain the following relation was derived:

$$\log(M) = 1.7320 + 0.0028T - (0.0820 + 0.0010T)\log(R) \tag{2}$$

The logarithmic basis of 10 is used. Although differences between resistance along and transverse to the grain were minimal, a relation was also developed for measurements made along the grain:

$$\log(M) = 1.6883 + 0.0021T - (0.0777 + 0.0010T)\log(R) \tag{3}$$

Differences between resistance along the grain and transverse to the grain were especially noticed in climates of 65 %RH. Below and above this relative humidity, differences were minimal. In the samples tested in relative humidity of 33 %RH, the resistance in longitudinal direction was higher than in transverse direction. A selection of the results is observed in Figure 5. The figure shows test results and the fitted curves along with the resistance to moisture content conversion programmed in the Scanntronik software and the Gann Hydromette M4050 hardware. These resistance curves were reverse-engineered using a set of resistances ranging from 330 kΩ to 100 GΩ. The relation between longitudinal and transverse resistance is plot in Figure 5 as well in the right diagram. When moisture content is small, grain direction does not need to be considered.

Figure 5 shows that use of beech veneer can lead to significant over estimation of moisture content in the higher moisture content ranges, up to 5 M% in relative humidities of 83 %RH. The error is in the order of 2 M% in the low moisture content ranges. Determining the relation between resistance and moisture content on beech veneer proved to be necessary to allow a better determination of moisture content in the future.
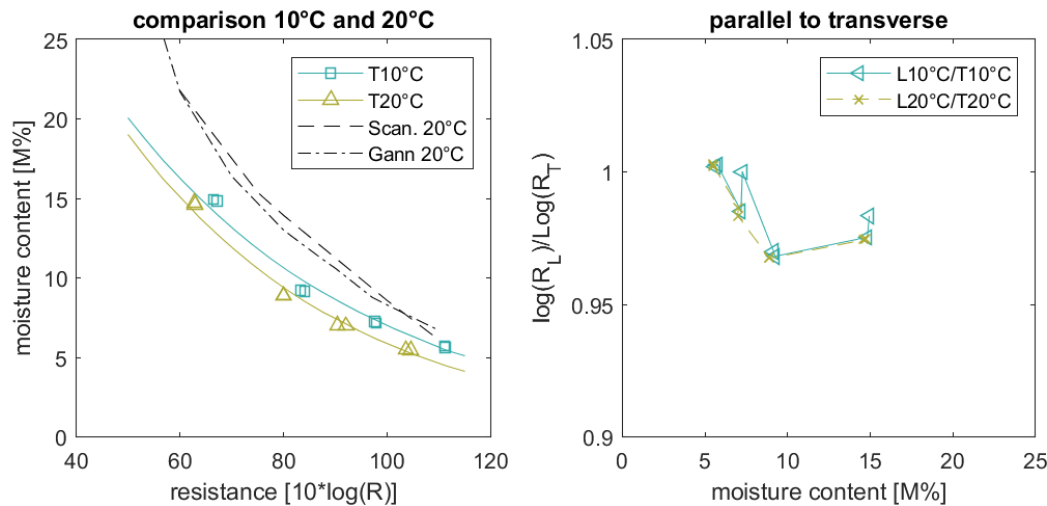
Figure 5: Measured resistance against moisture content transverse to the grain at 10 °C and 20 °C and the resistance curves for beech as programmed in the soft and hardware of Scanntronik and Gann Hydromette M 4050 (left); relation between resistance measured along the grain and transverse to the grain (right).

Table 2: Moisture contents calculated from the different instrumentation setups B, C, and D in comparison to setup A where electrical resistance is measured transverse to the grain.

Orientation to grain	Transverse A	Parallel A	Transverse B	Parallel C	Transverse D
Average moisture content	9.4	10.0	6.6	10.1	9.6
Difference with Transverse A	-	0.6	-3.8	0.7	0.2

Average measured moisture contents calculated from setups B, C, and D are presented in Table 2. The table shows the moisture contents calculated with the obtained resistances from each setup calculated with Equation (2). It also shows the average differences with the suggested standard setup, being transverse to the grain in setup A where the electrodes are oriented transverse to the veneer layups.

The table shows, that if the resistance curve from equation (2) is used for measurements made longitudinal to the grain, an average difference of 0.6 M% or 0.7 M% is obtained depending on the orientation of the electrodes. As observed in Figure 5, this difference is only large in relative humidities of 65 %RH. If measurements are made transverse to the glue line, an average underestimation of moisture contents of 3.8 M% can be expected. Finally, whether predrilling is done with a drill of 3.0 mm or 3.5 mm, an average overestimation of the moisture content of 0.2 M% can be expected. If the obtained spreads are included in these differences, it is expected that only setup B shows significant differences to setup A. The extra tests show that measuring across glue lines is strictly discouraged.

2.3   Measurement of relative humidity and temperature in the sorption method

2.3.1   Application of the sorption method in monitoring campaigns

Moisture content can also be determined using relative humidity and temperature measured in a small cavity in the wood. The method is called sorption method by Dietsch et al. (2014) or the bore hole method in Li et al. (2018). The monitoring method has been implemented in Norwegian bridges owned by the Norwegian Public Road Administration (Dyken and Kepp, 2010), recall Figure 1 (right). Melin et al. (2016) uses the method to measure moisture content in art and other objects of cultural heritage in museums. The author claims that a higher accuracy is achieved than with the electrical resistance method, since measurement depth can better be defined. In the measurement of electrical resistance, the path with least resistance governs the measured resistance along the area in contact with wood. Li et al. (2018) mentions that this monitoring method can however only be applied in the hygroscopic range of wood. Electrical resistance methods can be used in the hygroscopic and over hygroscopic range. Which makes the electric resistance method more suitable to identify leakages in bridge decks or to monitor drying processes of soaked structural elements. However, the sorption method is insensitive to existing electric fields, salty environments, and if sensors can recuperate from condensation without loss of measurement accuracy,

a wide application can be foreseen. Otherwise, sensors need to be exchanged and recalibrated every several years (Norsk Treteknisk Institute, 2013). Further development of the method could also be implemented in monitoring methods using fibre optics for instance where multiplexing reduces the need for pulling cables from sensor to logger etc., see also Franke and Schiere (2017).

2.3.2 Conversion of relative humidity and temperature to moisture content for spruce

The sorption method requires the use of sorption isotherms to convert measure relative humidity and temperature to moisture content. That means that these should be known or determined through experiments before the measurements start. Dyken and Kepp (2010) performed tests in temperatures from -20 ˚C to 20 ˚C in different relative humidities and set up a second-order polynomial equation to calculate wood moisture content for Nordic pine (Pinus sylvestris). Measurements were performed to form a basis for a practical formula, not to investigate all properties of the wood or of the measuring method. The authors suggest sorption isotherms cannot be used because the climate in a small cavity in the wood according to a moisture content and temperature is not the same as the moisture content of wood placed in an ambient climate. Measured differences between the newly established curve and the originally used Madison curve resulted in values in the order of 2 M% in comparison to the so-called Madison values obtained from Simpson (1998). The mathematical formula was however also used to calculate moisture content values measured right below asphalt surfacing during summer periods.

Skaar (1988) and Siau (1995) describe how adsorption of water on the cell wall is a complex process which can be modelled in the Dent model, BET model, or Hailwood Horrobin model. Simpson (1973) used the Hailwood-Horrobin model. A comparison is made between the following models or experiments that propose models to calculate the moisture content, see Figure 6.

- Simpson (1998) which suggested equations using RH and T to calculate moisture content of wood which overlaps with the Keylwerth and Noack (1964). These values are based on Sitka spruce,
- Toratti (1992) which suggest equations to calculate sorption isotherms using RH only,
- Rijsdijk and Laming (1994) experimentally determined the ad- and desorption isotherms of Norway Spruce (Picea abies, Central European grown),
- Frandsen (2007) suggesting mathematical equations using only RH based on the Hailwood-Horrobin formulations, and
- Fortino et al. (2009) which uses an equation based on RH and T of which the resulting EMC overlaps the equation suggested by Simpson (1998).

Melin et al. (2016) use ad- and desorption surfaces such as developed by Rode and Clorius (2004) to transfer measured relative humidity and temperature to moisture content. This forms a more physical basis than the second-order polynomial set up by Dyken and Kepp (2010). Rode and Clorius (2004) present a method to convert relative humidity and temperature to moisture content from -20 ˚C to 50 ˚C using data obtained from Hedlin (1968), Hansen (1986), and Kelsey (1957). As far as known, Hedlin (1968) provides the largest amount of sorption measurements made for wood below zero. These three latter authors developed or gathered sorption isotherms for wood placed in a climate, not for the climate inside a cavity in the wood.

Melin et al (2016) does not apply a temperature dependent adsorption curve above zero, Rode and Clorius (2004) do and base this on measurements made by Kelsey (1957). The moisture independent adsorption isotherm conflicts at a certain point with the temperature dependent desorption curve, i.e. the intersect. Both Melin et al. (2016) and Rode and Clorius (2004) however apply a temperature dependent desorption isotherm with data obtained from Kelsey (1957). Rode and Clorius (2004) developed the sorption surfaces for moisture contents below zero and use a depression of moisture content in relation to temperature. Rode and Clorius (2004) further note that Hedlin's measurements of the desorption curve concern the initial desorption and overestimate the actual moisture content if ad- and desorption would be followed up continuously below zero. The ad- and desorption surfaces above and below zero were reconstructed and observed in Figure 7. Note that the relative humidity below 0˚ C is calculated for vapour above ice instead of super cooled water. Whether the extrapolation to -12 ˚C to -20 ˚C is realistic is not known.
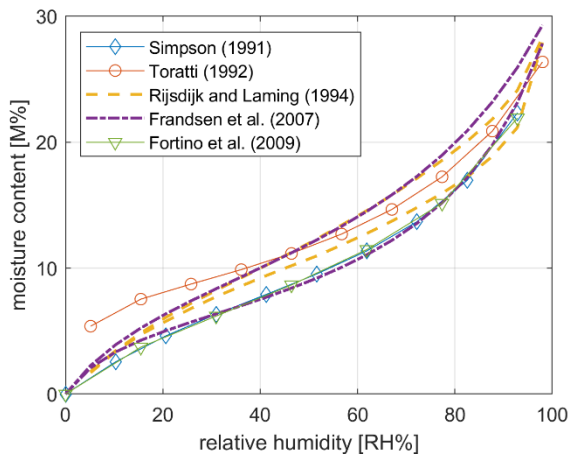
Figure 6: Comparison of mathematical equilibrium moisture content models for Spruce found in literature for a temperature of 20° C
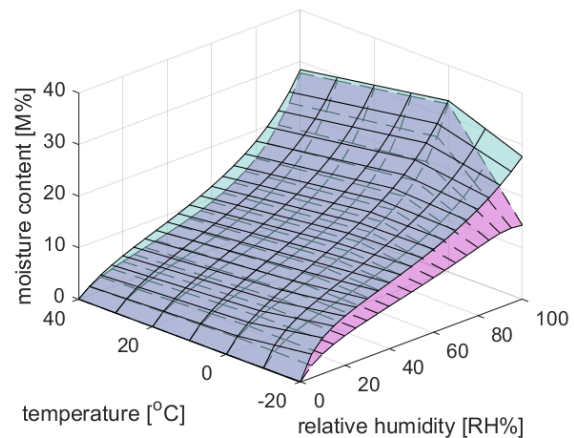
Figure 7: Illustration of ad- (red) and desorption surfaces (blue) built for spruce based on methods suggested by Rode and Clorius (2004)

Melin et al. (2016) does not mention anything with regards to the statement made by Dyken and Kepp (2010), that the relative humidity in a small cavity in a large piece of timber is different from the relative humidity around a small specimen of wood at equal moisture contents. Melin et al. (2016) use these sorption surfaces to calculate moisture content of structures measured with a small temperature and relative humidity sensor in a method called bore hole by Li et al. (2018). Below zero, Simpson's (1998) equations require relative humidity calculated over ice to give most accurate values. Extensive validation was however not made.

2.3.3 Sorption isotherms for beech veneer

Sorption isotherms for beech veneer can be obtained from the building physics brochure (Pollmeier, 2018). These were digitalised, and a mathematical formulation of the sorption isotherms was developed using the Hailwood-Horrobin theory (Simpson, 1973).

$$u_{emc} = \frac{1800}{M_p}\left(\frac{K_1\phi}{1-K_1\phi} + \frac{K_2K_1\phi}{1+K_2K_1\phi}\right) \tag{4}$$

In which:

$$M_p = 234 + 1.13T + 1.99\cdot10^{-2}T^2$$
$$K_1 = 0.770 + 8.502\cdot10^{-4}T - 1.47\cdot10^{-6}T^2 \tag{5}$$
$$K_2 = 4.17 + 5.127\cdot10^{-2}T + 3.27\cdot10^{-4}T^2$$

Where T is the temperature in °C and ϕ relative humidity. This equation can be used to convert measurement of humidity and temperature in a cavity in the wood to moisture content. The sorption isotherms provided by the building physics brochure are however published for a temperature of 20 °C and above. Hence, values for temperatures below 20 °C are extrapolated from this graph.

Along with the tests performed in Section 2.2.8 with samples of 80 mm x 80 mm x 40 mm, smaller blocks of 40 mm x 40 mm x 40 mm were cut from the beech veneer beams as well. These were used to verify the sorption isotherms. The smaller blocks were climatized in the same conditions as the larger blocks. The overlap between the moisture content from the mathematical formulation and from the measured moisture content on the small samples is observed in Figure 8. Table 3 shows that differences between the fitted curves and the measured moisture contents are above 3 M%.
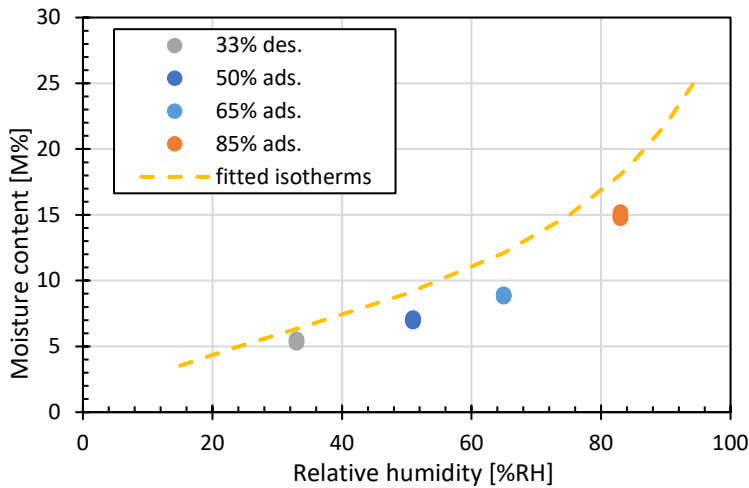
Figure 8: Fitted sorption isotherm and the calculated moisture content from smaller wood samples. Note that the moisture content calculated from the samples conditioned in 33% are likely on the desorption isotherm and the rest is on the adsorption isotherm.

Table 3: Moisture content as calculated from fitted mathematical curves and moisture content calculated from smaller blocks

	33 % des.	50 % ads.	65 % ads.	85 % ads.
Fitted isotherms	6.3	9.0	12.1	18.1
Measured moisture	5.4	7.0	8.9	14.7

2.3.4 Additional comments concerning uncertainties

It should be noted that diffusion of vapour through the lumens is faster than that the cell walls can absorb or release water into the cell lumens itself. Measured relative humidities might not directly correspond with the real moisture content of wood in dynamic conditions. Methods as proposed by Frandsen et al. (2007) and implemented by Fortino et al. (2016) should be used to better investigate the behaviour of relative humidity in a small cavity. Petara et al. (2016) use a different approach than the latter two sources to the hysteresis of wood in varying relative humidities and temperature. These allow detailed analysis of static and dynamic properties of this measurement method as well.

2.4 Non-physical effects in moisture content measurements

Calibration curves providing the correction of measured resistance or climate to moisture content have been set up in constant or semi-static climatic conditions such as a climate chamber. However, monitoring campaigns deal with varying climatic conditions, measuring a constantly varying resistance, which is used to calculate moisture content. Through the different steps that are needed to finally obtain the measured moisture contents, there is a risk of non-physical effects being present in the analysis of moisture content, i.e. moisture content changes that are not real, also explained in Dyken and Kepp (2010). This can occur for instance to a timber member warming up due to exposure to solar radiation, through which the centre of the cross-section warms up. This reduces the measured resistance and increases the measured moisture content after temperature correction. It is not realistic to expect that moisture content of larger cross-sections changes in the order of 1 M% over the range of a day.

Similarly, the resistance type method has also shown to be affected by magnetic fields around the instrumentation. Electrical systems being switched on or off result in unrealistic moisture content increases. These types of uncertainties can hardly be corrected or accounted for. They do however affect data analysis. Moving averages have been suggested to correct for strongly varying effects, but it is not expected that that can average out all the encountered effects. It is suggested to filter moisture content measurements using a median filter for instance prior to the application of a moving averages. Skaar (1988) also explains how measurement of electrical resistance in varying moisture content can either underestimate or overestimate moisture content.

3 Climate Scenarios and Moisture Content in Timber Structures

3.1 Monitoring objects

The ambient climate and moisture content in timber structures and on timber bridges is monitored with different objectives, duration, and results, e.g. in Gamper et al. (2014), Cruz and Custódio (2006), Franke et al. (2015). Some are monitored to investigate moisture gradients, detect leakages, or obtain equilibrium moisture contents. The ambient climate depends on the building occupation and use and on the meteorological weather, local topography or environment, and altitude. Moisture content follows the variations in ambient climate. Since climate and moisture were not investigated yet in some structures, new monitoring campaigns were started. These new results were combined with available results into data that could be interpreted based on one single parameter. The new monitoring campaigns were selected and obtained in close cooperation with the practitioners and research partners. The buildings and structures were mainly erected in 2017 and 2018 and are in Switzerland:

- The riding hall in Einsiedeln was instrumented because the region is known to have high relative humidities over the year. The effect of the local climate should be analyzed in addition to the ambient climate due to user service. Riding halls are known to be wetter due to the moistening of the soil to prevent too much dust developing during riding. The hall was instrumented with Scanntronik Mugrauer GmbH equipment to measure moisture content at four different depths in two locations. Each of the locations was also instrumented with sensors to measure moisture content through the sorption method. More details are shown in Appendix A.2.

- Three alpine ski stations near Andermatt were instrumented. The structures were all located above an altitude of 1500 meters above sea level. These structures are well ventilated and instrumented with Scanntronik Mugrauer GmbH equipment to measure moisture content at four different depths in two locations. Each of the locations was also instrumented with sensors to measure moisture content through the sorption method. More details are shown in Appendix A.1.

- The two open ice rinks in Delémont and Le Locle are nearly identical timber structures but in different regions with different user service (period of ice over the year), and local ambient climate. Both ice rinks are instrumented with two moisture content sensors. Moisture contents were logged with the Scanntronik Mugrauer GmbH equipment. The moisture content was not measure above the ice, but at a reference location above a grandstand. The reference locations were accessible with considerably less effort than the areas above the ice. More details are shown in Appendix A.3.

- A newly erected ice hockey training facility in Davos was instrumented because of the special architectural concept. Moisture content above the ice and in transition area between a heated fitness facility and cool ice hall climate was of interest. It was expected that condensate could build in this area. The locations of interest were located too far apart to allow use of cables, therefore the Omnisense equipment was used. More details are shown in Appendix A.4.

- The reinforced bridge of Andelfingen was instrumented to investigate moisture content developments in beech veneer. The northernmost portal frame was instrumented in two locations at two depths from the surface. Moisture content was also measured in two reference blocks that could, if needed, be removed for extra analysis in a laboratory. Beech veneer is not commonly used in Service Class 2 (SIA 265:2012) applications. The moisture content and climate were logged with the Scanntronik Mugrauer GmbH equipment. More details are shown in Appendix A.5.

The location of all monitoring objects observed within the research project in Switzerland is shown in Figure 9. The figure shows:

- the newly instrumented structures,
- the bridges where instrumentation had already been placed and monitoring was continued,
- two structures from which measured data was received, and
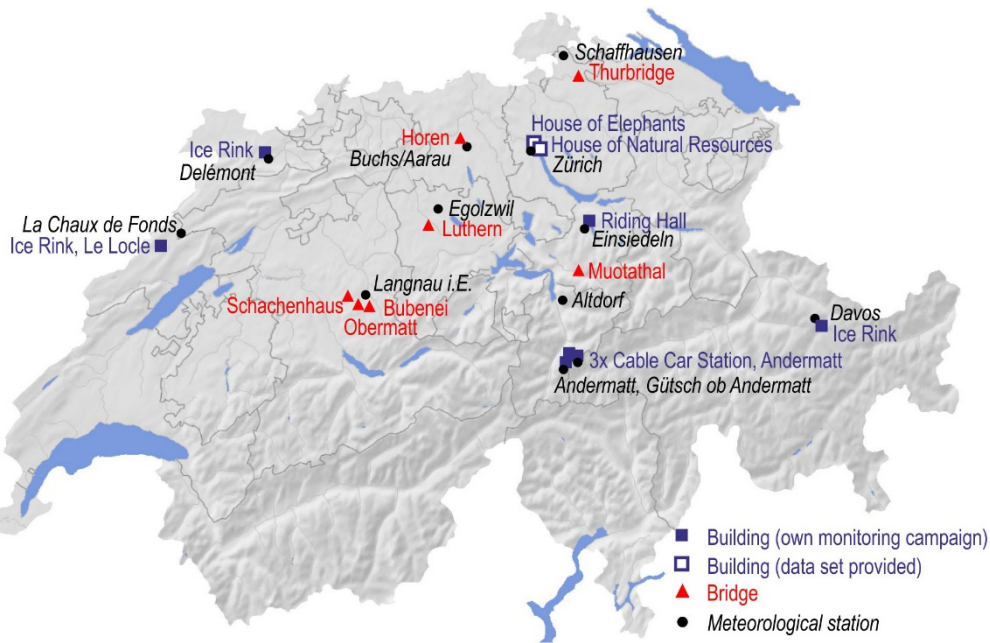- meteorological stations used to compare measured values with.

Figure 9: Map of Switzerland with instrumented bridges and buildings and meteorological stations serving as reference

3.2 Analyses method of climate and moisture content values

3.2.1 Envelopes of moisture content and climate

All the gathered time traces of moisture content and climate are shown in Appendix A. The measured data is analysed using the minima and maxima value over one year. This is done both for the wood moisture content and climate and presented as an envelope of the measure data. The developed envelopes can be used by practicing engineers and planners a support tool towards the design of a building. They also quickly allow to assess whether measured moisture contents are in ranges where the relative humidity is measured. Figure 10 shows the annual developments of relative humidity and moisture content over a year (left) and a comparison between the two (right). The moisture content was measured at 15 mm depth. The period where the ice rink is in operation is easily distinguished, i.e. from 1st September to 15th of April. The plotted data was filtered with a moving average filter.
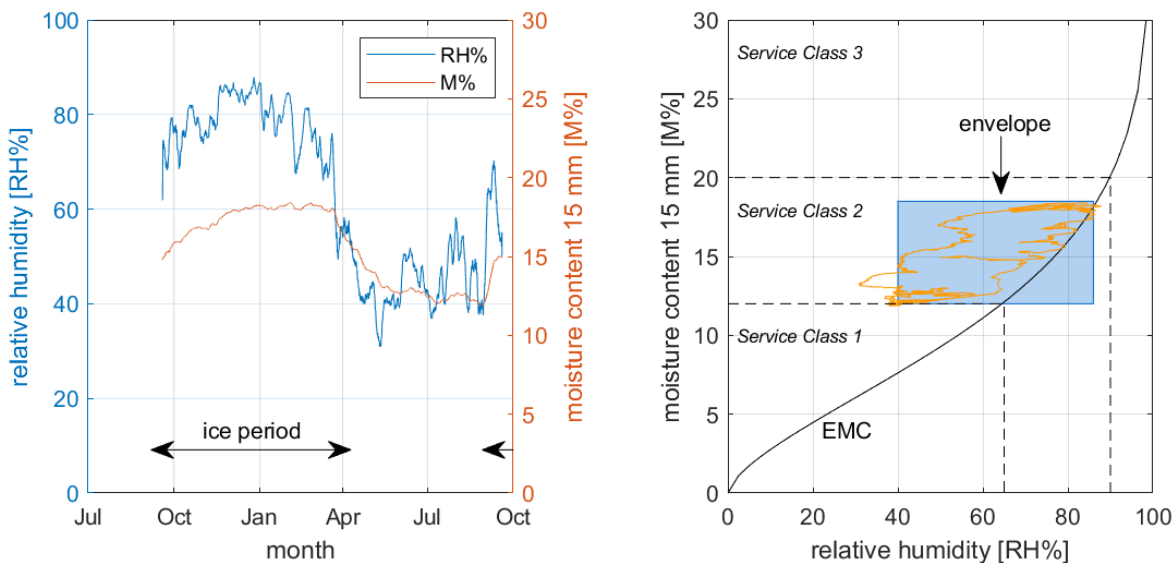
Figure 10: Example of data extraction of the data from ice rink B2 at measurement location M2 with the time series (left) and the comparison of relative humidity and moisture content at 15 mm depth (right); measuring data used from Gamper et al. (2014)

If moisture content on the surface would be compared to the relative humidity, the envelope would theoretically follow the theoretical equilibrium moisture content (EMC). Response of the moisture content at 15 mm depth however is delayed, with a smaller amplitude. The minimum relative humidity was omitted of the envelope since it concerns only one peak which is concerned to be due to a special climatic event and it did not affect the moisture content much. It would be included in the envelope once it would be observed more often.

The envelope helps to calculate the difference in moisture content throughout the year. This is the maximum minus the minimum moisture content.

$$\Delta u_{15\,mm} = \max(u_{15mm}) - \min(u_{15mm}) \tag{6}$$

It should be noted that the maximum moisture content in heated buildings occurs during the summer months, and the minimum moisture contents during the winter months. The data in Figure 10 shows the moisture content developments in an ice rink, where the maximum moisture contents are achieved in winter time, and the minimum in summer.

A similar value called $\Delta u_{surface}$ can also be calculated using the theoretical equilibrium moisture contents calculated at the surface using temperature and relative humidity. The relation between the two is then calculated as:

$$r_u = \frac{\Delta u_{Surface}}{\Delta u_{15\,mm}} \tag{7}$$

This value defines the relation between the moisture content developments. If this value is high, large variations of short duration occur at the surface. If it is small, variations in relative humidity at the surface are smooth and not very large either. The two parameters in Equation (6) and Equation (7) are used to simplify climates in different types of structures in Section 5.3.

3.2.2 Extrapolation and interpolation of moisture content profiles

Moisture content measurements are made at various depths from the surface. This depends on the goal of the monitoring campaign, i.e. to know moisture gradients like in Gamper et al. (2014), to know risk of decay like in Yiang et al. (2017), or to detect leakages of protective layers in timber bridges like in Franke et al. (2015). Most of the measurements were performed with partially insulated, nail-type electrodes (GANN) at a depth of 15 mm, 25 mm, 40 mm, or 70 mm from the surface. Moisture contents were in these cases derived at 15 mm from the surface like explained in Figure 10. In the cases where measurements were performed at different depths, moisture contents need to be interpolated or extrapolated.

Analytical solutions to moisture content diffusion offer a mathematical basis to in- and extrapolate the moisture contents across the timber cross-section. Two equations can be used. Eq. (8) is the error function proposed by Crank (1975):

$$n(x,t) = erfc\left(\frac{\frac{L}{2} - x}{\sqrt{Dt\pi}}\right) \tag{8}$$

in which L is the entire width of the cross-section, x is the distance from the surface, D is the diffusion value and t the time.

Eq. (9) is proposed by Siau (1971):

$$n(x,t) = 1 - \frac{1.27}{e^{(2.47\tau)}}\cos\left(\frac{\pi x}{L}\right) + \frac{0.425}{e^{(22.2\tau)}}\cos\left(\frac{3\pi x}{L}\right) \tag{9}$$

in which $\tau = 4tD/L^2$. Eq. (9) is to be chosen if $\tau < 0.1$. This is when the moisture content distribution is calculated for semi-infinite bodies, an assumption that holds shortly after boundary conditions at the surface are changed. Time t is selected as 90 days (approximately one season), after which the width of the body mainly helps to decide whether the moisture content distribution is a distribution in a finite or in a semi-finite body. The difference between the moisture content distribution at the measured location
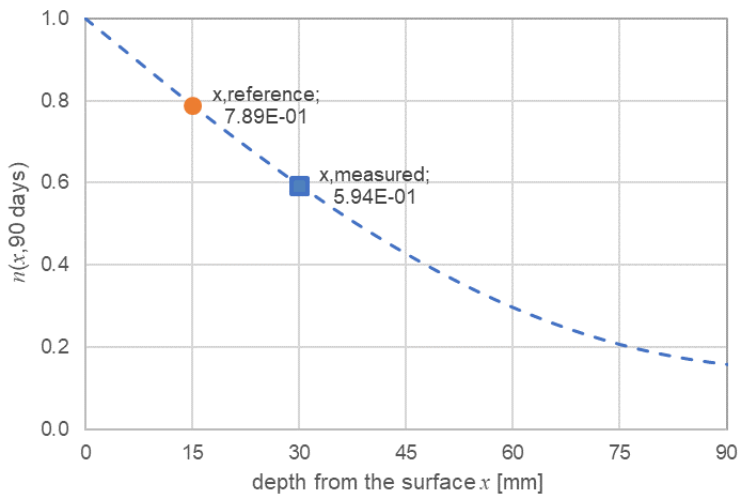
Figure 11: Example in which the moisture content variation measured at x = 30 mm depth is recalculated to a moisture content variation at x = 15 mm depth from the surface

and at 15 mm depths from the surface is then simply calculated as the ratio between the $n(15\,\text{mm}, 90\,\text{days})$ and $n(x_{measured}, 90\,\text{days})$. An example where moisture content is measured at 30 mm depth in a 200 mm wide beam is shown in Figure 11. The moisture content variation is multiplied by $0.79/0.59 = 1.34$.

3.3 Timber structures in alpine regions

Experience with timber construction in the alpine region is mainly obtained with smaller residences, but the increase in recreational tourism has led to the construction of refuges and restaurants on high altitudes with large spans and high-quality requirements. The ski resort located between Andermatt and Sedrun expanded its infrastructure in 2017 and 2018 with several newly constructed cable ways. Most of the corresponding stations were erected in timber because it allows a short construction time. The three cable car stations in the alpine region of Andermatt-Sedrun are on different altitudes: one in the village of Andermatt at an altitude of approximately 1500 meters above sea level (m a.s.l.), one in the village of

Figure 12: Picture of the ski station in Andermatt (upper left), Nätschen (upper right), Schneehüenerstock during construction (lower left) and a map (source: openstreetmap) with their locations between Andermatt and the Oberalp pass
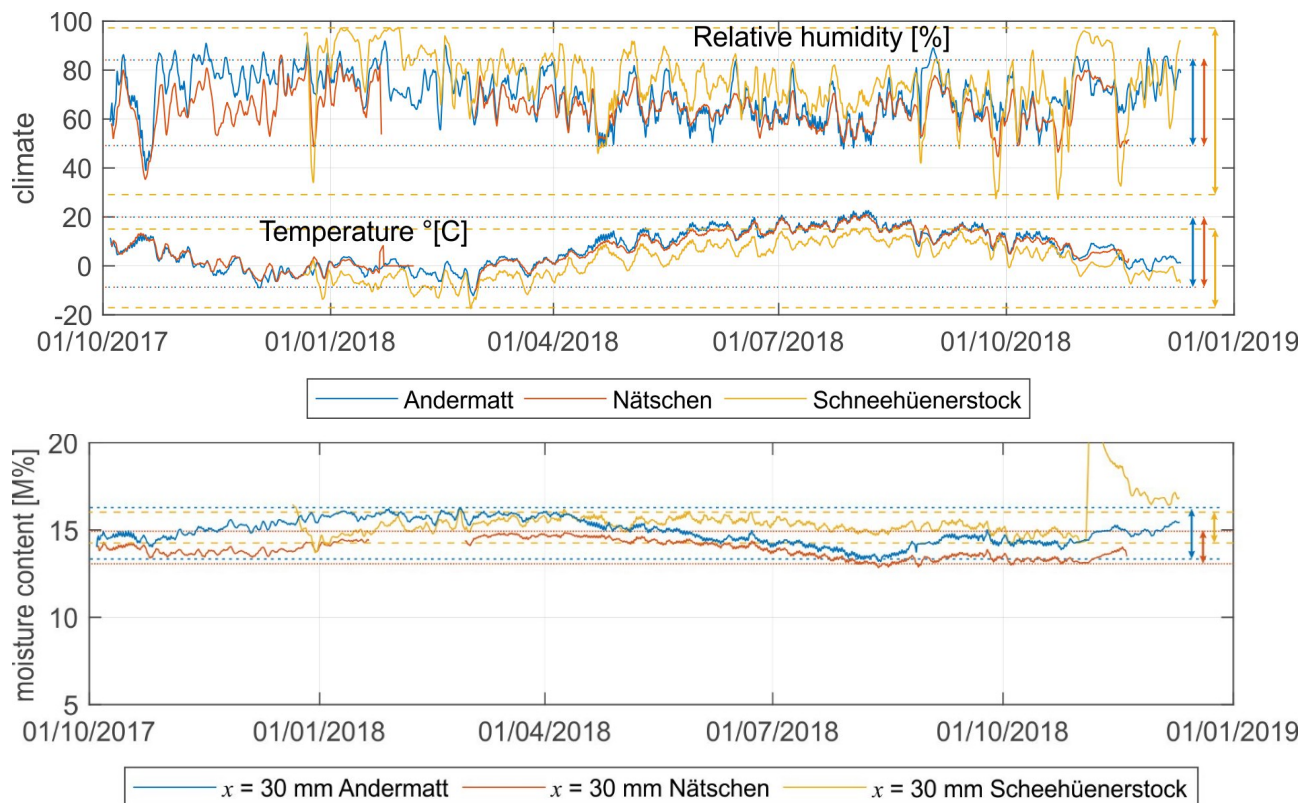
Figure 13: Climate and moisture content monitoring in the alpine region of Andermatt-Sedrun

Nätschen at approximately 1900 m a.s.l. and one on the Schneehüenerstock at approximately 2600 m a.s.l. Pictures of the three stations and their location in the area Andermatt/Oberalp are shown Figure 12 along with their location.

The time traces in Figure 13 show the climate and the measured moisture contents at all three reference locations. The climate data shows that the temperatures are below zero for a large part of the winter period, up to four months in total. Since measurement of moisture content with electrical resistance methods is not recommended under these conditions, see also Section 2.2, only values measured trough sorption method are plotted.

The climate at the Andermatt and Nätschen station appears to be relatively constant throughout the year with temperatures from -10 ˚C up to 20 ˚C and a relative humidity from 50 to 85 %RH. At the Schnee-hüenerstock the temperature is between -20 ˚C to 10 ˚C, but relative humidity shows nearly the double range reaching from 30 %RH up to high values of 98 %RH. The high and low values concentrate in a short period from autumn to winter. In the spring and summer time the amplitudes are more moderate.

The moisture contents via the sorption method are measured at 30 mm depth. Throughout the year, the average moisture contents in all three structures lie around 15 M%. The moisture content variation at the Schneehüenerstock is smaller than that observed in Andermatt and Nätschen.

In addition to the comparisons between the different stations, also comparisons between two instru-mented locations at the stations itself are made. The following two comparison are made at the station of Andermatt with (1) the reference location and (2) instrumented location near a large opening oriented eastward. The second comparison is made at the station of Nätschen where the moisture content at the reference locations is compared to the moisture content measured on a beam that penetrates the façade. The end grain of this beam is protected by a board that prevents the direct impact of rain. The comparison is made in Figure 14 where the measured envelopes of the extra locations of interest is plotted in green. The figure shows that the moisture contents at the two locations is lower than at the reference locations. The higher ventilation is a possible cause of the lower moisture contents.
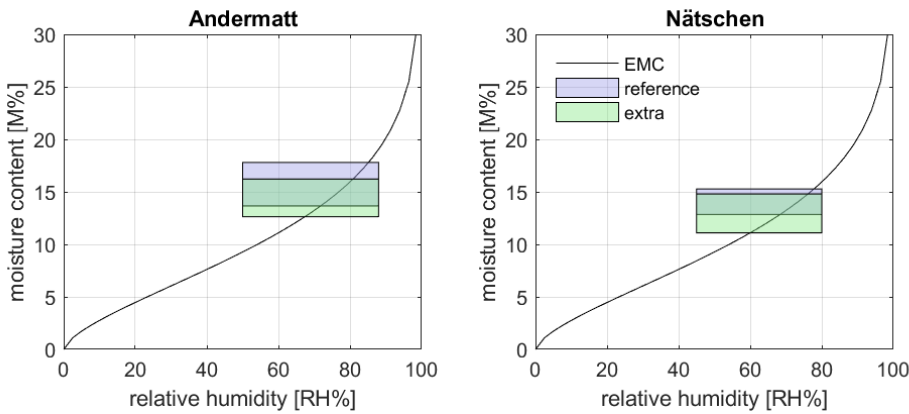
Figure 14: Comparison of moisture contents measured in the between the reference location and extra location of interest in the cable car station of Andermatt and Nätschen.
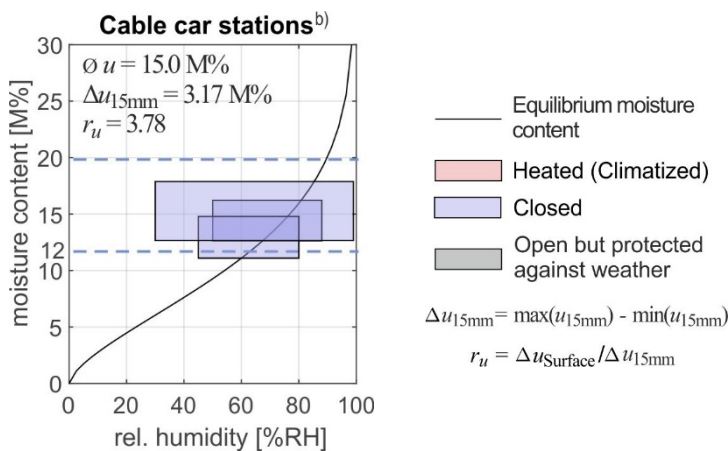

Figure 15: Envelope of moisture content vs. relative humidity measured at the monitored cable car stations of Andermatt-Sedrun

The envelopes of the moisture content and relative humidity are shown in Figure 15 for all three cable car stations. These represent moisture content variations at 15 mm depth and were scaled using principles described in Section 3.2.1. Each box represents one cable car station. Cable car stations should be assigned to service class 2. The average moisture content is 15 M% with a delta Δu_{15mm} of 3.17 M%.

3.4   Riding hall

In addition to riding halls observed and published in south Germany a new riding rink erected in Einsiedeln was instrumented. Riding rinks are often considered to be damper than other ventilated buildings because the sand in which the horses train is artificially wetted to prevent dust formation. Secondly, Einsiedeln is one of the damper regions in Switzerland according to the meteorological data gathered at the weather station. About 45% of the days between 2014 and 2018 had an average relative humidity of 90 %RH and higher, shown in Appendix A.2.1. The riding hall and its location are shown in Figure 16. The timber structure is a frame with trussed beams. Along the entire length of the building, right under the windows, a gap of several centimetres facilitated the ventilation of the inner space. One main load bearing member in the rear end of the hall was instrumented. One position close to a window and the other one more to the middle of the hall. More details are found in Appendix A.2.2.

The temperature inside the riding hall was continuously above 20 °C during the summer period, see Figure 17. The upper left figure shows a comparison of the measured temperature with the temperature recorded by the weather station. An average difference of almost 4 °C between the two values was calculated. The upper right figure shows that the relative humidity measured at the weather station was about 12 % higher on average throughout the year than the relative humidity measured in the riding hall. This is caused by the temperature difference between the riding hall and the weather station. The lower two figures show the measured moisture contents obtained through electrical resistance and sorption method. The equilibrium moisture content is plotted as well.

Moisture content in the first year of instrumentation does not exceed the 16 M% to 17 M%. The moisture contents measured through the sorption method are higher than those measured through the electrical resistance method. This is not necessarily observed in other instrumented buildings, see also Section 3.6, and remains open for further research. Analysis included possible temperature differences (material and air) and measured relative humidities (sorption method and air). It is also possible that the conversion curves, such as discussed in Section 2.2 do not overlap. The comparison of the envelopes of the riding halls published and observed show a close range with an average value of 15.4 M% and a delta of ± 4.44 M%, as shown in Figure 18.

Figure 16: View of the inside of the riding hall and the location of the riding hall within Einsiedeln
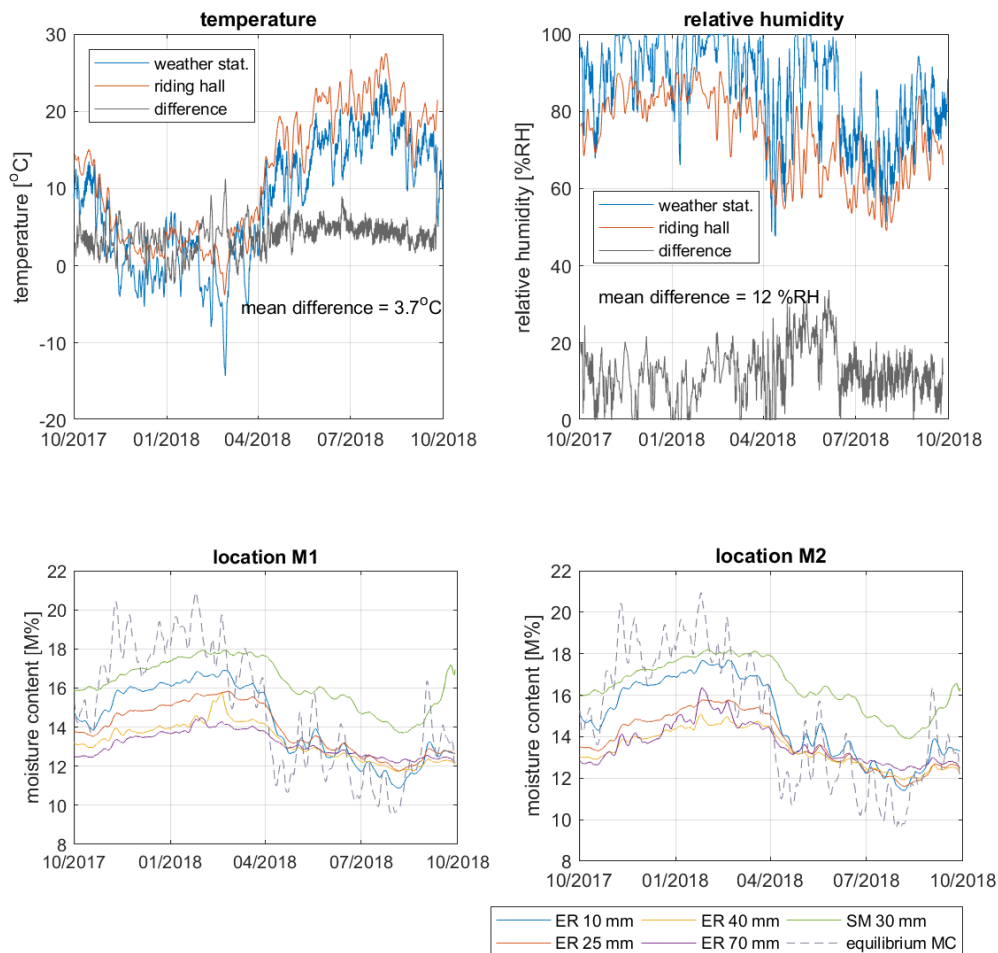
Figure 17: Moisture content monitoring in the riding hall in Einsiedeln close to the glass façade and more towards midspan in the riding hall of Einsiedeln using the electrical resistance (ER) at different depths and the sorption method (SM)
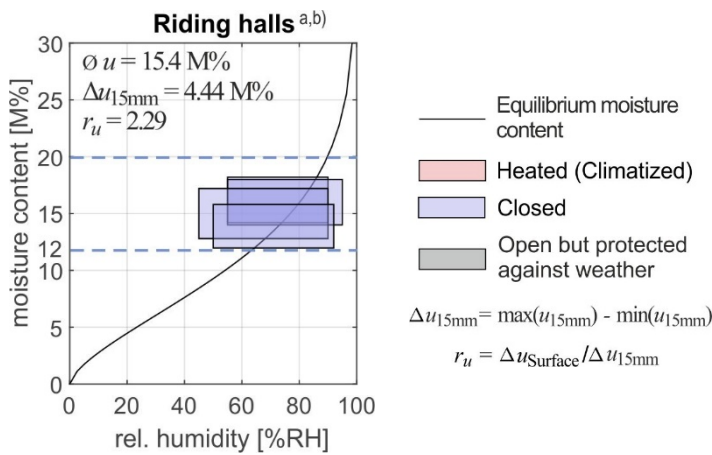
Figure 18: Envelope of moisture content for riding halls

3.5 Ice rinks

3.5.1 Open ice rinks

Two partially open ice rinks of Delémont and Le Locle were instrumented in the Jura mountains of Switzerland, shown in Figure 19. The years of construction are 2011 and 2004, respectively. The objective is to investigate the impact of the surrounding meteorological climate, user profile, and environmental on the moisture content of the timber structure. The frame structure with truss member is nearly identical of both open ice rinks. The ice rink of Delémont is located on a lower altitude of 440 m a.s.l. than the one of Le Locle, at an altitude of 1000 m a.s.l.

Figure 19: Pictures of the outside and inside of the ice rinks of Delémont (upper left) and Le Locle (upper right) (sources unknown) and pictures of the interiors of the Delémont ice rink with the ice formation on the downward facing surfaces of the load bearing members (bottom right)

The meteorological data over 2014 until 2018 shows that the Delémont (DLM) region suffers relative humidities of 90 %RH or more for about 44 % of the days per year. The higher region Le Locle, station L achauds-de Fonds (CDF), only 30 % of the days per year, see Figure 20. Le Locle experiences 10 % more sunshine duration than Delémont. The temperature difference between the two locations is related to the difference in altitude, i.e. -6°C per 1000 m increase in altitude.

The beams were instrumented at the edges of the ice surface. Instrumentation over the ice surface was not possible due to accessibility during installation time. Future instrumentations are however recommended over the ice surface. The difficulty is though that although the moisture contents above the ice are higher than around the it, reliability is lower as moisture content measurements are likely made below or around zero. This means that the electrical resistance method is not recommended. The sorption method would be the most accurate method. Both methods were applied in the instrumentation of the closed ice rink of Davos discussed in the next section, where the ice rink was instrumented during construction.

During visits of the ice rinks of Delémont and Le Locle, traces of water are however clearly visible on the structure and roof. In autumn and winter, ice formation on the bottom side of the load bearing members was observed, as well as decolouration of the lower one or two lamellas of beams in the trusses. The situation could unfortunately not be inspected closely but can be seen Figure 19 bottom right. Apart from the ice formation, the ice rink's personnel also mentioned occasional fog formation inside the ice rink on otherwise clear days. In Delémont an extra ventilator was used to in these cases to improve ventilation throughout the structure. Traces of fungi or decay are not observed in either structure suggesting that the annual variation of climate also provides sufficient drying capacity throughout the rest of the year.
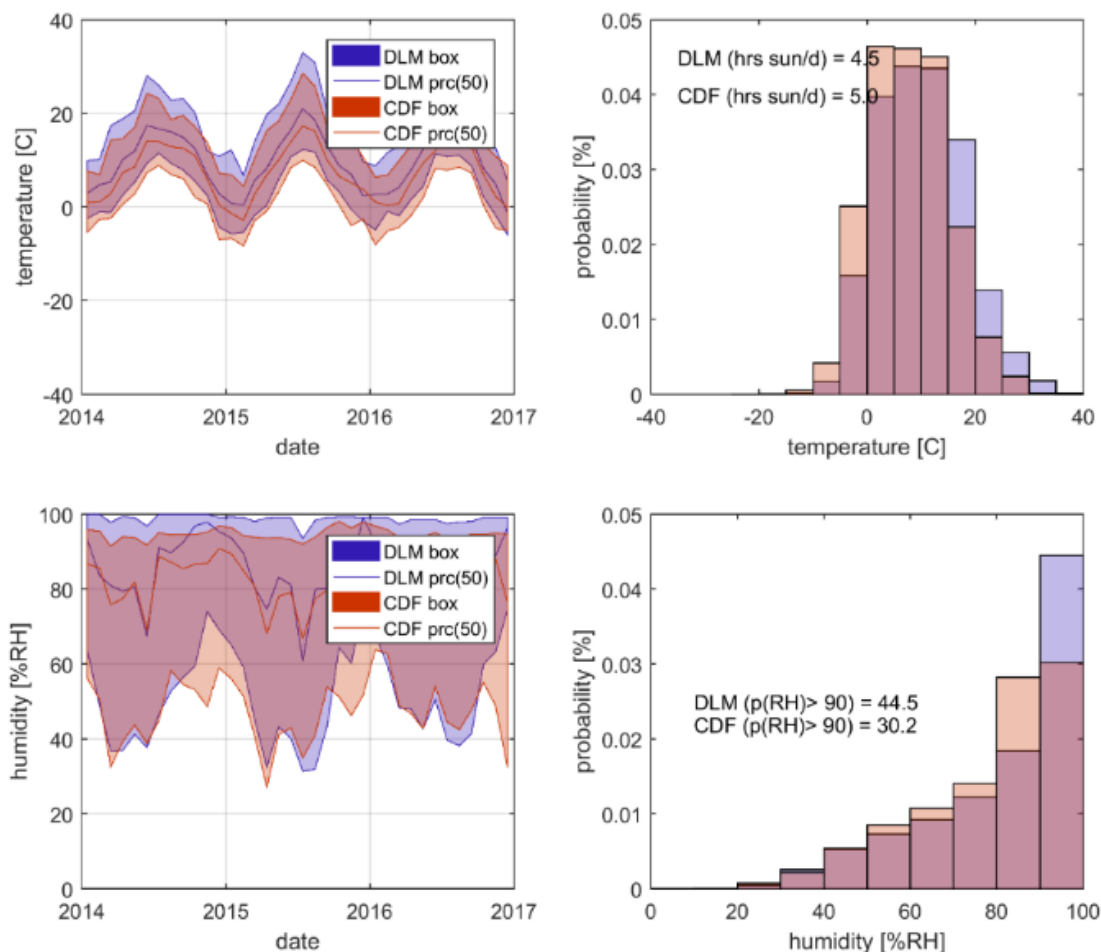
Figure 20: Comparison of meteorological data of stations Delémont DLM, 439 m a.s.l. (left) and La Chaux-de-Fonds CDF, 1017 m a.s.l. (right) for the last three years
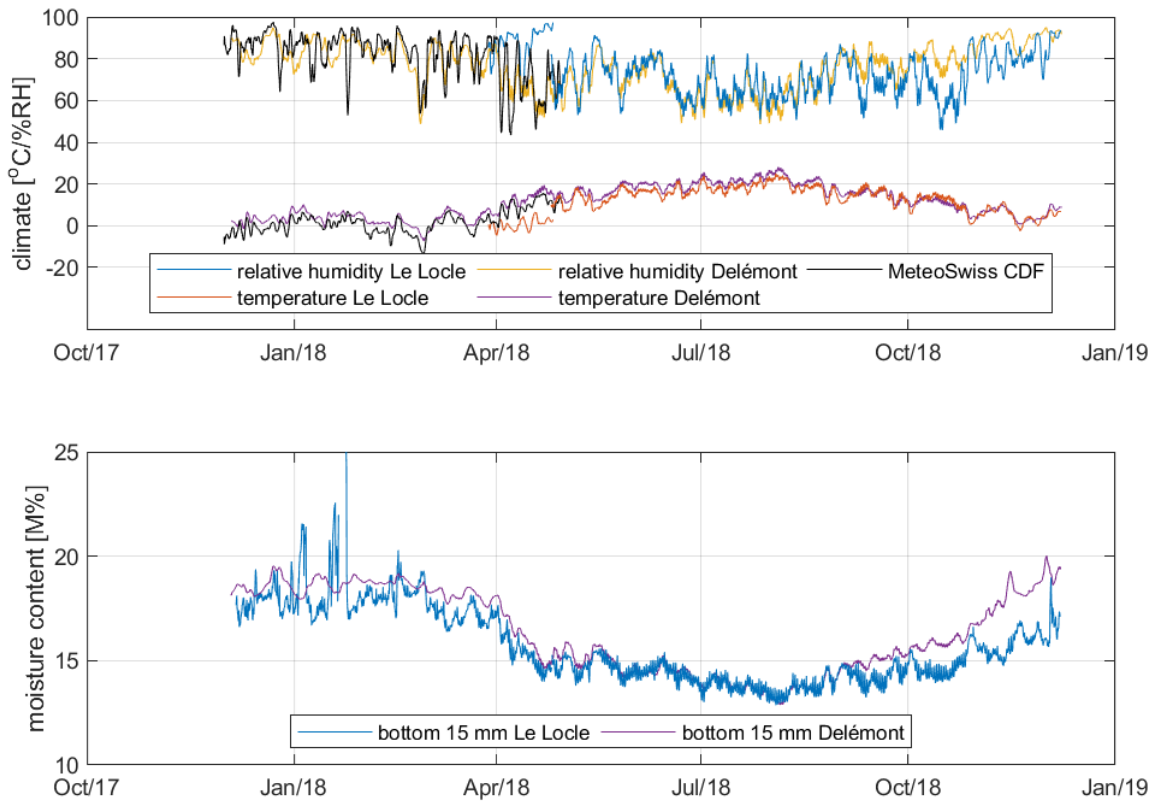
Figure 21: Measured climates and moisture contents on the bottom faces of the load bearing beams in the ice rinks of Le Locle and Delémont

Time traces of measured climates and moisture contents on the bottom faces of the load bearing beams are plotted in Figure 21. The climate at the ice rink of Le Locle is replaced with climate from the meteorological station of La Chaux-de-Fonds for the first period due to a malfunctioning climate logger. This data is visualized through a black continuous line. Whereas the measured moisture content at the ice rink of Le Locle showed some peaks suggesting condensate building during the winter months, the data of the ice rink in Delémont does not show this. On the other hand, the moisture contents in the ice rink of Delémont increase more rapidly in the autumn than the moisture contents in the ice rink of Delémont.

Whether measurements can directly be compared is difficult to say. The measurements in the ice rink of Le Locle were made on one of the edge beams and not in the centre of the ice rink like was done in Delémont. Both beams span over the ice surface though.

3.5.2 Closed Ice rink

A new ice rink in Davos was instrumented upon request of the timber construction company and the and responsible structural engineer. The ice rink was intended for training purposes of the local team. Inside the training facility, a gallery above a part of the ice surface was constructed that was intended as a fitness area, i.e. heated area. Concerns about high moisture contents around the supporting beams of this gallery were part of the reason for a monitoring campaign. A dehumidifier was installed to control high relative humidities occur in the hall.

The ice rink was instrumented with the wireless equipment offered by Omnisense. Eight *S2*-sensors were installed, each equipped with two relative humidity sensors and a wood moisture content sensor. One relative humidity sensor was used to monitor the climate at the beam's surface and the other to monitor the climate in a cavity. Moisture contents obtained through the electrical resistance method and the climate measurements could be compared directly. The obtained moisture contents were modified such that they would match those obtained by the Scanntronik equipment, see also Section 2.2.

Figure 22: View of the outside and inside of the ice rink during construction

A summary of the measured climate and moisture contents are observed in Figure 23. The figure shows the differences between the temperatures and relative humidities of the ice rink and fitness facility on the gallery. The moisture contents of the structure located above the ice is around 12 M% to 13 M%, except for the gage located above the tribune. The moisture content measured in the heated fitness facility reduces significantly. The development of moisture content in the load bearing member supporting the gallery seems to be little reason for concern (bottom plot) as moisture contents are between 9 M% and 12 M%. Two sensors temporarily malfunctioning due to a disconnected cable.
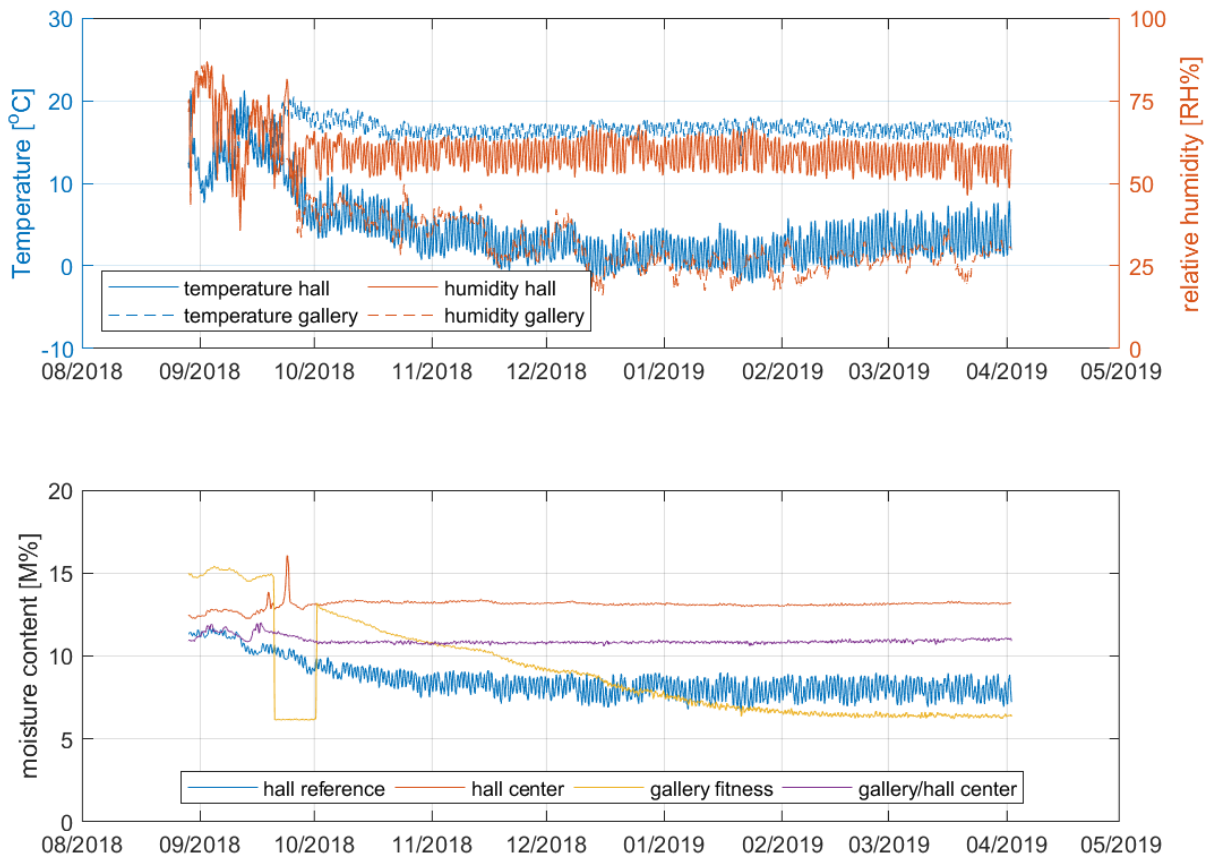
Figure 23: Summary of the measured climate and moisture content (depth of 15 mm) in the training facility of the Davos ice hockey club
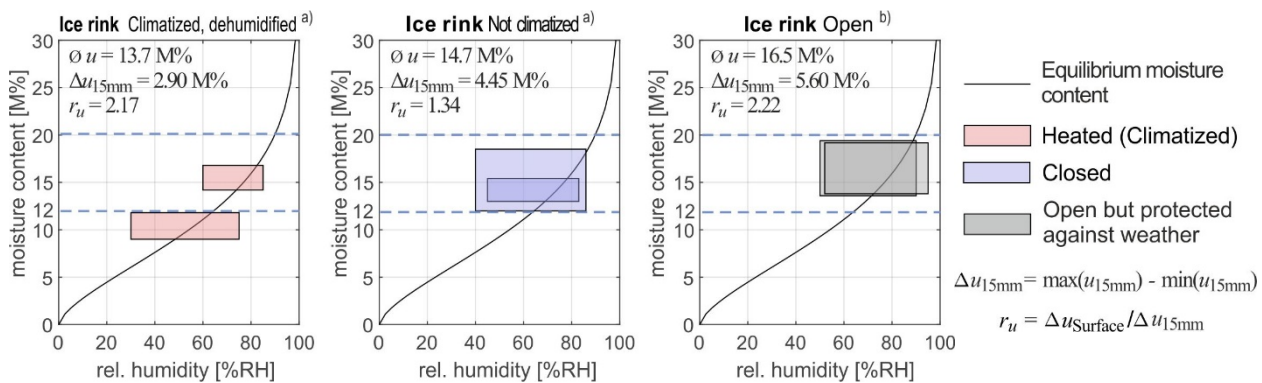
Figure 24: Envelopes of the moisture content for ice rinks, distinguished after operating service and construction type

3.5.3 Summary of ice rinks

The measured values observed in the ice rinks are compared with values published (Gamper et al. (2014)). The ice rinks were distinguished after closed and heated, closed and not climatized, and open. The range of the moisture content shows, that ice rink mainly could be assigned to Service Class 2 but open ice rinks should be considered as in Service Class 3. If ice rinks are heated and controlled dehumidified it is possible to reach moisture content values below 12 M% and Service Class 1 could be applied. It is however noted that the open ice rinks experience the highest average moisture contents as well as the highest variations. It is noted that the moisture content between the surface and the 15 mm depth reaches the 22.6 M% if the average moisture content $\emptyset u$ is added to the variation Δu_{15mm} times the ratio r_u divided by two, see also Section 3.2.1.

Data of the ice rink in Davos was not included since the obtained data did not span a year yet. It would however be included as a heated/climatized ice rink and the obtained envelopes would be plot in the left diagram.

3.6 Measured moisture contents throughout the depth from the surface

Moisture content measurements were obtained at different depths from the surface to measure the effect on depth on the moisture content variations. This is interesting in newly erected structures, where timber elements were produced at an average of 12 M%. The moisture content on the outer surfaces will quickly adjust to the surrounding climatic conditions. However, the inner parts of the cross-sections will react far slower and moisture content will not adjust as fast. This process is observed in Figure 25 where moisture content variations of the monitored buildings in Einsiedeln, Andermatt and Nätschen are shown. The theoretical equilibrium moisture content at the surface, along with the moisture content that was measured at different depths is plotted. Both the results with the electrical resistance and the sorption methods can be compared.

Some care must be taken using the moisture contents measured in Andermatt and Nätschen as these were measured close to, or around freezing temperatures. As the peaks were omitted though it is expected that the plotted moisture contents are representative enough. Temperatures at the station of Schneehüenerstock were lower and electrical resistance measurements are more unreliable. The figure shows though that the average moisture contents at the inner parts of the cross-sections are lower than at the surface. As measurements are continued, it will be interesting to see if how quickly the annual equilibrium is achieved.
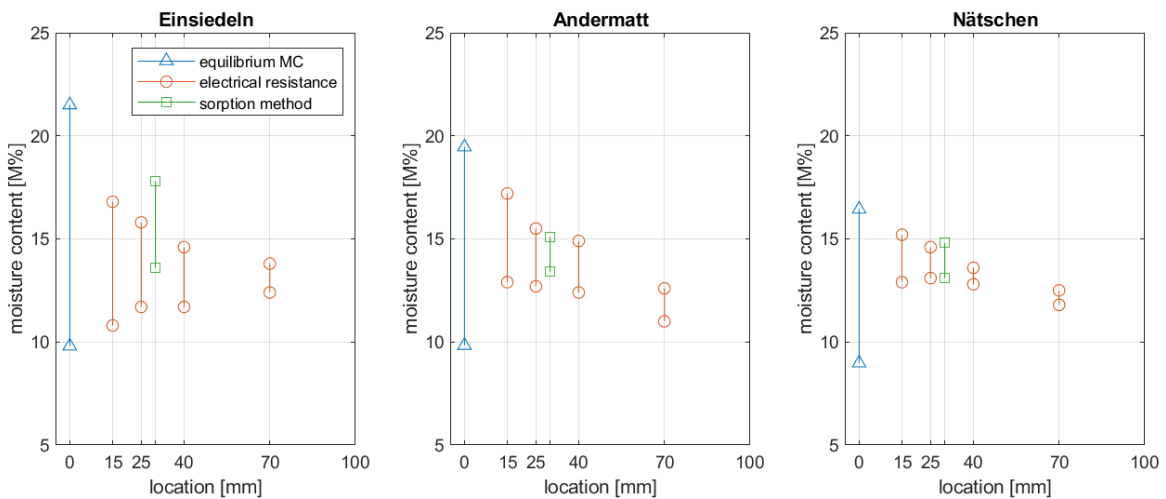
Figure 25: Moisture content measurements at different depths from the surface and different methods

3.7 Elephant house

The Elephant house in the zoo of Zürich was erected in 2014 and has a timber roof as free form shell with a diameter of 85 meters, as shown in Figure 26. Moisture content is monitored in 14 locations in the roof by the facility management of the zoo. The moisture content measurements are performed using the humimeter by Schaller GmbH. It is a sensor that is constantly connected to a power source and makes measurements using 15 V to 29 V. The measurement range is 9 M% to 150 M% wood moisture content.

The moisture contents shown in Figure 27 span measurements made from September 2014 to June 2017. This is compared to a theoretical equilibrium moisture content that was calculated using data from the climate loggers in the building. It should be noted that this sensor was in a different layer of the building skin than the moisture content sensors, data is not therefore not directly comparable. It is also noted that the moisture content sensors indicate a moisture content below their measuring range. This was verified with the manufacturer but as far as known the wood seems to be very dry in the roof. The fact that the measured moisture contents are out of range of the sensor also could indicate the real moisture content is even lower than the plotted values. A reference measurement or visual inspection was not made. The measured moisture content was this low since the installation of the equipment which is also a suspicious. This would indicate that the building material itself is already delivered in this very dry state.

The difference between the reference climate and the measured moisture content is expected to be due to the layup of the building skin and the presence of the glass roofing. This positively affects the drying behaviour. As the moisture content sensors are between the relative humidity sensor just below the roof, moisture content would be expected to be between a theoretical moisture content calculated between inside and outside climate.
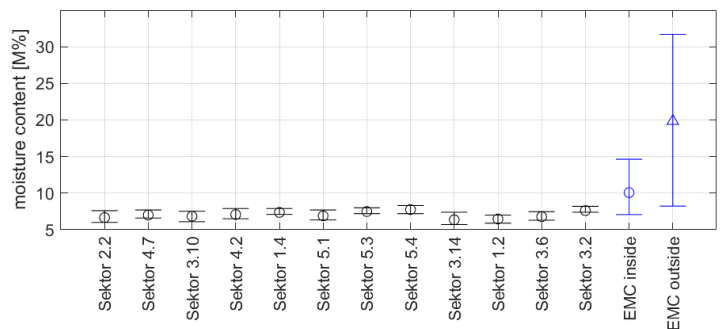
Figure 26: Inside of the elephant house at zoo Zurich, Source: https://www.waltgalmarini.ch/portfolio/elefantenanlage-zoo-zuerich/ (13.02.2019)

Figure 27: Monitoring the moisture content and climate of elephant house at zoo Zurich

3.8   House of Natural Resources Hönggerberg Campus ETH Zurich

The House of Natural Resources (HoNR) is found on the Hönggerberg Campus of the ETH Zürich. It is an office building of three floors erected as a post-tensioned timber frame with composite slabs. The main load bearing structure consists of beech instead of spruce or other softwood. The moisture content was measured in the building envelope and in a floor of beech CLT by ETH Zürich. Figure 28 shows the results for a period of autumn 2015 until summer 2017. The moisture contents within the structure are lower than those measured in the building skin. Although beech and spruce are compared (CLT versus façade), this is supported by difference in relative humidity measured inside the building and at the façades.

The moisture contents in the façade concerns moisture contents measured in spruce. The moisture contents measured in ash are not plot. Figure 28 also shows the envelopes of the measured moisture contents versus the measured relative humidity in the façade. The variations in moisture content are limited as the measurements were made at a depth of 50 - 60 mm from the surface.

The envelopes were determined using data of 2016 only. The time traces show that there is however a blind spot. It is however not known whether this data contains extreme values.
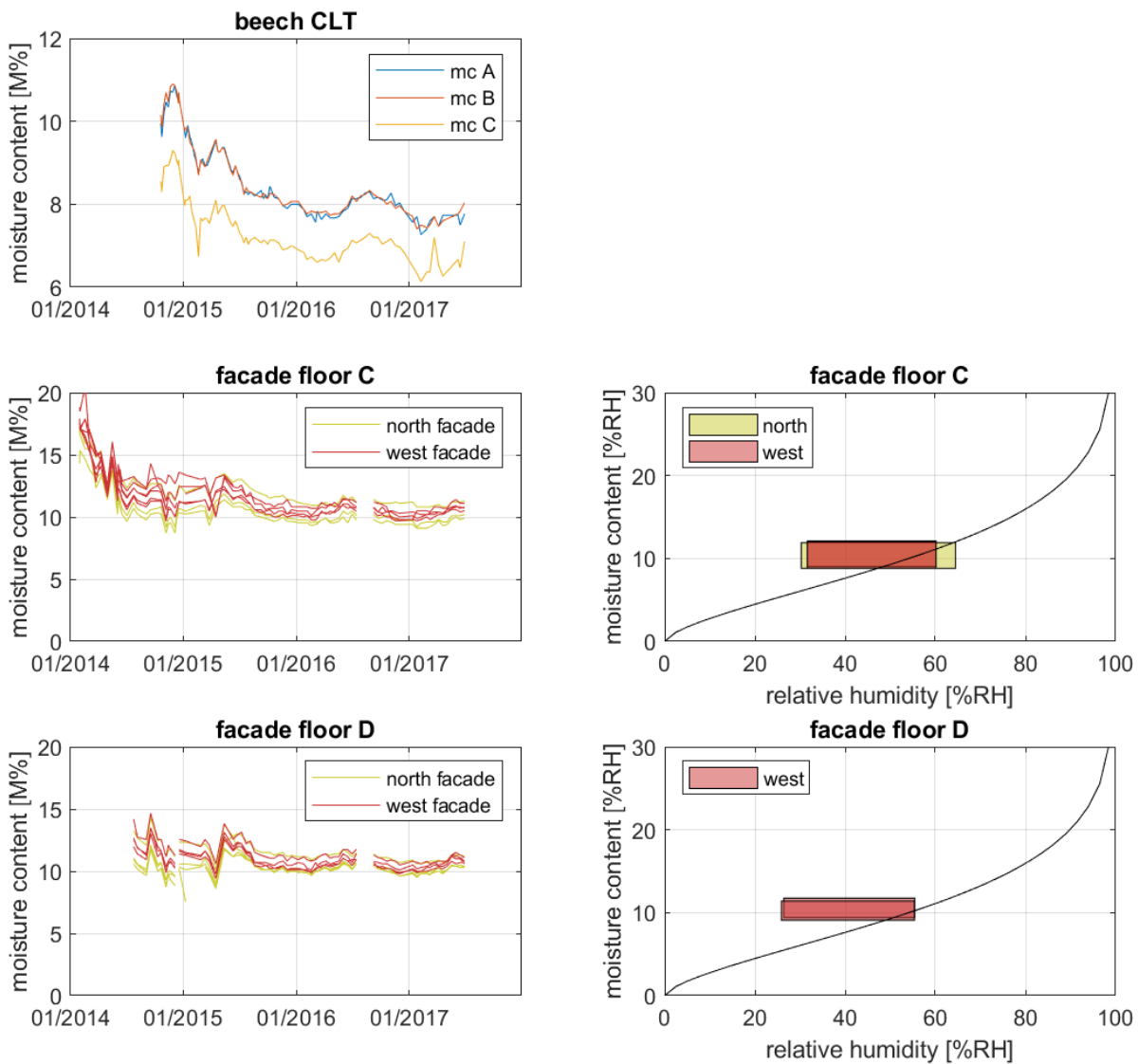
Figure 28: Monitoring results of the moisture content at House of Natural Resources, moisture content (left) and envelope curves for two sensors for west side and one sensor for north side (right)

3.9 Summary of typical climates in and around timber structures

In summary, all monitored and analysed objects from literature are plotted in envelope curves of the moisture content, as shown in Figure 29 and described in Chapter 3.2.1. In addition to the curves, the average values and the deltas at a measuring depth of 15 mm are included. Each box in the diagram represents one monitoring object in Switzerland or Southern Germany (Gamper et al. (2014)). The following observations concerning these structures are made. These concern the observations in the monitored data and exceptions are possible:

- Swimming pools: the measured climate contained several blind spots, but graphs with moisture content show stable conditions in general. The climate in the monitored structures was regulated.
- Sports halls: Relative humidities and corresponding moisture contents are low to very low. Moisture contents might be a little higher than that observed in the production halls. Moisture contents are lowest in winter and increase towards the summer time.
- Production halls: Moisture content and climate profiles are like that of the sports halls. Climates might be dryer though. Here too, moisture contents in winter time are lower than in summer time.
- Ice rinks: Two ice rinks were heated/climatized, two had a closed building envelope (not heated or climatized) and two were well ventilated. Moisture contents in the climatized ice rinks are generally lower than in the ventilated structures. In general, the high relative humidities in the closed and ventilated ice rinks that are generated during autumn and beginning of the spring time. Periods with building of condensate were omitted from the data analysis.
- Riding rinks: Although the structures are closed, large variations in climate are observed. Climate in the building presumably follows the climate around the building to a large extent meaning that moisture contents in winter are higher than in summer time.
- Livestock halls: The agricultural buildings contain livestock and were often well ventilated through one side of the building being fully open. Yiang et al. (2017) conducted an extensive monitoring campaign in these building types, particularly focused on the risk of wood decay. High moisture load is caused by cleaning (with water) that is required regularly. It is also argued that the evaporation of sweat and breathing of the livestock contributes to the high relative humidities encountered in the structures.
- Storage halls: The storage halls contained a closed building envelope, but through which smaller doors or windows ventilation was possible. These structures contain the lowest moisture contents of all the ventilated structures.
- The instrumented ski stations in the alps show moderate moisture content and climate envelopes throughout the year. One of these stations shows high variation in surrounding climate, but as these peaks are only of short duration they do not lead to high moisture content variation throughout the year. The station is located just behind a mountain ridge between the northern pre-alps and the inner alps.
- Envelopes of moisture content and climate around the bridges is plot in the last diagram. Moisture content measurements were made in eight bridges, but as some measurements were made deep into the timber material, it was not possible to extrapolate measurements made there to moisture contents at 15 mm depth. This extrapolation is only possible up to depths of 50 mm. More analysis of climate around bridges and the moisture contents is made later in Chapter 4.

The figure also shows that, assuming glulam would be produced between 12 M% and 15 M%, that it would dry for use within heated structures and moisten for use in ventilated structures. Moisture content variations in heated structures are small than those in ventilated structures.

The lowest moisture contents in ventilated structures are observed in the storage halls. Within the heated structures these are seen in the production halls. Although no data on heated structures in mountainous regions has been obtained yet, it is expected that this can be quite low as temperature differences with outside climate are larger than in low areas, leading to very low relative humidities.
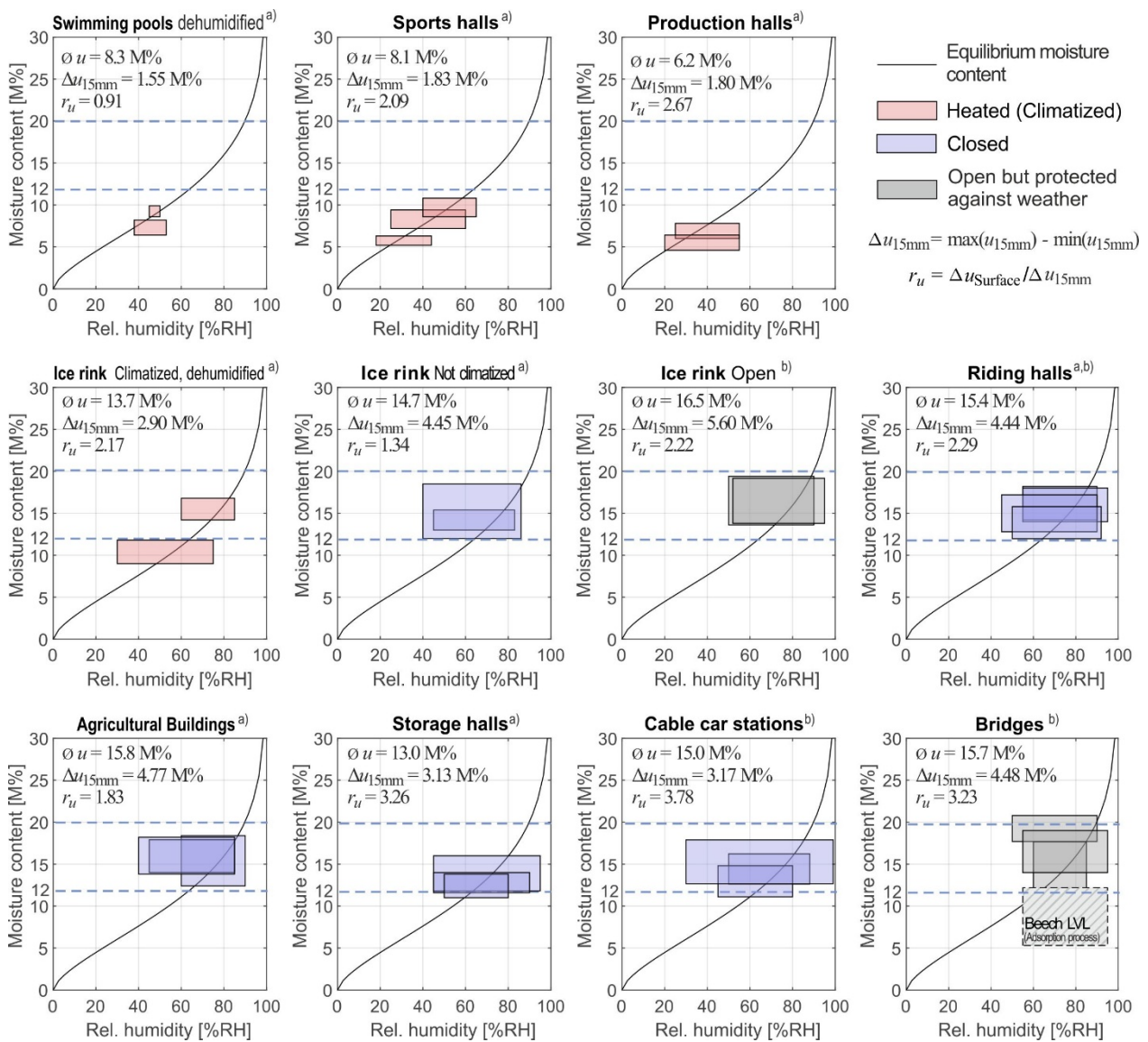
Figure 29: Overview of relation between the envelopes of measured relative humidity and measured moisture content at 15 mm depth from the surface

4 Timber Bridges

4.1 General

Timber bridges have a long tradition, but they are underrepresented for modern bridge constructions. An extensive report on timber bridges in especially Switzerland is found in "Timber Bridges, potential and limits" published by the Bachofer and Cozett (2013). The document contains statistical information on where bridges can be found throughout the country. A total of 340 timber bridges throughout Switzerland was inventoried in detail in their year of construction from 1300 to 2010. From 1900 onwards, timber bridges in Switzerland were built especially between 1930 and 1950, a total of 35, and from 1980 to 2010 with a total of 36, 47, 49 in the last three decennia. Building timber bridges again is popular since 1980. The increase in number of erected timber bridges between 1930 and 1950 is explained by financial crisis and wars limiting the import of raw material like steel.

Bridges without a roof structure to provide protection of constructive details, are first built in the 1960s. Between 2000 and 2010, 49 of 66 timber bridges were built without a roof. The protection of constructive details was performed through the road deck. Since the 1960s, two new types of load bearing structures were introduced into the design of timber bridges. Apart from the used truss and strutted systems, arch bridges and large beams were introduced as a main load bearing system. The latter two load bearing systems are more common now than the more traditional ones.

Most bridges are built for pedestrian traffic or cyclists. The difference in number of bridges that was built for single lane road traffic is small. The number of two-lane bridges being built grows gradually to a total of 18 between 2000 and 2010. Since 1970, the total number of bridges with a span lower than 10 m is 9%, between 10 m and 20 m is 24%, between 20 m and 30 m 39%, between 30 m and 40 m 25%, and longer than 40 m is 3%.

Authorities and planning engineers still pose questions regarding the impact of the climate, the changes of dimensions due to shrinkage and swelling, quality assurance, long-term behaviour, durability and maintenance. For sustainable and durable timber buildings, it is mandatory to consider the impact of the moisture content.

Table 4: Overview of timber bridges analyzed

Bridge/Erection	Characteristics	Measuring period	
Horen 2008	31.0 m long, beam bridge, Block-glued Spruce Glulam	since Oct 2009	Switzerland
Muotathal 2009	33.4 m long arch bridge, Block-glued Spruce Glulam	Oct 2009 - Dec 2011	Switzerland
Obermatt 2007-2008	32.0 m long, beam bridge, Spruce Glulam	Dec 2010 - 2014	Switzerland
Schachenhaus 2000	20.4 m long, timber-concrete composite bridge	Mar 2011- 2013	Switzerland
Bubenei 1988	45 m long, arch bridge, Spruce Glulam, Deck of cross pre-stressed glulam	since Jul 2012	Switzerland
Andelfingen 1814/2018	71 m long, covered bridge, reinforced with LVL from beech	since Aug 2017	Switzerland
Hoengesberg 2014	66.5 m long bridge with three spans, middle span is an arch, Spruce Glulam	since Aug 2015	Germany
Schwäbisch Gmünd 2012	25.3 m long, timber-concrete composite bridge, slow traffic bridge, spruce Glulam	since Oct 2016	Germany
Werdau 2011	15.4 m long, spruce Glulam	since Oct 2016	Germany
Evenstad bridge 1996	180 m long, with 5 arches a 36 m, traffic bridge	since Winter 2000	Norway
Daleråsen 2001	68.9 m, arch structure	since July 2001	Norway
Flisa 2003	196.3 m long with three spans, truss system	since 2003	Norway
Klemetsund 2005	87 m with seven spans	since August 2005	Norway
Måsør 2005	82.5 m, largest span with 50.1 m as arch structure	since Sept. 2005	Norway

During this project, long-term monitoring data observed or published at selected timber bridges were used to analyse the effect of regional climate and microclimate effects on timber moisture content. The investigation focuses on the moisture gradient that develops over the total cross-section under daily changes of the climate.

The local climate and moisture content could be monitored on seven timber road bridges in Switzerland. Some monitoring campaigns were initiated in previous research projects and were extended in this project. One reinforced historic timber bridge in Andelfingen could be newly instrumented. The bridge is reinforced with laminated beech veneer, which is a relative modern wood product. The material is especially used in heated structures which are generally dry, see Figure 29. Little experience on the long-term reaction to moisture content variations experienced in Service Class 2 has been gained yet. Additional monitoring data could be used from three timber bridges within a monitoring campaign in Germany at FH Erfurt, project "Protected Timber Bridges", and five timber Bridges monitored by the Norwegian Public Road authority. Table 4 gives an overview of the timber bridges considered, the detailed information is summarized in Appendix A.5 to A.14.

4.2   Reinforced bridge Andelfingen

The existing and covered 200-year-old bridge crossing the river Thur in Andelfingen was repaired and reinforced during the spring of 2018. Four new beech laminated veneer frames were installed (one at the north entrance, two in the middle at the central support, and one at the southern entrance) of which the most northern one was instrumented with electrodes. The frame was coated after the construction work to delay moisture content variations. The bridge and the instrumented corner are observed in Figure 30. The beech veneer frames are coated with a green colour. Along with the instrumentation of the frames also two separate uncoated blocks were instrumented to capture the extremes and possibly deinstall one and investigate in more detail in the laboratory. The instrumentation allows comparison of coated and uncoated load-bearing members. The frame was instrumented with four pairs of electrodes, two in upper beam and two in a column, and two per block located on the eastern side of the bridge.

A summary of the time traces of the measured climate and moisture contents are seen in Figure 31. The instrumentation was performed in the beginning of June 2018. A malfunctioning Gigamodul was replaced two weeks after initial instrumentation. The moisture content at instrumentation is very low due to the low moisture content, around 7 M%, the beech veneer is usually delivered in. During autumn, moisture contents increase faster in the uncoated block members than in the coated load bearing members. Note that the moisture content measurements on the load bearing members were made in longitudinal direction to the grain, those on the uncoated blocks transverse to the grain. The corresponding equations are developed in Section 2.2.8.

Figure 30: Bridge crossing the Thur in the village of Andelfingen with a view on the instrumentation and two dummy blocks on the north side of the bridge
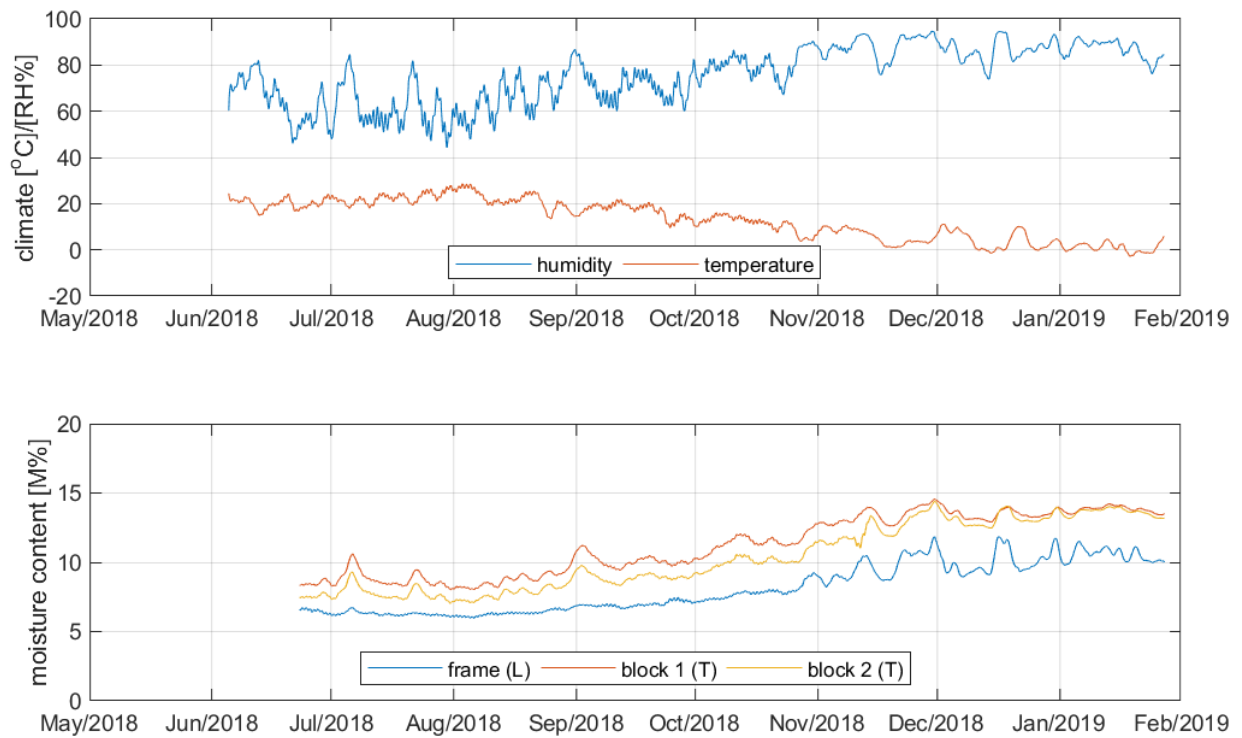
Figure 31: Climate and moisture content measurements made on the bridge of Andelfingen (L: longitudinal and T: transverse)

4.3   Bridge Bubenei

The bridge Bubenei is in the Emme valley (Emmental) between Eggiswil and Schüppach. The bridge has a span of 45 meters and was designed for traffic loads up to 40 tons, see Figure 32. The main load bearing system consists of two arches. During inspection, high moisture contents were observed in the west side of the bridge. Excessive wetting through a leak in the asphalt surfacing was believed to be the cause of this defect. The asphalt surfacing was replaced halfway 2012. A monitoring system was installed to observe the drying behaviour of the timber. Currently, dry wood is only found at sensor 1.3 for instance (west). The east side of the bridge is dry which is observed in the lower diagram. As a reference, average moisture contents at this bridge will later be taken 16.5 M% and 18 M% obtained from the east side of the bridge. The median moisture content at this location was at 17.7 M%. More time traces of the moisture contents are observed in the Appendix A.6.

Figure 32: Picture of the Bubenei bridge from the east side bank (Eggiswil side)

Figure 33: Picture of the Obermatt Bridge (upstream)
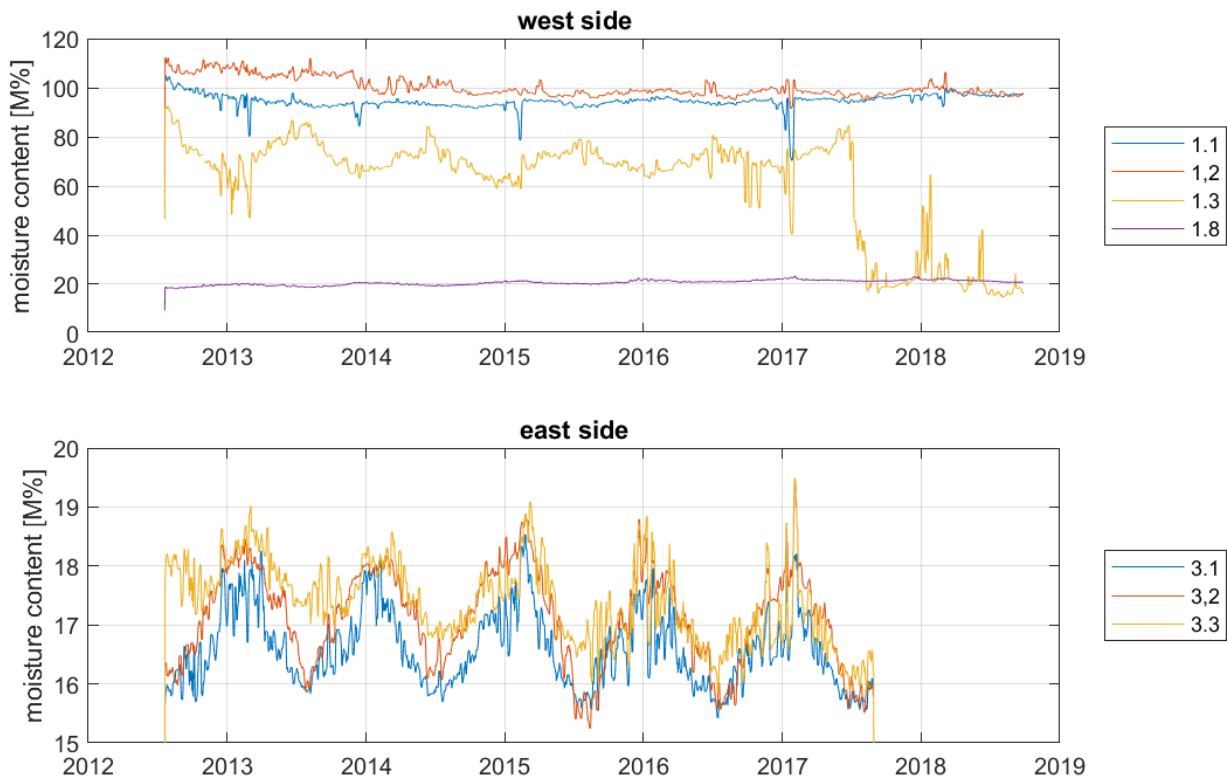
Figure 34: A summary of the moisture content measurements made on the Bubenei bridge

4.4   Bridge Obermatt

The bridge Obermatt is in the Emme valley (Emmental) as well, at couple of kilometres distance from the bridge Bubenei. The bridge has a span of 32 meters and was designed for traffic loads up to 40 tons, Figure 33. The main load bearing system consist of two beams.

Figure 35 shows the moisture content measurements made throughout the span of four of the total of about eight years. Measurements were not made for two years, but instrumentation was not completely removed. The figure shows how moisture content monitoring can assist in the early detection of leakage in the asphalt surfacing. The leakages could be forwarded to the owner/authorities and maintenance programmes were started before major damages occurs.

The bottom figure shows the measurements made in spruce where no high variations in moisture contents were found. Here, yearly average moisture contents between 13 M% and 19 M% were measured. The median of all average moisture contents was at 16.5 M% and the peak is found at 17.5 M%. More time-traces can be found in Appendix A.7.

4.5   Measurements of moisture contents at selected German and Norwegian bridges

The University of Applied Sciences in Erfurt is monitoring seven timber structures, see Koch et al. (2017). The moisture content of three of these bridges, the ones of Hoengesberg, Schwäbis Gmünd, and Werdau will be discussed in more detail.

The Hoengesberg bridge spans a total length of 66.5 meters and is suited for general traffic loads. It is a bridge of three sections where the middle span is an arch instrumented with four moisture content sensors. The middle section crosses a river while the outer sections span the river beds. Moisture content measurements range between 15 M% and 20 M%. The moisture content measurements made over the river show smaller fluctuations than those at the bridge ends. The latter are however made in the end grain of the load bearing members. The data at these locations also seems to be affected by water condensate (spikes).

Figure 35: A summary of the moisture content measurements made on the Obermatt bridge where a leakage could clearly be detected thanks to the installed monitoring system.

The bridge at Schwäbis Gmünd spans a total distance of 25.3 meters and is designed for pedestrians and cyclists. Four moisture content measurements were made above river bed and four above the water that is crossed. The sensors measured moisture contents at 2 cm, 4 cm, 6 cm, and 8 cm depth from the surface. Means of the moisture contents at the eight locations range from 15.8 M% to 16.8 %. Due perhaps to the small span, differences between the moisture contents measured above land and above the river are not distinguished.

The Werdau bridge spans a length of 15.4 m. Five moisture content measurements are made above land and three above the river. The available monitoring data spans a period of almost two years. The average moisture contents are between 15.7 M% and 17.3 M%, with a median at 16.2 M%. The moisture contents made above river bed are slightly higher than those measured over the river. It should be noted that the averages contain two winters and only one summer (dry period).

The report of Norsk Treteknisk Institut (2013) presents an overview of monitoring data obtained from five timber bridges throughout Norway. Focus of these measurements were tension in the dilatation, tension in the bars of the stress laminated decks, and wood moisture contents in the decks and load bearing members. Moisture content measurements are typically performed with relative humidity and temperature sensors placed inside the wood. Whenever measurements were made in treated timber (creosote), also a dummy block with untreated spruce was installed for comparison. The bridges treated are the Evenstad bridge, the Daleråsen, Flisa, Klemetsund, and the Måsør bridge.

The Evenstad bridge was built in 1996. It contains five arches of 36 meters long spanning a total of 180 meters. The bridge is a one lane bridge designed for full traffic loads. The bridge is located halfway between Oslo and Trondheim. Moisture content was not measured in a dummy element of untreated spruce. Moisture contents in the decks were between 8 M% and 11 M% throughout a monitoring period of more than 10 years. Temperatures below zero are found for extended periods of the year, on average between four to five months.

The Daleråsen bridge was erected in 2001 and spans a length of 68.9 m divided into two nearly equal spans of arched structures. The bridge was designed for full traffic loads for its use by agriculture and forest-related vehicles. Only wood moisture content measurements were made here. The bridge is located close to Oslo. Moisture content in the dummy elements decreased from 14 M% to approximately 10 M% over a period of roughly 12 years.

The Flisa bridge replaced a single lane steel bridge for a two-lane traffic bridge with a sidewalk. The total length of the bridge is 196.3 m, subdivided into three nearly equally divided spans. The load bearing structure is designed as a truss structure. The bridge is located between Oslo and Trondheim. Moisture content in the dummy element was about 15 M% over a period of almost 9 years.

The Klemetsund bridge is a pedestrian bridge with an untreated spruce in the stress laminated decking. A watertight foil was applied on the upper side though to prevent wetting by rain. The bridge spans a total length of 87 m divided into seven smaller spans. Measurement of temperature and relative humidity was made just below the asphalt surfacing, halfway the height of the timber prestressed deck and at the bottom of the timber prestressed deck. Interestingly the moisture contents close to the surface of the asphalt surfacing showed a lower moisture content, around 11 M% to 12 M% and the ones close to the surface moisture contents around 14 M% to 15 M%. This was observed on several locations in the bridge. The extra heat absorbed by the asphalt could help to reduce the moisture contents in the timber.

The Måsør bridge is an 82.5 m bridge with the largest span covered by a 50.1 m long arch structure. The bridge is located north of Trondheim and is designed with two lanes for all traffic. Both the arches and the deck were monitored. Moisture contents in the arches varied around 14 M%. In sensors close to the edge annual variations between 12 M% and 16 M% were observed over the course of six years. Moisture contents in the road deck were around 16 M% but showed less variation as these were also deeper into the material.

From all bridges no significant difference was observed between measurements of humidity and temperature between creosoted elements and untreated elements (dummy elements). Some problems arose sometimes due to condensation for instance. Some sensors also had to be recalibrated after unrealistic measurements were obtained.

Figure 36 shows the location of the bridges from Switzerland, Germany, and Norway listed in Table 4 on maps with average temperature and relative humidity developed by Nikleswki (2018). The measured average moisture contents are plot in Figure 37. Differences in color gradients for temperature are distinguished between northern and central Europe. Regarding the locations of the different bridges as to relative humidity, differences are not easily obtained. Since moisture content is not affected as much by temperature as it is by relative humidity, relation between moisture content and location cannot be drawn (yet). Some areas are more humid or dry than others, but measured data from bridges considered here is not available. As seen in Figure 37 though, average moisture contents measured in Norwegian bridges are lower than those measured in Switzerland and Germany. As the moisture content in the Norwegian timber bridges was also monitored in dummy elements, moisture contents measured in treated elements was omitted from plotted values.
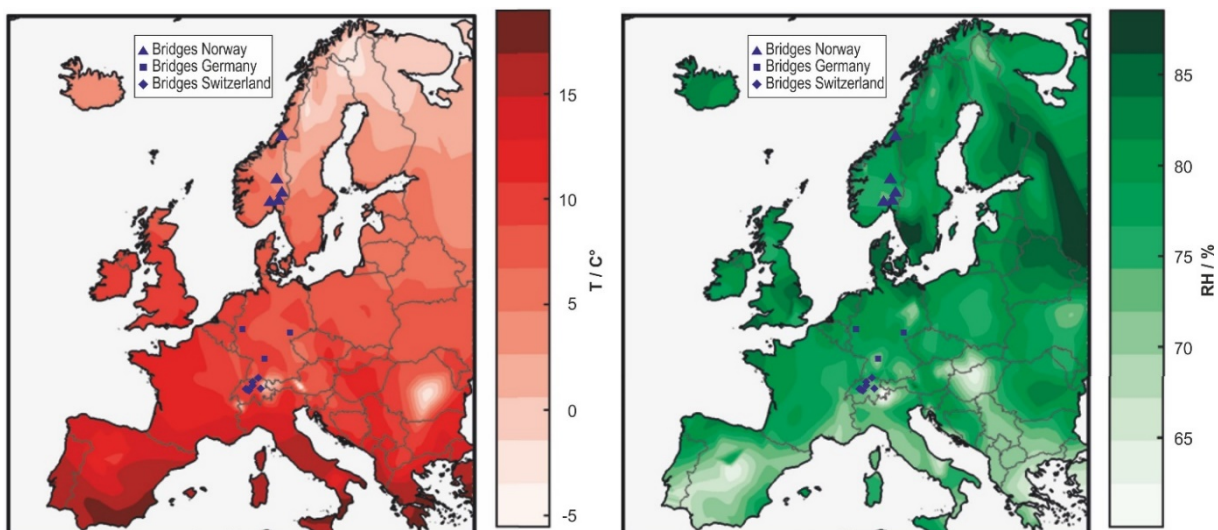
Figure 36: Temperature (left) and relative humidity (right) (Niklewski, 2018) of Europe with the location of monitored bridges listed in Table 4 and plot in Figure 37
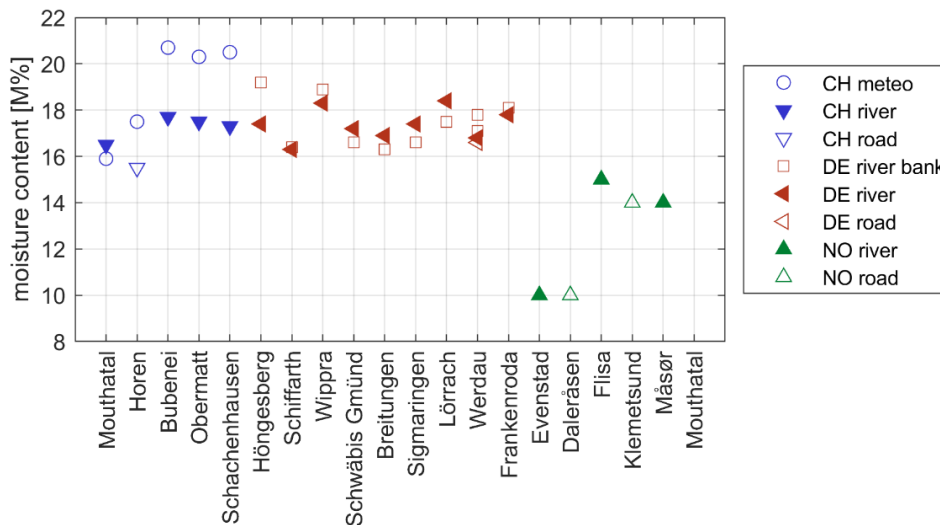
Figure 37: Visualization of measured moisture content in bridges over water and road in Switzerland, Germany, and Norway. Plotted values are averages of available data.

4.6 Summary of average moisture content regarding crossing situation

In summary, the average moisture content of the timber bridge monitoring campaigns was compared among each other and to nearby meteorological weather stations, as shown in Figure 37. Instrumentations generally included monitoring of climate and moisture content and duration stretched over a couple of years. Moisture contents under 20 M% are a measure for the sound state of the timber structure. The doubts were raised as to whether higher moisture contents could be expected above rivers and roads due to the presence of a water body or spray.

In case of the Swiss timber bridges, comparisons with reference climate were made from data obtained from meteorological stations in the objects' vicinities. The moisture contents were calculated using equations for equilibrium moisture content using temperature and relative humidity of Simpson (1973) at regular intervals between 1 and 3 hours. In the case of the German monitoring campaigns, climate around the bridges was measured as reference data, Koch et al. (2017). The Figure 37.shows that moisture contents over 20 M% can generally not be expected. Also, whether the moisture content over water bodies is higher than over roads can also not be distinguished from the data. The Norwegian bridges show the smallest average values. As the Norwegian timber bridges are known to be coated and impregnated, special care was taken to use measurements from uncoated or unimpregnated blocks. It is not clear what the possible cause is of these low average values.

4.7 Recommendations for the planning and design of timber bridges

4.7.1 General recommendations

Building timber bridges is possible thanks to the enormous effort timber industry makes, even of single people, to promote the use of timber for bridges, (Bachofer and Conzett 2013). Planning engineers, architects and authorities rise questions regarding the long-term behaviour and durability of timber bridges. Several points are expected to impact the behaviour of timber bridges and lead to higher moisture content or less durability compared to other construction material like concrete and steel. Municipalities or traffic authorities demand a financial study comparing timber to concrete or steel alternatives. This delays construction and decision processes.

According to the monitoring data, the moisture content does not exceed maximum allowable levels under normal conditions, i.e. 20 M%. However, damages still occur, and proper design remains a challenge. The real benefit of monitoring bridges is the fact that leakages or other reasons for water accumulation can be detected at an early stage. The structures' operational lifetime benefits greatly from these interventions.

Discussions with experts and literature research lead to the following conclusions:

- Building in forest environments does not necessarily mean that average moisture contents in the structure will be higher, however the risk that this occurs is. This is explained by:
  - Vegetation and plants growing around structural details, preventing proper drying after contact with water or high humidity. The drying is accelerated through sufficient ventilation. Care should be taken in the maintenance plan to remove bushes and plants overgrowing structural members or blocking ventilation (Burkhart and Kleppe, 2017).
  - Clogging of drains caused by falling leaves in fall, dirt accumulating, twigs and branches, litter, etc. This should generally be taken well care of according to Bachofer and Conzett (2013), no matter where the bridge is built.
  - Reduced overall ventilation due to sheltering by the forests.
  - And increased presence of fungi or animals attacking the wood.

- Building over rivers does not necessarily result in higher moisture contents than in open land:
  - Rivers could provide increased humidity levels, but the structure often benefits from the increased ventilation around open spots or waterways.
  - Although road bridges or other structures around roads are often at risk due to spray caused by traffic. The impact is questioned as increased temperature and ventilation by the traffic is expected to promote the desorption process. The main challenge in these bridges is to make sure that no standing water accumulates and that details are designed well enough to allow ventilation and water drainage.
  - Snow does little harm because fungi will not grow when it's cold (Burkhart and Kleppe, 2017).
  - Topography influences the microclimate around a bridge, however a higher moisture content over waterbodies or roads cannot be distinguished from measurements Müller et al. (2017) and Koch et al, 2017). Uncertainties in measurements are perhaps too large.

It should be realised that the findings mentioned above only applies to average annual moisture content. Whatever the locations or the effect of the obstacle to overcome has on the amplitude of climatic variations around the bridge is not well understood yet.

4.7.2 Structural details

Timber bridges are customized through the choice of the timber structure, road surface, and wood preservation by gladding's and covers. Design of timber bridges involves personal experience with design of timber bridges, literature, and personal preferences, Bachofer and Conzett (2013). Universities, universities of applied sciences, or research institutes could provide a central role in the general support to designers and planners to continuously improve design of details, methods to protect timber against decay, design and development of new connections and materials, etc. Experiences show that structural details which are planned for Service Class 2 can in practice easily be as in Service Class 3 through missing moisture and rain protection or reduced air circulation. The main risk for timber bridges are draping water and prevention of drying potential. The objectives are durable and protected timber bridges according the definition in EN 1995-2:2004.

Legend
a) Bridge with underlying traffic road
b) Bridge with overhead traffic road
c) Covered bridge
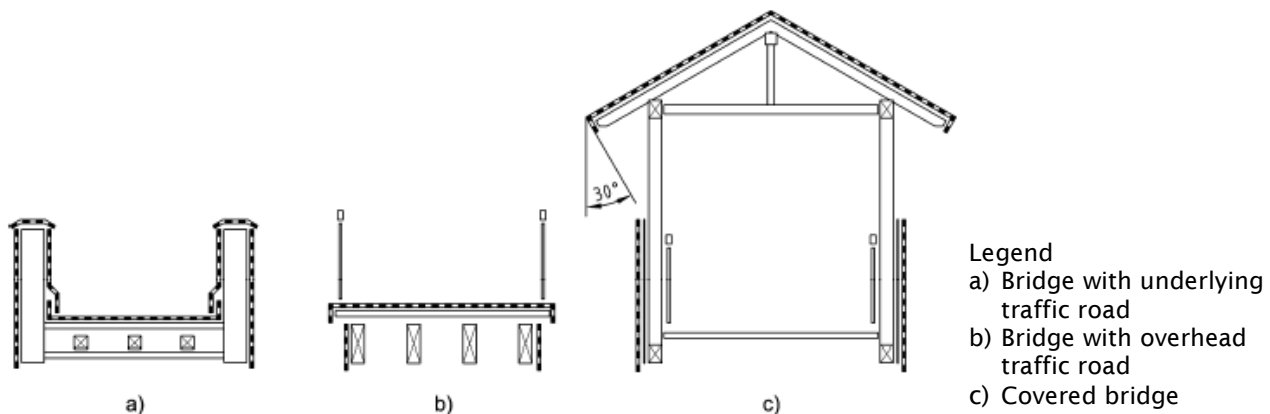
Figure 38: Structural classification of timber bridges, protected bridges according to DIN EN 1995-2/NA:2011

- Protected timber bridges can be assigned in service class 2, Figure 38.
- The bridge expansion joint should be planned as closed.
- The water management (drain systems) is important and needs to be checked after erection and during service.
- Monitoring of the moisture content in hot spots e.g. bridge expansion joint or area wide on the road deck

For the planning of constructive details, the following work can be recommended:

- Bachofner R., Conzett J. (2013) Brücken aus Holz: Möglichkeiten und Grenzen, Forschungsprojekt AGB 2003/012, Bundesamt für Strassen, Schweizerische Eidgenossenschaft
- Seidel A., Keil A., Hafner A., Özdemir Ö., Jacob-Freitag S. (2019) Drüber und drunter – Brücken aus Holz, Qualitätsgemeinschaft Holzbrückenbau e.V., ISSN-Nr. 0466-2114
- Seidel A. et al. (2019) Entwurf von Holzbrücken, holzbau handbuch, Reihe 1, Teil 9, Folge 1, Qualitätsgemeinschaft Holzbrückenbau e.V., ISSN-Nr. 0466-2114
- Seidel A. et al. (2019) Tragwerksplanung von Holzbrücken, holzbau handbuch, Reihe 1, Teil 9, Folge 2, Qualitätsgemeinschaft Holzbrückenbau e.V., ISSN-Nr. 0466-2114
- Simon A., Arndt R., Jahreis M., Koch J. (2019) Musterzeichnungen für Holzbrücken, Qualitätsgemeinschaft Holzbrückenbau e.V., ISSN-Nr. 0466-2114
- Brünninghoff H., Heimeshoff B., Sengler D., Samuel S., Rampf G. (1988) holzbau handbuch, Reihe 1 Entwurf und Konstruktion, Teil 9 Brücken, Folge 1 Planung, Konstruktion, Berechnung, DGfH Innovations und Service GmbH, München
- Augestein M., Dittrich W., Geohl J. (2000) holzbau handbuch, Reihe 1 Entwurf und Konstruktion, Teil 9 Brücken, Folge 2 Details für Holzbrücken, DGfH Innovations und Service GmbH, München
- Qualitätsgemeinschaft Holzbrückenbau e. V. (2006) Detailzeichnungen, https://holzbrueckenbau.com/ wp-content/uploads/QHB_Detailzeichnungen.pdf, 12.12.2018
- Luggin W. F. (2010) Brücken aus Holz – Standardisierte Detaillösungen und Wartung, 1. Internationale Holzbrückentage, Bad Wörishofen
- Schwaner, K. (2004) Schutz und Dauerhaftigkeit von Holzbrücken, 10. Internationales Holzbauforum, Garmisch-Partenkirchen.
- Schickhofer G., Unterwieser H. (2005) Wartungsmanual für Holzbrücken – Ein Leitfaden zur Brückenüberwachung, Technische Universität Graz
- Pousette A, Malo KA, Thelandersson S, Fortino S, Salokangas L, Wacker J (Editors) (2013), Durable Timber Bridges, Final report and guidelines, RISE Research Institutes of Sweden, SP Rapport 2017:25, ISSN 0284-5172, Skellefteå, Sweden

4.7.3 Gladding's and coatings

Applying coatings or sealing systems do (strongly) reduce the moisture content variations in the timber members. However, they increase the risk of moisture entrapment and increase the maintenance costs if damage occurs. Traditionally timber structures which are exposed to weather are protected by structural elements e.g. claddings or effective overhang against driving rain, compare Figure 39.

- Claddings can be very beneficial in the protection of main structural members, however the effects on moisture content are not quantified. They prevent direct impact of rain but also prevent faster drying by reducing ventilation and protection from sunlight. The claddings are often sacrificial and need to be replaced occasionally.
- During design of protective layers, robustness of each of these layers should be considered. One single layer is sufficient if the layers are robust, but multiple layers should be applied when the individual layers are weak (Burkhart and Kleppe, 2017).
- Driving rain needs to be considered carefully in design of details (Burkhart and Kleppe, 2017).
- Leaching of surplus material quantity is a problem. Louvers can help in this protection but need to be properly designed. Properly designed cladding should also be sufficient. Note that it is okay if these protective measures need to be replaced occasionally.

- Coating like applied in some Scandinavian countries can block moisture transport around the surface of the structure, but as mentioned can also prevent drying and cause accumulation of moisture in the structure. This is often not easily observed during inspections as the wood is not visible. Coating can reduce extremes in moisture in timber elements, but can also increase surface temperatures, which can go up to 70 ˚C when dark coatings are used (Pousette et al., 2013). Coatings on well protected elements needs to be maintained every 25 years.
- Impregnations like performed in Norway, with creosote or copper-based fluids, increase the hydrophobicity of the structure and or protect the timber from biological attacks. This has a potential toxic impact on the environment of the structure as well but reduces maintenance costs and increases the structures' operational life (Burkhart and Kleppe, 2017). The reduction of moisture induced cracking will also have appositive effect on the durability of the structure. Tall oil is currently considered an alternative to the creosote impregnation, Pousette et al. (2017).

Figure 39: Bridge Neumatt with protected truss system using gladding (left) and Bridge Horen with weather protection by structural overhang

4.7.4 Connections

No standardized recommendations are given on the design and performance of connections under moisture induced stresses. For connections in timber bridges the following aspect should be considered:

- Consideration of corrosion assurance in connections with mechanical fasteners.
- Control of the maximum size of timber connections, which is not limited in European standards. This can lead especially in shear connections with slotted in steel plates to high moisture induced stresses and exceeds of timber strengths. The application of reinforcements in these connections could help, but research on this topic is still needed.
- The choice of material should be closely considered when possible so that durability of connections is increased. Condensation grows on cold surfaces (Burkhart and Kleppe, 2017). This can prevent needless accumulation of moisture of increased humidity around the connections. Choice of material could also involve choice of more resistant wood type for details with higher risk of decay.
- Ventilation should be considered for all details, especially the important ones. Considerations are to include enough space to prevent capillary flow, include dripping rims, etc. as stressed by both Burkhart and Kleppe (2017) and Bachofer and Conzett (2013). Once details are also easily accessible or enough space around them is provided, these can easily be cleaned and inspected if necessary.
- Key points are the anchorage points of prestressed decks and the connections of kerb and crash barrier.
- Asphalt sealing systems on timber decks should be made according to SN 640451.
- To reduce openings and the impact of water closed bridge expansion joints should be used.
- The use of homogeneous material in the connections is recommended.

Bachofer and Conzett (2013) mention that sufficient experience is available designing load bearing structures up to 50 m. Beyond this, perhaps new concepts of how to build sufficiently large timber cross-sections needs to be gained. Too little knowledge is available on how response to torsion loads or reaction to moisture content distributions is. Production and transport of these large cross-sections needs to be investigated as well.

The longest span of the two-lane traffic Bridge Flisa is 70 m and is set up as a truss. The splices and connections consist of slotted in steel plates and dowels. The DuraTB project (Pousette et al., 2017) investigated the possibility to build longer bridges as massive arch bridges or network arch bridges where the cable arrangement supporting the road deck deserves special attention. Normally, cables would be oriented vertically but here cables are to be shaped like spokes of a bicycle wheel, see Figure 40. In this way, bending loads on the arches are reduced and convert any type of traffic load into a compression load in the timber arch.
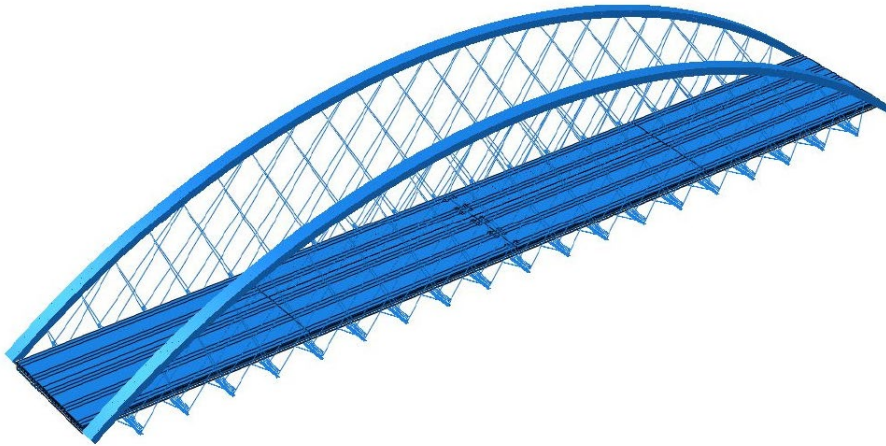
Figure 40: Structural model of a study for a 111 m massive arch bridge with a spoked cable configuration for the road deck (Pousette et al. 2017)

5   Analyses of Meteorological Data

5.1   Climate and moisture content regions in Switzerland

The question is regularly asked whether there are any areas with high risk of elevated moisture content levels in Switzerland. As far as known problems with moisture content have not developed yet in the alpine region, generally known for its dryer climate. To investigate this in more detail measured data was downloaded from the data portal of MeteoSwiss website Idaweb. The daily averages were downloaded over a span of 30 years, from 1 January 1980 to 31 December 2009. This period was selected as the climatic averages are generally calculated over 30 years. The averages are updated now every 10 years. Temperature and relative humidity at 2 m above the grown were downloaded for a target of 110 meteorological stations. Data was not available for 30 years on all these stations.

Swiss climate is affected by the presence of the Alps, the Atlantic Ocean, and Mediterranean climate. Within the Alps, dry climates are found, and arctic temperatures can be reached in winter time. The central plateau is at an altitude of roughly 500 m above sea level, is mild and affected more by prevailing currents from the westerly and northerly direction. It is also a region that is known for a cloudy overcast in autumn and winter. Most areas in Switzerland, including the Jura mountain ridge, have plenty of rainfall throughout the year. The alps act as a climate barrier and therefore the south is affected more by the Mediterranean Sea, with milder winters (MeteoSchweiz[3], 2018).

Maps with design snow and wind loads per area are available in the SIA 265:2012. Note is made that equilibrium moisture contents in the pre-Alpine region (north of the Alps) and the Jura are higher. Within the Alps itself, equilibrium moisture contents are to be assumed lower than normal. How much higher and lower this is and if this should affect the design, is not mentioned. It does mention that the designing engineer should consider local effects.

The Köppen and Geiger maps described in Kottek et al. (2006) offer a classification of climates. General application of these maps is for instance in agriculture or medicine. A set of climates is defined based on temperature and rainfall per region. Detailed distributions can be found within this classification, but at least three climates are distinguished in Switzerland: (1) Cfb: warm temperate, fully humid, warm summer, (2) Dfc: snow, fully humid, cool summer, and (3) ET: polar tundra. The latter two are found in the Alpine region. In Austria four climates are found with an additional variation of the second climate class, indicating hot instead of warm summer. Germany is practically covered by only the first climate. The Köppen-Geiger classification indicates that separate climates can be found, but whether it can be used to appropriately predict expected moisture content in timber structures is to be better investigated.

Theoretical equilibrium moisture content was calculated for 262 locations in the US and 122 locations across the globe in Simpson (1998). The purpose of these calculations was to know what the moisture content of timber could be if it was stored outside. The theoretical equilibrium moisture content was calculated per month using relative humidity and temperature. Autumn is the wettest period and spring is the driest. However, further analyses use monthly data, these are representative for the seasonal trends. The calculated monthly average moisture contents for Geneva, Bern, and Zurich are shown in Table 5. Little difference between these is found. These cities are all located in the central plateau. The moisture content was calculated using the Simpson (1973) equation using the relative humidity over ice. The relative humidity data on the Idaweb data portal is offered often as relative humidity over super cooled water. This is however not always the case. All stations were checked and if needed there were converted to the relative humidity over ice. However, some instrumentation was changed over the course of the 30 downloaded years meaning that it is well possible that erroneous data was used in the calculations. Using the relative humidity over ice however should result in conservative values.

Table 5: Theoretical equilibrium moisture contents (M%) per month in three different cities (Simpson, 1998)

[M%]	March	June	September	December
Geneva	13.0	12.0	13.7	16.3
Bern	13.7	12.5	14.1	18.3
Zurich	13.0	13.1	14.9	18.3

For Switzerland we applied the biogeographical regions for assessment of the meteorological climate impact on timber structures. Switzerland can be distinguished in six different regions according to the meteorological climate, as shown in Figure 41. Figure 42 shows the topographical map of Switzerland where the meteorological stations marked again. This impact of the altitude is analysed in Chapter 5.2. The corresponding equilibrium moisture content according the meteorological climate values are plotted as average value in Figure 43 and as possible annual variation in Figure 45. The equilibrium moisture content is calculated according to Simpson (1973). The map of average moisture content shows that in the alpine regions the moisture content is less than the Jura, Central plateaus and Northern alpine regions of Switzerland. These values directly support the advice in SIA 265:2012 p.21 where is written that "The moisture content in Jura and Northern alps a little bit higher and in the alpine region a little bit lesser assumed." However, the map is one first approximation step and local effects on the climate should be considered carefully e.g. shadowing from neighborhood, wind circulation or vegetation. The annual variation represents the average delta between the 95% and 5% quantile of each of the 30 years (1980-2009). The distribution of the annual variation deltas is comparable grouped to the biogeographical zones from Switzerland.
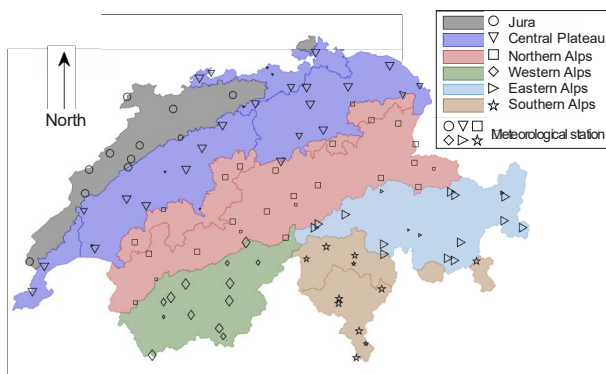
Figure 41: Biogeographical regions of Switzerland including the meteorological stations considered
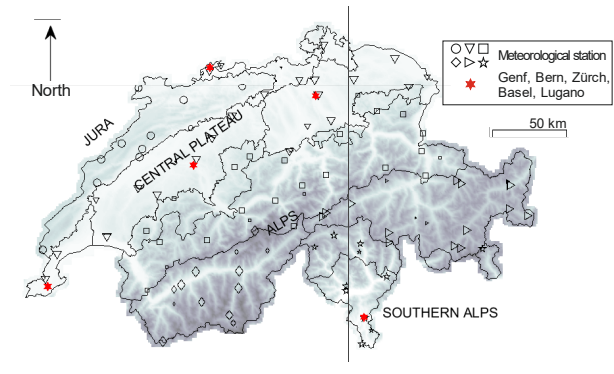
Figure 42: Topographic map including the meteorological stations considered
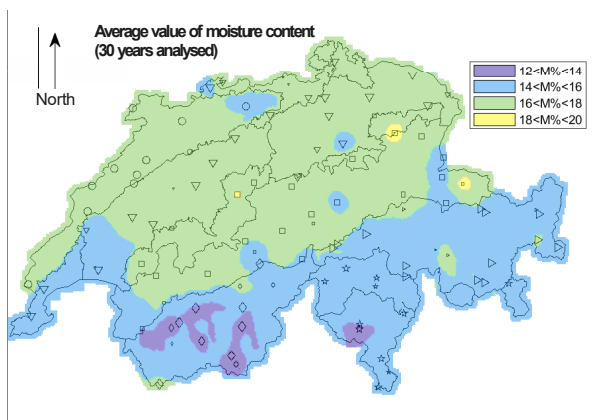
Figure 43: Map of average equilibrium moisture content based on 110 Meteorological station over 30 years (1980-2009)
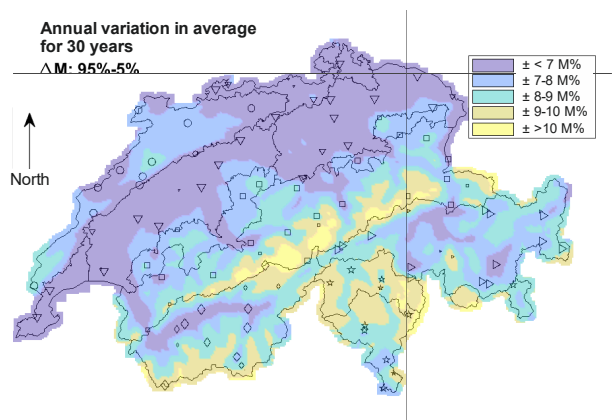
Figure 44: Annual variation of the moisture content in average

5.2 Moisture content dependency on region and altitude

The equilibrium moisture content was analysed according to the impact of the season, location and altitude, as shown in Figure 45. The general conclusions are:

- Over the course of the year, the period between October until March is considered wet in the low areas. There is a negative correlation between moisture content and altitude in this time of the year. During summer, moisture contents are equal over all altitudes.
- Moisture contents around 1500 m a.s.l. remain stable throughout the year. Below this level, winters are wetter than summers. This is generally observed in climatic data. Above this level, cold seasons are dryer than warm seasons, the opposite of what is seen in low areas.

When observing the winter period in more detail:

- Average moisture contents in the central Plateau and the Northern Alpine region reach values up to 19 M% to 21 M%. This is slightly higher than the maximum values observed in the Jura mountains which are around 18 M% to 20 M%.
- The three dryer regions could be considered as the Western, Eastern, and Southern Alps. The higher moisture contents in winter are found between 16 M% to 18 M%.

It is important to note that the moisture contents on which these conclusions are based are calculated with Simpon's (1973) equations. The Simpson equation tends to underestimate the moisture content by a couple of percentages as observed in Figure 6. The relative differences should however still be equal.

The conclusion is that especially lower areas in cold periods of the year are likely to experience high moisture contents. Whether the climatic data really covers all wet areas of the country is not guaranteed. Building in timber in the high altitudes does not seem to be a problem. If timber was not already a material
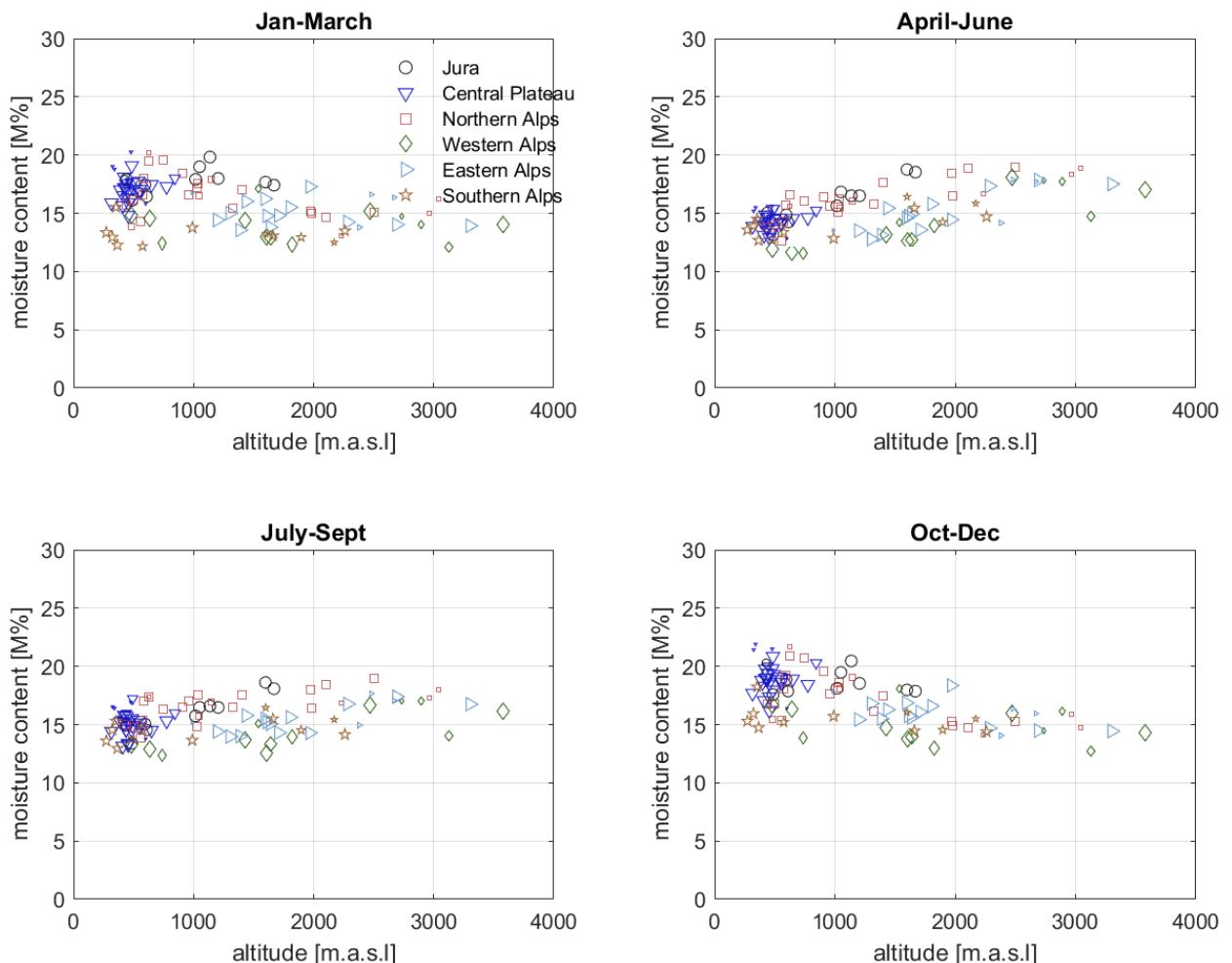
Figure 45: Dependency of moisture content on season, location, and altitude
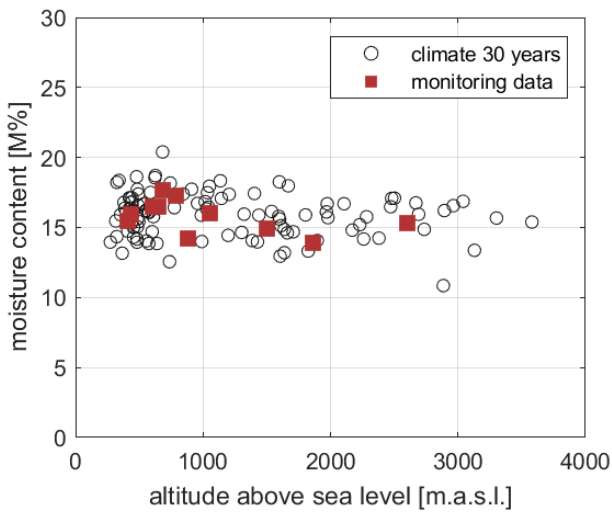
Figure 46: Comparison of theoretical moisture content calculated from meteorological data with the measured average moisture contents in the monitored objects

of choice for difficult reachable areas, this analysis shows that the low relative humidities can be expected too. The fact that moisture content drops in winter also improved performance regarding snow load bearing capacities.

A final comparison is also made where the moisture content of the monitored objects in Chapter 3 is compared to the theoretical moisture content calculated from the meteorological data, see Figure 46. The figure shows that increasing altitude generally reduces moisture content in well ventilated structures.

5.3 Simplification of seasonal climate conditions

For the approximation of the moisture content of timber members and the distribution over the cross-sections or the calculation of moisture induced stresses, a simplified climate model over the year could be applied. Instead of the daily or seasonal changes, a model based on the cosines shape or a simple step model can be applied, as summarized in Table 6. These models will further be used and stated as "Richtklimas". The starting point of these climates are the normal climate condition (20 °C/65 %RH) with an equilibrium moisture content of 12 M% in timber. The mean equilibrium moisture content was set to 9 M% for indoor climates according to Service Class 1 (SC1) and 16 M% for outdoor climates but whether protected according to Service Class 2 (SC2). By using the specified values for the moisture content from chapter 0, variations of $\Delta u_{Fk1} = 1.83 \cdot 2.15 = 3.93$ M% and $\Delta u_{Fk2} = 4.13 \cdot 2.32 = 9.58$ M% could be calculated for sports halls in SC1 and riding rink in SC2 respectively.

5.4 Sample for the approximation of the moisture content during service and erection

The research results to the impact of the user/ambient climate and the meteorological whether on timber structures is used for two case studies a riding ring and a sports hall. First the regulations regarding the SIA 265:2012 are applied by assigning the member first and then applying the service class. Secondly the approximation of the distribution of the moisture content over the cross-section using the service profiles according to chapter 0 and the meteorological weather impact during erection time and start of use according to chapter 5. In both cases the regulation from SIA 265:2012 are confirmed by the new research approach. The new research approach gives further details about the distribution over the cross-section.

Table 6: Models for the simplification of climate impact

Model of change of climate according cosines shape
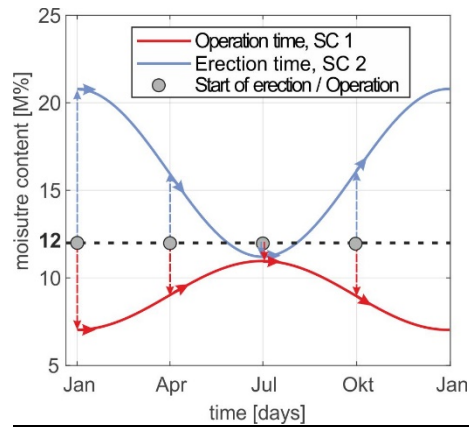
$$u(t)_{SC1} = 9 + \frac{\Delta u_{Surface}}{2} \cos\left(2\pi \frac{t}{365} + \pi\right) \qquad (10)$$

$$u(t)_{SC2} = 16 + \frac{\Delta u_{Surface}}{2} \cos\left(2\pi \frac{t}{365}\right) \qquad (11)$$

where:

$$\Delta u_{Surface} = \Delta u_{15\,mm} \cdot r_u$$

t Time in Days, $t = 0 \,\hat{=}\, 1^{st}$ of January $\qquad (12)$

Model of change of climate according step change
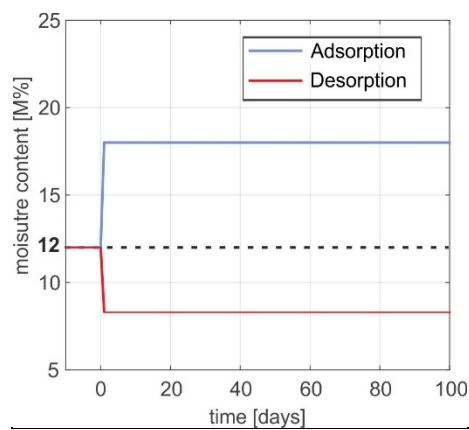
$$u(t \leq 0) = 12\,\text{M\%}$$
$$u(t > 0) = 12\,\text{M\%} + \Delta u \qquad (13)$$

Table 7: Example for approximation of moisture content

Situation	Riding rink located in Basel (closed and unheated)	Sports hall located in Zürich (closed and heated)
According to SIA 265:2012 *Table 2* *Table 3*	Position of the member: $u = 15 \pm 3\,\text{M\%}$ Service class 2: partly protected against whether exposure $u = 12 - 20\,\text{M\%}$	Position of the member: $u = 9 \pm 3\,\text{M\%}$ Service class 1: protected against weather exposure $u \leq 12\,\text{M\%}$
Research approach	Benchmark $u_{15\,\text{mm}} = 15.4 \pm \dfrac{4.44}{2}\,\text{M\%}$ Benchmark $\Delta u_{Surface} = 4.44 \cdot 2.29 = 10.2\,\text{M\%}$	Benchmark $u_{15\,\text{mm}} = 8.1 \pm \dfrac{1.83}{2}\,\text{M\%}$ Benchmark $\Delta u_{Surface} = 1.83 \cdot 2.09 = 3.8\,\text{M\%}$
Location	Region Basel: $14 \leq u \leq 16\,\text{M\%}$, $\Delta u = \pm 7\,\text{M\%}$	Region Zürich: $16 \leq u \leq 18\,\text{M\%}$, $\Delta u = \pm 7\,\text{M\%}$
Begin of service time *Change from 12 M% to u (x M%)*	$u(\text{January } t=0)_{SC2} = 16 + \dfrac{10.2}{2}\cos\left(2\pi\dfrac{0}{365}\right) = 21\,\text{M\%}$ $u(\text{July } t=180)_{SC2} = 16 + \dfrac{10.2}{2}\cos\left(2\pi\dfrac{180}{365}\right) = 11\,\text{M\%}$	$u(\text{January } t=0)_{SC1} = 9 + \dfrac{3.8}{2}\cos\left(2\pi\dfrac{0}{365}+\pi\right) = 7\,\text{M\%}$ $u(\text{July } t=180)_{SC1} = 9 + \dfrac{3.8}{2}\cos\left(2\pi\dfrac{180}{365}+\pi\right) = 11\,\text{M\%}$
Cross-section		
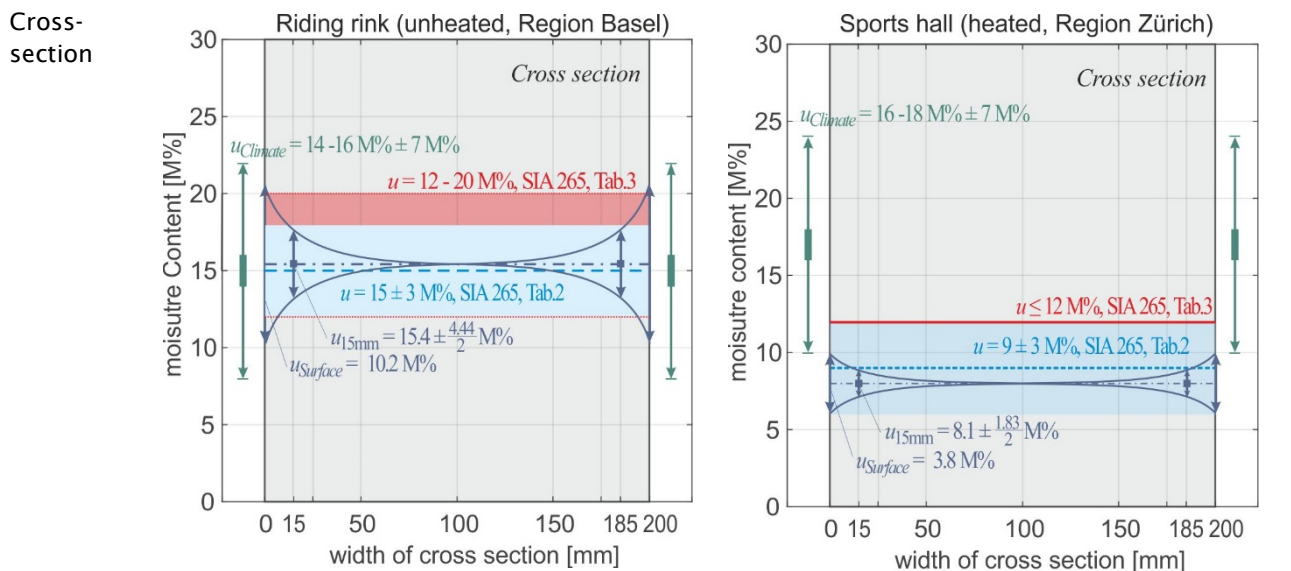
6 Numerical Simulation of Moisture Diffusion and generated Stresses

6.1 Fundamentals

The topic of moisture induced stresses has been on the international research agenda for a couple of decennia. A first overview of work listing findings on this topic is given in the following list:

- Wood drying and shape stability, Ormasson et al. (1999)
- Stability of historic artwork, furniture, and instruments, Kanoopka and Kaliske (2016), Luimes et al. (2016)
- Deformation and fracture in wood-based panels after production, Gereke and Niemz (2010), Hassani et al. (2016)
- Models to simulate moisture content distributions, Siau (1971), Crank (1975), Droin-Josserand et al. (1989), Wadsö (1994), Krabbenhoft und Damkilde (2004), Frandsen et al. (2007)
- Models to simulate moisture induced stresses in glulam members, Ranta-Maunus (1990), Toratti (1992), Hanhijavirni (2000), Angst and Malo (2012), Angst-Nicollier (2012), Hassani (2014)
- Models to simulate crack initiation and growth, Saft and Kaliske (2013), Franke and Quenneville (2011)
- Quality assurance of timber structures, Häglund (2010), Fragiacomo et al. (2011), Müller and Franke (2015)
- Inventories of damaged timber structures, Frese and Blass (2011), Müller and Franke (2015), Dietsch und Winter (2018)
- Experimental monitoring of climate and moisture content in timber structures, Gamper et al. (2012), Dietsch et al. (2015), Franke (2016a)
- Experimental work to determine moisture induced stresses in glued laminated timber, Mohler and Steck (1980), Jönsson (2004), and Angst and Malo (2013)
- Experiments to determine material parameters for moisture transport and moisture induced stresses, Wimmer et al. (2013), Gereke (2009), Olek et al. (2005), Toratti und Svensson (2000), Frandsen et al. (2007)

The variety of topics and the amount of results and insights are large, yet little of these results have found their way to the daily construction practice. It is imagined that this could be due to the complexity of the problem. From all this work though, modelling of the different aspects is schematised into three different steps visualized in Figure 47 (Schiere, 2016). It is suggested that climate and environment precede step 1, and that repair follows step 3.

The purpose of modelling is to isolate effects, investigate sensitivity of results to material parameters, and vary material properties, cross-section dimensions, drying loads etc. within an oversee-able amount of time and costs.

simulation	model	input factors
moisture diffusion	Fickian, non-Fickian, multi Fickian, glue lines, coating	wetting, drying, temperature, relative humidity, transport directions, surface emission factors
stresses and strains	elastic time dependent external loads	hygro-expansion, elastic properties, load duration, mechano-sorptive effects, creep, moisture content dependency
material failure	plastic deformation fracture reinforcement	Specimen size, material strength, loading direction, moisture content dependency, fracture model

Figure 47: Schematic model of modelling moisture induced stresses and following faire of (local) material
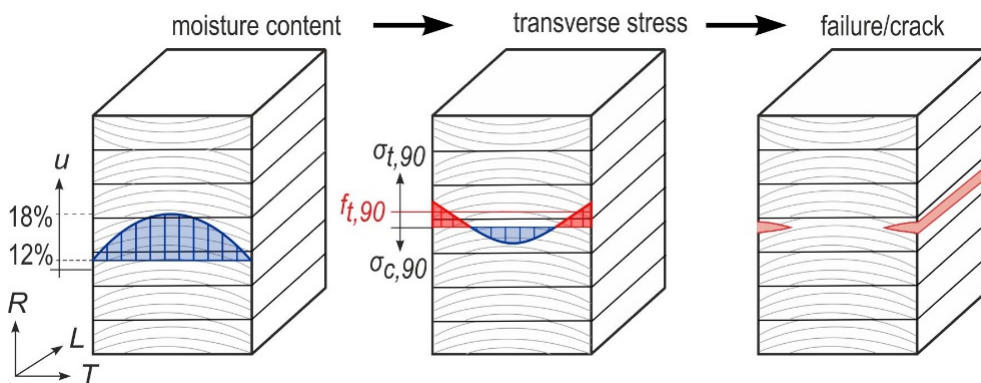
Figure 48: Moisture content and stress distributions in glulam beams during drying processes, tensile stresses at the surface and induced visible crack initiation
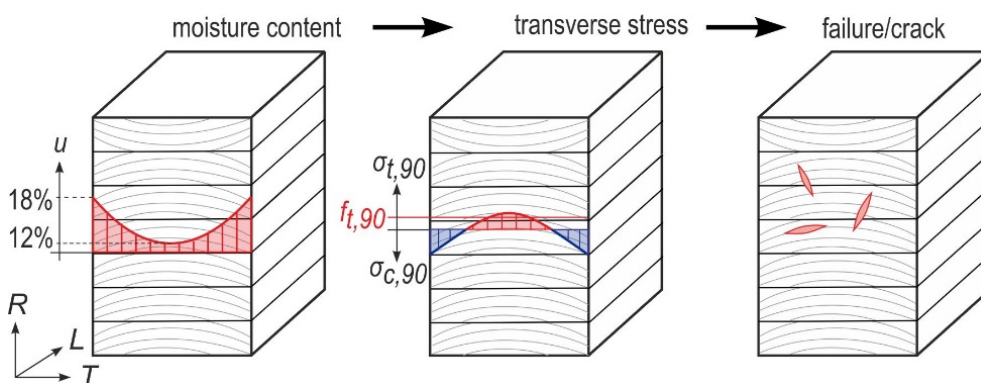
Figure 49: Moisture content and stress distributions in glulam beams during wetting processes, tensile stresses in the midplane and induced invisible crack initiation

Figure 48 and Figure 49 explain the crack initiation and growth due to moisture content variations in the cross-sections. During drying processes, the tensile stresses at the surface of cross-sections induce visible cracks. These can be observed and measured when moisture content at the surface if the cross-section is lower than at the centre of the cross-section. In seasons where the climate is moist compared to the annual average, these cracks will tend to close again.

During wetting processes, tensile stresses develop in the midplane of cross-sections and lead to crack initiation and growth invisible to the eye of the inspector.

6.2   Moisture diffusion

Like observed in moisture content and hysteresis, different models are available to simulate the moisture diffusion in timber cross-sections:

- A single-phase Fickian moisture diffusion model averaging moisture diffusion through cell walls and cell lumens such as explained by Siau (1971) or Cranck (1975) and used by amongst others Droin-Josserand et al. (1989), Fragiacomo et al. (2011), Angst-Nicollier (2012), De Backer et al. (2018).
- A single-phase non-Fickian moisture diffusion model such as described by Wädso (1994) or Krabbenhoft and Damkilde (2004).
- A double-phase Fickian moisture diffusion model, distinguishing the diffusion of moisture through the cell lumen and cell wall, and describing the exchange between the two such as by Frandsen et al. (2007).
- A single- or multi-phase non-Fickian moisture diffusion model including thermal effects: a fully coupled hygro-thermal model such as in Fortino et al. (2013) or Fortino et al. (2016).
- A fully hygro-thermal coupled model with a physical description of hysteresis such as described by Petara et al. (2016).

Modelling of vapour transport through cell walls and lumens is commonly based on Fick's second law for diffusion. As described in Equation (14), the diffusion velocity D gives the relation between moisture content u over time and over space (position in the material).

$$\frac{\partial u}{\partial t} = D \frac{\partial^2 u}{\partial x^2} \tag{14}$$

Previously mentioned diffusion models include either a temperature, moisture, or time dependent diffusion value. Frandsen et al. (2007) separates the moisture diffusion through the cell wall and cell lumen and formulates the amount of condensation and evaporation on the cell wall itself from and to the surrounding air. Instead of using moisture content u, the author uses formulations based on concentration c, both for the vapour in the cell walls and lumens. The exchange of concentration between the two is expressed as $\dot{c}$ in Equation (15).

$$\frac{\partial c_b}{\partial t} = D_b \frac{\partial^2 c_b}{\partial x^2} + \dot{c}$$
$$\frac{\partial c_v}{\partial t} = D_v \frac{\partial^2 c_v}{\partial x^2} - \dot{c} \tag{15}$$

Fortino et al. (2019) added temperature dependent equations to be able to model moisture content fluctuations in environments with fluctuating temperatures. Similar equations have been implemented in programs like WUFI by the German Fraunhofer Institute although differences in implementation will of course result in a spread of results (Krus, 1995 and Künzel, 1995).

6.3   Surface emission coefficient and film resistance of coatings or glue

The surface emission coefficient and film resistances of coatings are related such that they can be integrated into one parameter in the boundary condition of the driving load. Adhesive, like a surface coating between wood and air, tends to delay moisture diffusion between two timber pieces, see Hassani (2014) or Gereke and Niemz (2010).

The surface emission factors are not studied in this report, partly due to the large spread of material properties. Along with this, it is also believed that most structures treated in this report concern structures which are ventilated. This reduces the need to accurately account for a surface emission factor. The film resistance by coatings will affect the wetting and drying behaviour of timber, see Fortino et al. (2016) or Rugenstein (2017), but this is not considered in detail either in this report.

6.4   Stress and strain developments generated by moisture variations

The stress-strain relations to calculate deformations and generated stresses are continuously studied, amongst others in the studies listed in Section 6.1. Of interest are the generated stresses perpendicular to the grain, primarily due to the high hygro-expansion factors and the low tensile strength perpendicular to the grain. The general stress-strain relation used to calculate the generated moisture induced stresses is formulated as follows:

$$\dot{\varepsilon}_T = \dot{\varepsilon}_E + \dot{\varepsilon}_\alpha + \dot{\varepsilon}_{ms} + \dot{\varepsilon}_c \tag{16}$$

Where the total strain is a summation of the elastic strain, hygro-expansive strain, the mechano-sorptive strain, and the time-dependent creep strain. The mechano-sorptive creep contributes to the relaxation of the stresses due to moisture content variations. The difference with time-dependent creep ε_c is that moisture content variations are not needed. Either one- or two-dimensional formulations are found for the separate components. The general elastic deformation is written as:

$$\dot{\varepsilon}_E = C\dot{\sigma} \tag{17}$$

Where C is the compliance matrix, i.e. the inverse of the elasticity matrix. Gereke and Niemz (2010) also add a component in which a change of elastic properties, for instance due to moisture content, can also be included. In the case of a one-dimensional formulation, an effective stiffness E_{eff} is used which can vary over the cross-section according to radial and tangential stiffness and the location of the pith with respect to the board edge (Häglund, 2007).

The hygro-expansive strain can, just like the elastic strain, be formulated for the one-, two- and three-dimensional case. The general formulation is:

$$\dot{\varepsilon}_\alpha = \alpha \dot{u} \tag{18}$$

The symbol α represents the hygro-expansive factors in longitudinal, radial and tangential direction. One-dimensional formulation is possible by replacing α by α_{eff} and using the radial and tangential components and location of the pith with respect to the board edge (Häglund, 2007).

The mechano-sorptive strain components are formulated differently for the one- or the two- and three-dimensional case. In the two- and three-dimensional case, the strain is formulated as follows:

$$\dot{\varepsilon}_{ms} = m\sigma|\dot{u}| \tag{19}$$

The coefficient m incorporates the mechano-sorptive parameters. In the one-dimensional case, the radial and tangential components are lumped into one number. However, differences between mechano-sorptive values for drying or wetting are easily be incorporated:

$$\dot{\varepsilon}_{ms} = \sigma(m|\dot{u}| + \beta\dot{u}) \tag{20}$$

Where β represents the reduction of m in case the timber is in the desorption phase. The formulation seen in Equation (20) is used by Häglund (2010). A more elaborate overview of the above-mentioned equations is also found in Schiere (2016).

The time-dependent creep strains are often not incorporated in calculations concerning moisture induced stresses perpendicular to the grain. Toratti and Svensson (2000) argued that the mechano-sorptive relaxation was larger than relaxation due to time-dependent creep. Methods to incorporate time-dependent creep into deformation of structures is however used in Toratti (1992) and in Fortino et al. (2016).

6.5 Validation of moisture transport and generated moisture induced stresses

The moisture distribution numerically modelled was compared with experimental investigations done by Jönsson (2004) as shown in Figure 50. The moisture content of a glued laminated member with a cross-section of 90 mm in width and 270 mm in height was increased (wetting process) from 9 M% to 16 M%. Figure 51 shows the resulting stresses for an adsorption process investigated by Jönsson (2004) on the same glued laminated cross-section of 90 mm in width and 270 mm in depth. The simulations show a good agreement with the experimental results and validates the model predictions. An influence of the glue lines of glued laminated timber on the moisture diffusion or moisture transport was not considered since the moisture transport were parallel to the glue lines.
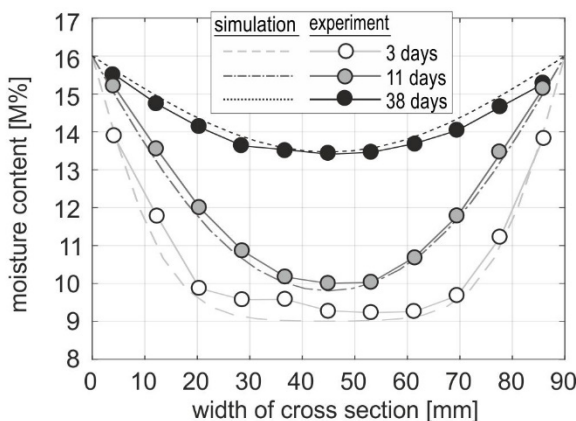
Figure 50: Numerical distribution of moisture content in comparison to experimental results on a glued laminated cross-section of 90 x 270 x 16 mm³ under adsorption process from 9 to 16 M% done by Jönsson (2004)
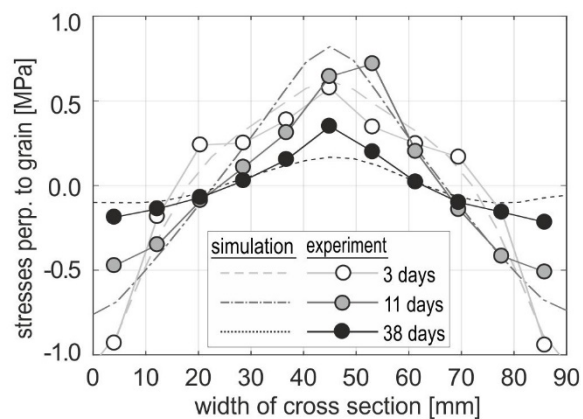
Figure 51: Numerical stress distribution and development in comparison to experimental results on a glued laminated cross-section of 90 x 270 x 16 mm³ under adsorption process from 9 to 16 M% done by Jönsson (2004)

6.6 Fracture and failure of wood

6.6.1 Moisture related damage in timber

The importance of the relation between moisture content and structural reliability is shown through assessment studies where it was observed that moisture content changes, high moisture contents, or low moisture contents could implicitly be related to almost half of the evaluated cases of structural damage or failure, Frese and Blass (2010). A similar study concluded that moisture content changes accounted for about one third of the observed structural damage (Dietsch and Winter, 2018). An example where invisible moisture induced damage, i.e. center of the glulam cross-section failed perpendicular to the grain, is in the old ice rink of Kandersteg in the Swiss Canton of Bern (Sigrist et al., 2013). Cracks perpendicular to the grain on the surface of the load bearing glulam beams were also observed. Aicher et al. (1998) observed failure of notched beams in DOL tests after several wet days preceded again by dry period. Moisture effects are also mentioned in Frühwald et al. (2007) as cause of damage, especially right after erection of buildings, where timber is moist during construction and dried shortly afterwards when heated.

One of the difficulties is that tensile strength perpendicular to the grain is affected both by volume and by moisture content. The volume effect is explained in Gustafsson (2005) and supported by data obtained from experiments. The effect of moisture on tensile strength is estimated at about 2.3% reduction per percent in moisture content increase from data presented by Gerhards (1982). Smith et al. (2003) mentions a 1.5% reduction per percent in moisture content increase. Using data obtained from Möhler and Steck (1980) in Figure 52, the reduction of tensile strength can be estimated to a value of 3.0% per increase in moisture content. The tests were performed with specimens of a cross-section of 30 mm by 30 mm and a height of 220 mm. This is for the average strength only. Data shows though that a peak in the 5th%-quantile tensile strength is observed at about 12 M%.

Several approaches to fracture of wood that were considered in this project, along with their applicability to moisture induced stresses, are discussed in the following sections.

6.6.2 Weibull stress approach

The Weibull theory is explained by the fact that in a small volume, a small number of defects can be expected to be present. In a larger volume, more (undetectable) defects will be present, hence reducing the amount of allowable stress per volume. Fracture perpendicular to the grain depending on stressed volume is formulated as:
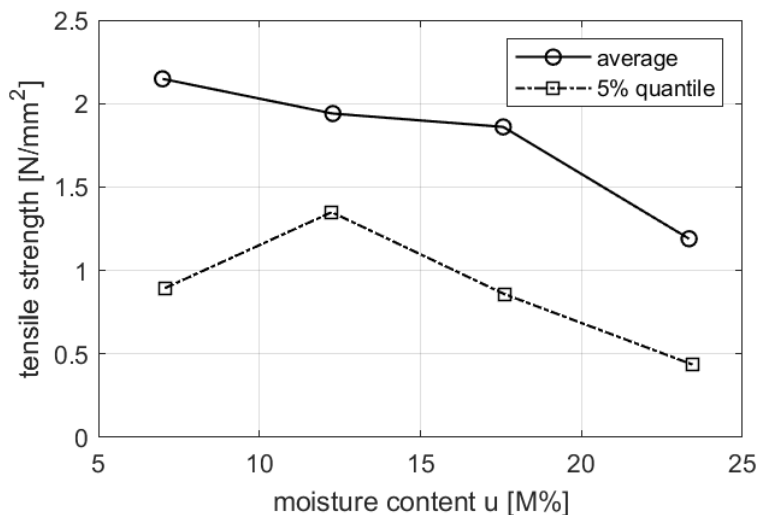
Figure 52: Measured strengths perpendicular to the grain depending on the moisture content by Möhler and Steck (1980) on specimens with a cross-section of 30 mm x 30 mm

$$\frac{f}{f_0} = \beta \left(\frac{V}{V_0} \right)^m \tag{21}$$

In which f is the fracture strength, f_0 is the reference fracture strength, β is a scalar, V is the volume considered and V_0 is the reference volume. Value m indicates the spread of the material properties, in this case fracture. If reference fracture strength f_0 of 1 and volume V_0 of 1 is chosen, fracture strength f can be calculated directly. Mean fracture strength perpendicular to the grain, based on a various number of tests is for instance proposed as:

$$f = 1.5 V^5 \tag{22}$$

In which f is in N/mm^2 and V is in dm^3. Meaning that a mean strength of 1.5 N/mm^2 can be expected when loading a volume of 1 dm^3. One of the properties is that an infinitely small volume has an infinite strength, both not being realistic.

To calculate the failure probability related to a volume where stresses are distributed unequally, the following formulation is used:

$$P = 1 - e^{-\int_v g(\sigma) dV} , \tag{23}$$

where

$$g(\sigma) = \left(\frac{\sigma}{f} \right)^m \tag{24}$$

in which the stresses need to be integrated over the volume. Numerically, i.e. using discrete volumes, it is implemented as follows:

$$P = 1 - e^{-\sum_{i=1}^{n} \left(\frac{\sigma_i}{f_i} \right)^m} . \tag{25}$$

6.6.3 Probabilistic Fracture Mechanics

The Probabilistic Fracture Mechanics (PFM) theory is based on a combination of the generalized Linear Elastic Fracture Mechanics (LEFM) and Weibull stress theory (Danielsson, 2013). The generalized LEFM solves the problem of the stress peak at a crack tip being infinite. By averaging the stresses over this crack-tip it creates a larger plastic zone in which equal fracture energy is stored. A requirement for validity of the LEFM is that the crack length is also small compared to the volume it acts in.

Considering the mean stress over a certain volume, a simple fracture criterion can be established like the Norris criterion, except that the mean tensile and shear stresses are now considered:

$$\left(\frac{\sigma}{f_\sigma} \right)^2 + \left(\frac{\tau}{f_\tau} \right)^2 = 1 \tag{26}$$

Where the contribution of the shear stresses is omitted as soon as only mode I fracture is considered. Where the average stress is calculated over a length x_{ms}. The length over which the stresses are averaged is calculated as follows:

$$x_{ms} = \frac{2 E_I \mathcal{G}_{Ic}}{\pi f_\sigma^2} \tag{27}$$

Where parameters $\mathcal{G}_{Ic}$ corresponds to the fracture energy and E_I is calculated as follows:

$$\frac{1}{E_I} = \frac{1}{E_x} \sqrt{\frac{E_x}{2 E_y}} \sqrt{\sqrt{\frac{E_x}{E_y} + \frac{E_x}{2 G_{xy}} - v_{xy} \frac{E_x}{E_y}}} \tag{28}$$

In which the material properties can be inserted corresponding to the specified plane of fracture. The value $\mathcal{G}_{Ic}$ is set to 300 J/m² and the value f_0 is set to 3.0 MPa.

Finally, in the PFM the averaged stress distribution over a plane is used to calculate a dimensionless linear load factor called α_{Global}:

$$\alpha_{Global} = \left(\frac{1}{V_{ref}} \int_V \alpha^m (x, y, z) dV \right)^{\frac{1}{m}} \quad \text{with } \alpha = \frac{\overline{\sigma}}{f_\sigma} \tag{29}$$

The advantage of applying the above-mentioned methods is that they can be implemented in a post processing step. The value α_{Global} can then actually be used to determine what the margin in the material is until failure.

$$F_{Failure} = \frac{1}{\alpha_{Global}} F_{Load} \tag{30}$$

In Finite-Element Methods for instance, a unit load can be used to calculate the stress distribution. The resulting load factor can then be used to calculate at which load failure can be expected, assuming material response throughout the whole loading process is practically linear.

6.6.4 Interface elements (fracture energy)

Saft and Kaliske (2013) designed interface elements based on fracture energy principles to estimate crack initiation and growth. A special interface element was developed to simulate ductile fracture perpendicular to the grain. The study however did not incorporate mechano-sorptive or time-dependent relaxation yet. Luimes et al. (2018) also used interface elements estimate crack growth in historic timber paintings on wood panels subjected to climate variations. The study however only includes elastic strains, thermal strains and hygro-expansive strains. The principles of the interface elements were developed by Cid Alfaro et al. (2009).

Saft and Kaliske (2013) and Luimes et al. (2018) predefined the crack growth paths. This approach is reasonable since cracks growth directions are known or can be estimated from stress distributions.

6.6.5 Discussion of failure assessment methods

Aicher et al. (1998) used the Weibull approach to estimate when notched beams that were placed in varying ambient climate would fail. The stressed volumes were not only loaded by varying climate, but also by a tension load. The approach discussed in this publication shows that the Weibull approach works for members that are fully subjected to tensile stresses. The Weibull approach does not allow the estimation of crack initiation. Similar is thought of the PFM which is based on the Weibull approach. In cross-sections loaded only by climate variations, a combination of compression and tensile stresses will be found in the cross-section.

Using interface elements is expected to be the best opportunity to model crack growth in glulam structures. It requires a larger numerical effort than the more probabilistic methods where simple post processing of data can be performed. This approach also requires ore material parameters to be known and determined. The probabilistic methods can however be used in cases where the structural element or structural detail is loaded primarily in tension by static loads and loaded by climate variations in addition to this.

6.7 Material properties of softwood

6.7.1 Diffusion value

Available methods to determine diffusion values are all based on gravimetric methods. A change in the samples' weight over time is used as a measure for ad- or desorption of water. The wet and dry cup method have been standardized in the International Organization for Standardization (ISO) standard ISO 12572 (ISO, 2016). Koponen (1984) dried and soaked wood samples to determine the diffusion parameters in the hygroscopic and over-hygroscopic range. Olek et al. (2005) suggested a so-called inverse

analysis of the transient bound water diffusion, by iterating D in Fick's second law until a suitable overlap between experiments and calculations is found. In De Backer et al. (2018), both the inverse analysis by Olek et al. (2005) and analytical solutions offered by Crank (1975), are used to derive diffusion parameters for early Netherlandish oak. The diffusion values obtained with the inverse analysis resulted in slightly higher values than those obtained with the analytical equations.

Table 8 and Figure 53 illustrate the wide range of moisture diffusion values found in literature. The presented overview is not complete but illustrates the spread amongst both constant and moisture dependent diffusion values. In the figure, the constant diffusion values are only plotted in the moisture content range in which these were used. Diffusion values published by Fragiacomo et al. (2011), Hanhijärvi (1995), and Hassani (2014) show differences close to a factor of four, even though a same exponential dependency on moisture content was used. On the other hand, the latter two sources suggest diffusion values that only differ marginally. Differences are also minimal between values published in Koponen (1984), Angst and Malo (2010), and Aicher and Dill-Langer (1997), to which again values used by Fragiacomo et al. (2010) overlap. Koponen (1984), Droin-Josserand et al. (1989), and Saft and Kaliske (2013) present both transverse and longitudinal moisture diffusion values. The negative moisture content dependency of diffusion values along the grain is explained by domination of conductance of the wood cell's lumen. The positive moisture content dependency transverse to the grain is explained through the lower bonding energy of the sorption sites on the cell wall (Siau, 1995).

Unlike Saft and Kaliske (2013), published diffusion values do not distinguish between values in radial and tangential direction. Siau (1995) states differences between diffusion values in these two material directions are around 17% to 25%. Patera et al. (2016) only measured differences between radial and tangential diffusion in the lower hygroscopic range and concluded that these disappear in the higher hygroscopic range.

6.7.2 Young's modulus

The elasticity matrix can be used in two- and three-dimensional models. An overview of different values was already presented in Schiere (2016). Values from additional sources have been added to this overview in Table 9. As observed, there is a spread in the used values. However, relations between radial and tangential elasticity are always around 2:1, except for Saft and Kaliske (2013) where the difference between radial and tangential stiffness is 1.5:1. Gereke (2009) takes moisture content dependency of the material elasticity into account in calculation of a panel's warping under moisture load. The values are however not listed in Table 9.

Table 8: Table with mathematical formulations to calculate moisture dependent diffusion values

Reference		D [m²/s]
longitudinal		
Droin-Josserand et al. (1989)	A	$304 \cdot 10^{-10}\, e^{-17.7u}$
Koponen (1984)	B	*experiments*
Saft and Kaliske (2013) (p)	C	*large equation*
transverse (radial and tangential)		
Aicher and Dill-Langer (1997)	D	$4.17 \cdot 10^{-10},\, 0.1 < u < 0.2$
Angst and Malo (2010) (p)	E	$3.0 \cdot 10^{-10},\, 0.09 < u < 0.16$
Droin-Josserand et al. (1989)	A	$1.5 \cdot 10^{-10}\, e^{2.28u}$
Fragiacomo et al. (2011) (p)	F	$2.4 \cdot 10^{-10}\, e^{4.0u}$
Hanhijärvi (1995)	G	$8.0 \cdot 10^{-11}\, e^{4.0u}$
Hassani (2014) (p)	H	$6.78 \cdot 10^{-11}\, e^{4.0u}$
Koponen (1984) (p)	B	*experiments*
Saft and Kaliske (2013) (p)	C	*large equation*

u moisture content in fractions

h relative humidity in percentages

(p) mentioned as parameters for Norway spruce (Picea abies)
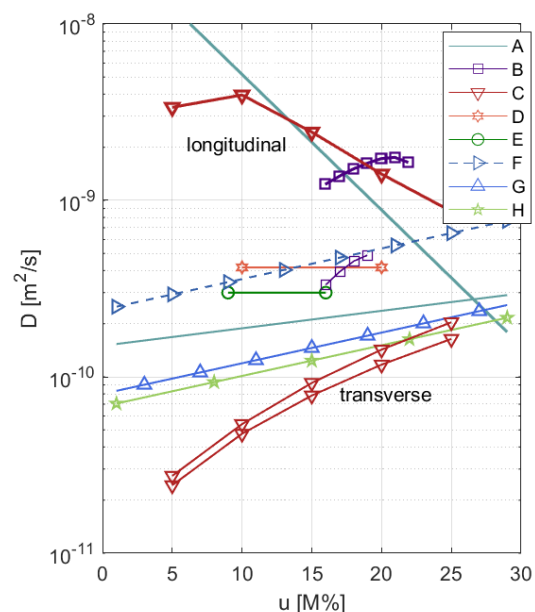
Figure 53: Comparison of diffusion values found in literature. The reference to the letters in the legend are found in Table 1.

Table 9: Used parameters in the elasticity matrix according to different authors

Property	Aicher and Dill-Langer (1997)	Gowda et al. (1998)	Fortino et al. (2009)	Angst and Malo (2012)	Saft and Ka-liske (2013)	Hassani (2015)	
E_l			12000	9700	9962	12002	N/mm²
E_r	1000	1000	900	467	635	823	N/mm²
E_t	600	500	500	216	429	423	N/mm²
G_{lr}			700	400	674	630	N/mm²
G_{lt}			700	250	661	745	N/mm²
G_{rt}	60	40	40	42	45	43	N/mm²
v_{lr}			0.038	0.017	0.45	0.407	-
v_{lt}			0.015	0.013	0.45	0.545	-
v_{rt}	0.31		0.558	0.50	0.24	0.31	-

6.7.3 Hygro-expansion values

In line with what is seen in the values obtained for the young's modulus, values used for hygro-expansion also vary between different authors. The difference between transverse hygro-expansion factors is more than a factor 2. However, the relation between the tangential and radial hygro-expansion is consistently around 2:1.

Table 10: List of hygro-expansion values found in different studies in %/M%

Source	longitudinal	radial	tangential
Rijsdijk and Laming (1994)		0.15 Green to oven dry	0.32 Green to oven dry
Toratti (1995)	$6.25 \cdot 10^{-3}$		
Aicher and Dill-Langer (1997)		0.07	0.14
Jöhnsson (2004)		0.11	0.22
Fortino et al. (2009)	$5.0 \cdot 10^{-3}$	0.13	0.27
Gereke (2009)	$5.0 \cdot 10^{-3}$	0.17	0.33
Angst-Nicollier (2012)		0.17/0.14 (wetting/drying)	0.34/0.28 (wetting/drying)

6.7.4 Mechano-sorptive creep

As mechano-sorptive creep is not studied as much as material elasticity or hygro-expansion, less parameters are found. A spread can still be observed in Table 11. Interestingly, the value β used by Aicher and Dill-Langer (1998), could lead to negative mechano-sorptive creep, which is a matter of interpretation perhaps. Svensson and Toratti (2002) derived only one value of m for wetting, drying and varying conditions.

Table 11: Mechano-sorptive parameters obtained from different studies

Component	Ranta-Maunus (1993) R/T/45˚	Aicher and Dill-Langer (1997)	Svensson & Toratti (2002)	Häglund (2008)	Angst and Malo (2012)	Gereke (2009)	
m_l						0.04	(N/mm²)⁻¹
m_r					0.07	0.15	(N/mm²)⁻¹
m_t					0.1	0.2	(N/mm²)⁻¹
m_{lr}						$8.0 \cdot 10^{-3}$	(N/mm²)⁻¹
m_{lt}						$8.0 \cdot 10^{-3}$	(N/mm²)⁻¹
m_{rt}					0.4	0.8	(N/mm²)⁻¹
m	0.12/0.08/0.17	0.035	0.33	0.085			(N/mm²)⁻¹
B	-0.07/-0.02/-0.08	-0.06		-0.045			(N/mm²)⁻¹
μ_{tr}					0.75		
μ_{rt}					1	1	

6.8   Sensitivity analyses to selected input parameters

6.8.1   Sensitivity to magnitude of diffusion value

As different parameters are available it is also relevant to know what the effect is of the variation. For spruce the diffusion parameter is around $2.0 \cdot 10^{-10}$ m²/s (Angst and Malo, 2010). However, values half or double this magnitude can also be found. Therefore, a step load is applied on a cross-section of 200 mm by 800 mm, modelled with a layup in which the pith distance is in the midplane and 50 mm below the board edge. The material elasticity is that obtained from Angst and Malo (2012). The diffusion parameter is varied between $1.0 \cdot 10^{-10}$ m²/s and $3.0 \cdot 10^{-10}$ m²/s in intervals of $0.5 \cdot 10^{-10}$ m²/s. The step load represents an increase of 6 M% from an initial moisture content of 12 M%. The resulting development of moisture induced stresses in the midplane and the surface are observed in Figure 54. The stress levels after 21 days (three weeks) of loading are observed on the left. The results show that diffusion speed does not have any effect on the achieved maximum tensile or compression stress levels when a step load is applied.

6.8.2   Response to variation of material elasticity and hygro-expansive parameters

The sensitivity to changes in material elasticity and to hygro-expansive parameters was not investigated. It is expected though that this relation is linear.

Figure 54: Development of moisture induced stresses in a 200 mm wide cross-section loaded by a stepwise moisture increase of 6 M%

7   Investigations and Case Studies using the numerical Model

7.1   Cross-section dimensions found in structures

Jöhnsson (2004) performed important research on a timber member of 90 mm wide and 270 mm high. This cross-section dimension was later also used in Angst and Malo (2012) and Angst-Nicollier (2012) for various studies including location of pith, and reinforcement of the beam with screws to mitigate risk of tensile cracks generating in the midplane of the cross-section. Gamper et al (2014) investigated the moisture variations in timber cross-sections of 21 different buildings located in southern Germany. These cross-sections monitored were from 160 mm to 240 mm wide, seen in Figure 55. The swiss website *swisstimberbridges.ch* contains a large amount of information, amongst others also on the construction. As far as possible, the cross-section widths were compared to the load bearing members obtained from construction plans and plot against the year of erection, see Figure 56. The website was carefully maintained until 2010. The diagram shows that block glulam beams were used in bridges from about 2010, thus this being only a recent development. Cross-section widths increased from about 160 mm to 240 mm from the 1970's to the year 2000. The diagram also shows an increasing trend in the size of cross-sections. Heavy traffic refers to loads of 40 tons or more.

Fortino et al. (2019) performed simulations on the pedestrian Älsvbacka Bridge in Sweden. The load bearing member of interest is 645 mm wide made of three separate 215 mm wide beams. Cross-section widths of single beams can in exceptional cases, be found up to 280 mm width. The depth of the cross-section ranges up to 2 meters, but deeper beams can also be found. A rule of thumb is that slenderness rations (depth/width) are around four as buckling resistances must also be met.

7.2   Effect of load amplitude and cross-section width

A variation is made on both the cross-section size and wetting load. Load steps of 3 M% to 16 M% were applied on cross-sections varying from a 100 mm width to 250 mm width. The aspect ratio was maintained at a constant value of four. Hence, the deepest beam is 1 m high. Figure 57 shows the dependency of tensile stresses in the cross-section's midplane. The pith is located 50 mm below the board edge. The figure shows that the maximum stresses are increase as the cross-section size increases. They do whoever take longer to develop.

To know if the stresses increase due to width only, a simulation is done where the cross-section width is varied, but the angle the annual rings make to the beam surface is maintained constant. Another way to see it, is that the ratio in which the angle varies over the cross-section is constant. The consequence is that pith distance from the board edge increases as the width of the of the beam increases. The results are observed in Figure 58, where the step load moisture increase of 6 M% was applied at an initial moisture content of 12 M%. It shows that the magnitude of the moisture induced stresses is related to the ratio between the annual ring angle in the midplane and that at the surface of the glulam cross-section. The stress distributions in beams of 160 mm, 200 mm, and 240 mm is seen in Figure 59 loaded by wetting and drying loads. The stresses that are plot are the stress distributions when the maximum tensile stress is achieved. During wetting, these take longer to develop than during drying.

Figure 55: Cross-section dimensions from 21 buildings monitored in southern Germany (Gamper et al., 2014)

Figure 56: Cross-section dimensions used in load bearing members of bridge construction obtained from swisstimberbridges.ch (data until 2010)

Figure 57: Maximum tensile stress due to selected step load magnitude in different cross-sections of width from 100 mm to 250 mm.

Figure 58: Dependency of tensile achieved stress levels in a closer analysis where either pith location or ratio of annual ring angle from edge to midplane was maintained constant

Figure 59: Transverse stress distribution depending on the cross section by constant slenderness at the point of maximum tensile stress perpendicular to the grain in wetting and drying.

7.3 Effect of cross-section aspect ratio

Angst and Malo (2013) varied the width of a cross-section while maintaining the layup of the glulam beam. The pith location, lamella-thickness, and total depth of the beam were not changed. The width of the glulam beams were 90 mm, 140 mm and 215 mm wide, while the depth was maintained at 270 mm. The aspect ratio, slenderness, or depth over width ratio of the cross-section varied from 3.0, 1.9, to 1.3. One of the results was that the highest stresses occur in the cross-section with a width of 140 mm. This contradicts the results seen in Figure 57 and Figure 58, where the increasing width led to higher moisture induced stresses. Here however, the aspect ratio was maintained at a constant value of 4.

The effect of the aspect ratio on the stress levels achieved in the glulam cross-section was investigated by adding two boards on the layup each simulation. The width of the glulam cross-section was maintained at 200 mm, whereas the depth was increased from 200 mm to 1000 mm, see Figure 60. The figure shows that the aspect ratio does not affect the stresses developed at the surface much. The stresses in the midplane converge at an aspect ratio of 2 or higher. This, together with the diagram observed in Figure 57, explains the conclusion made by Angst and Malo (2013). Here, the highest moisture induced stresses would occur in the glulam beam with a width of 140 mm and aspect ratio of 1.9.
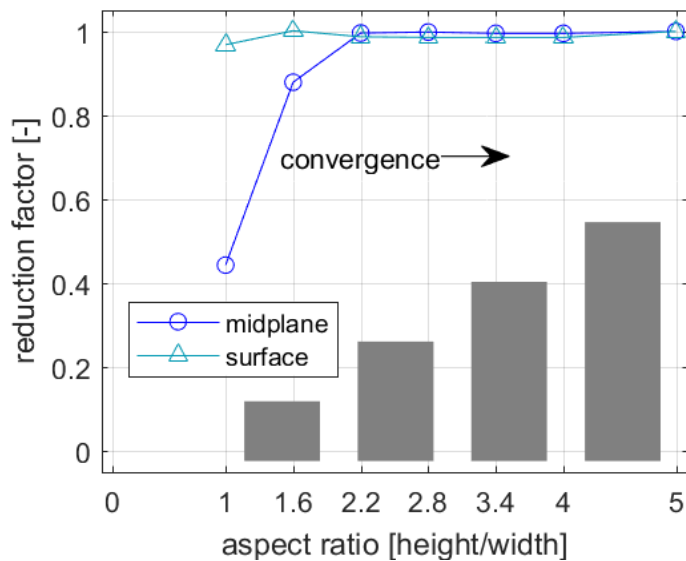
Figure 60: Effect of aspect ratio on stress levels on the surface and midplane of a glulam cross-section

7.4 Block glued glulam beams

The magnitude of the climatic variations affects the generated moisture induced stresses in the cross-section. Section 7.2 showed how the moisture induced stresses are also affected by cross section width. Low aspect ratios used in Section 7.3 showed that the geometry also can affect the generated stress levels. The block glulam beams form wide cross-sections by gluing single beams sideways onto each other. This is expected to affect the moisture induced stresses in two ways.

1. The ratio between the areas where the compressive stresses and the tensile stresses are present is different from those in slender beams. The tensile stresses are spread out over a larger portion of the cross section, resulting in smaller values. Note that in Section 7.2 tensile stresses increased due to cross section width at constant pith location.

2. Since the cross section is not slender anymore, effects of aspect ratio also start playing a role and reduce the total amount of generated stresses in the cross section.

This is however verified by setting up simulations where a stepwise climate is induced of $u = 12 \pm 6$ M%. The cross-section height is always maintained at 800 mm.

The calculated levels of moisture induced stresses in different widths of cross-sections is plotted in Figure 61. The stress distribution is plot at the point where the maximum tensile stress levels are achieved. Two beam widths were used to calculate stress levels up to total block glulam beam widths of 800 mm:

- four beams of 200 mm were needed to form a block glulam of 800 mm, and
- five beams of 160 mm were assembled to form a block glulam beam of 800 mm.

Figure 61 shows that higher tress levels are found in block glulam beams with an uneven number of single beams when submitted to wetting loads. In the block glulam beams with an even number of single beams, maximum stress levels are lower than in the uneven number of single beams. Converged stress levels remain around 0.5 MPa. The time needed for each of these beams to develop these stresses is different and all reach a maximum level long after the load was initially applied.
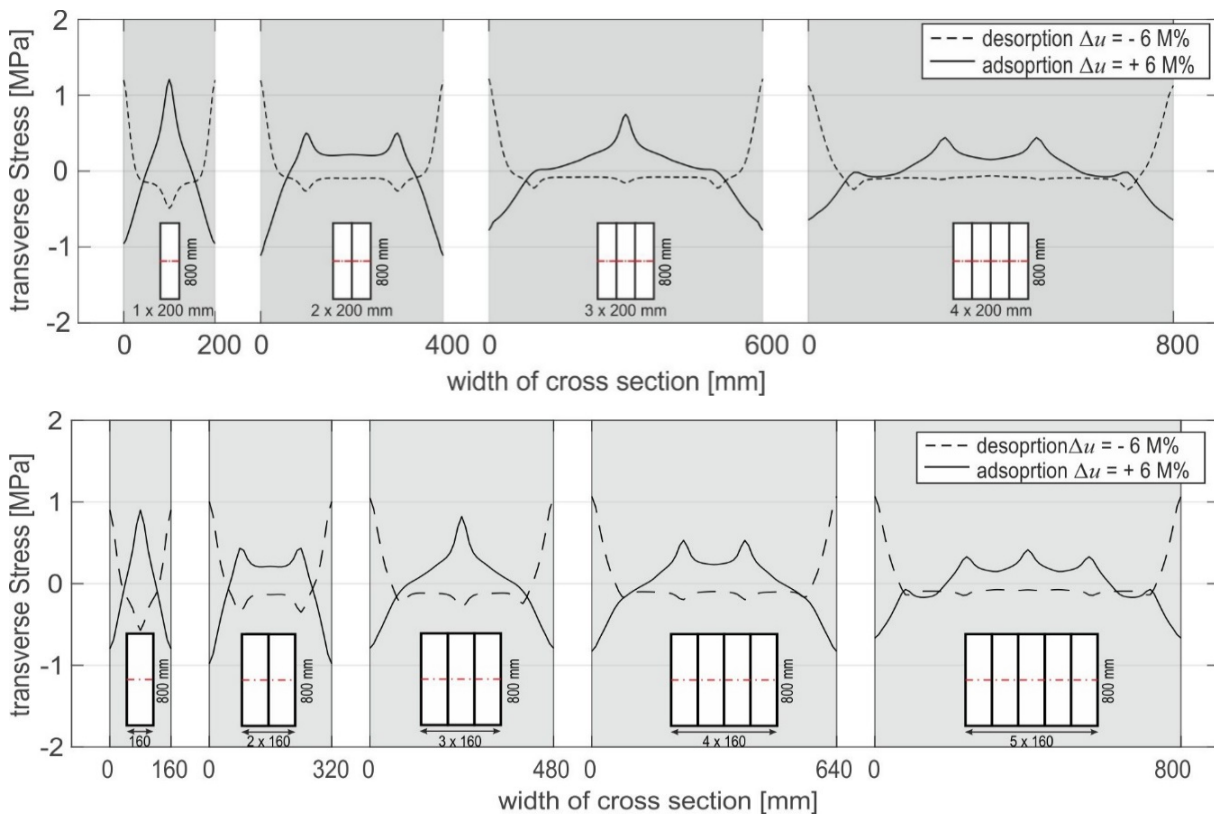
Figure 61: Transverse stress depending on the width of the cross-section, step load

When the beams are subjected to drying loads, width of the beam or number of beams used does not affect the level of maximum tensile stress. These simply occur shortly after the driving load has changed at the surface. This could be an explanation why almost all timber in building has at least some cracks perpendicular to the grain. It is suggested that these stress levels depend much more on the angle the annual rings make with the surface of the beam.

To verify if the aspect ratio affected the reduction of strains only a simulation was done where the cross-section width and height were maintained constant, and the number of single beams was varied, Figure 62. A beam with a cross section width of 360 mm is subdivided into two, three, four, six, and nine cross-sections. Here too, the stress distribution perpendicular to the grain converges once four beams or more are used in the cross section. It is noted that the cross sections simulated here are not necessarily economical for use in practical production lines or construction.
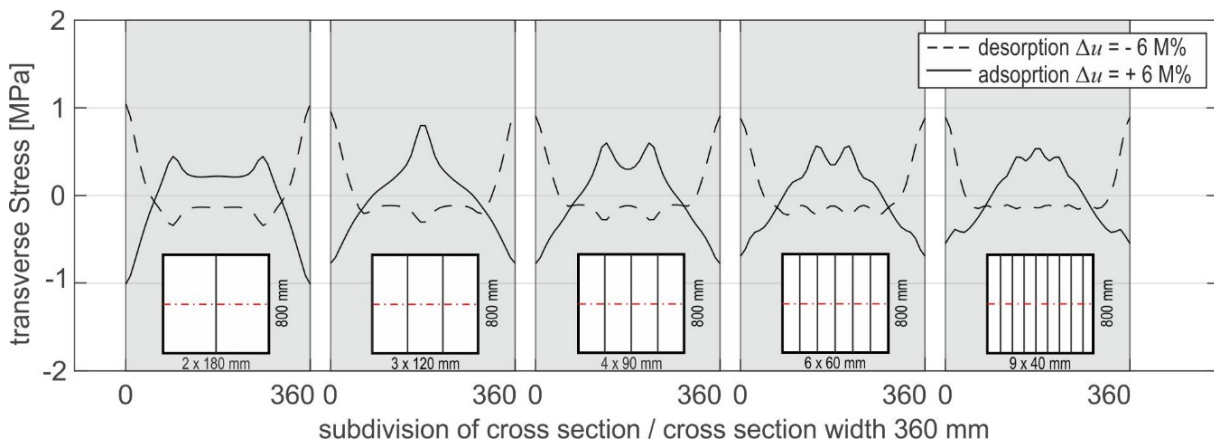
Figure 62: Transverse stress with different number of beams used in a same cross section width, step load

7.5 Influence of pith location or spread of pith per board

Angst and Malo (2013) varied the layup of the whole glulam beam and studied how this affects the moisture induced stresses perpendicular to the grain. The pith locations found in this study were in the board cross-section, on its edge, and outside the board cross-section. A more systematic variation of pith distance from the board edge was made to study the effect of the tensile stress levels in the midplane of the cross-section. The cross-sections size was maintained constant at 200 mm width using the pith distance in previous simulations as a starting point. The pith distance was varied to 10 mm, 30 mm, and 70 mm from the board edge. As observed in Figure 63, increase of the pith distance from the board edge does not result in a linear decrease of the tensile stresses in the midplane of the cross-section.
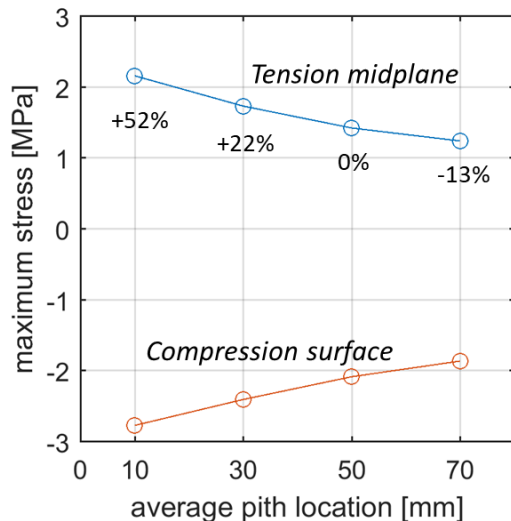
Figure 63: Comparison of maximum stress levels under a variation of the pith distance from the board edge. The values in the graph are with a pith distance of 50 mm to the board edge.

Pith eccentricity also affects the generated moisture induced stress levels. Looking into a more realistic board layup, it should be acknowledged that pith locations within a layup are quite randomly distributed. Boards that go into a glulam beam are selected on their strength class and not on the location these were cut from a tree trunk. Moreover, the pith within a board does not stay on the same position but varies due to cutting pattern, straightness of the trunk, drying stresses, etc.

A look into more realistic layups is made to make a relation between the idealised layup and a more realistic layup. Figure 64 shows a comparison of three different layups of a glulam beam: (1) the idealised layup, (2) a more realistic layup with spread of 7.5 mm standard deviation in pith eccentricity and pith distance from the lamella, and (3) with a higher standard deviation of 15 mm than found in variation (2). Note also that in variation (2) and (3), the upper board is flipped upside down. The stresses perpendicular to the grain are evaluated in the central half of the cross-section.

The effect of the pith spread on the developed stresses in the midplane and the surface is observed in Figure 65. For each standard deviation in spread, ten different simulations were performed. This was done to achieve some statistical convergence. Three important conclusions can be drawn:

- The obtained maximum tensile stresses at the midplane and the compression stresses at the surface start showing a spread. In the idealised layup, the minimum and maximum stresses are concentrated in one large peak.
- In the compression zone at the surface, the average of the maximum stresses does not move as the spread in pith location increases. This means that as the mean of these stresses does not change but the spread does increase, higher compression stresses can be expected at the surface of the beam due to increase of pith spread.
- In the tension zone at the midplane, the of the stresses decreases. However, the spread does. The result is that the maximum tensile stresses in general will decrease but that stresses around those values of the idealised setup can still be expected

A couple of notes should be made:

- What is seen for wetting, is also seen for drying. Hence, stresses at the surface will generally increase and stresses in the midplane will generally decrease.
- The characteristic tensile strength perpendicular to the grain of 0.4 N/mm² is exceeded in all simulations, whether drying or wetting loads are applied.

Average tensile strength of 1.8 N/mm² is not exceeded. The reference volume over which these are calculated is 1 dm³ (Blass und Schmid, 2001).
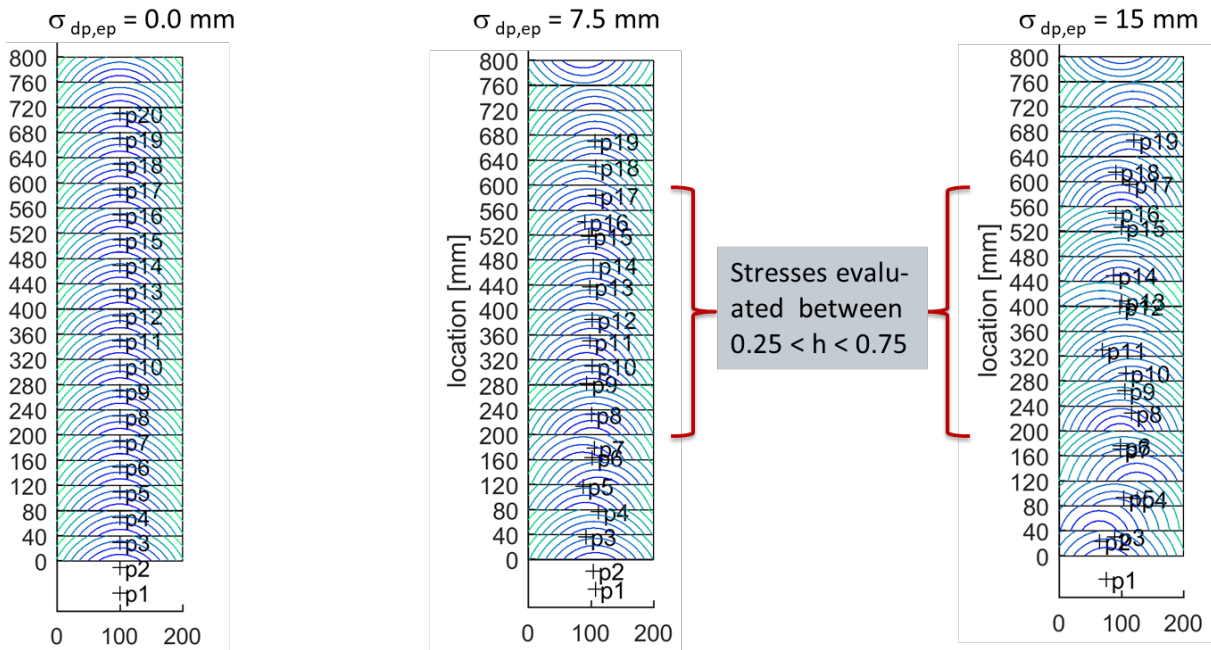
Figure 64: Glulam beam layup in the idealized condition (left) and the more realistic conditions (middle and right).
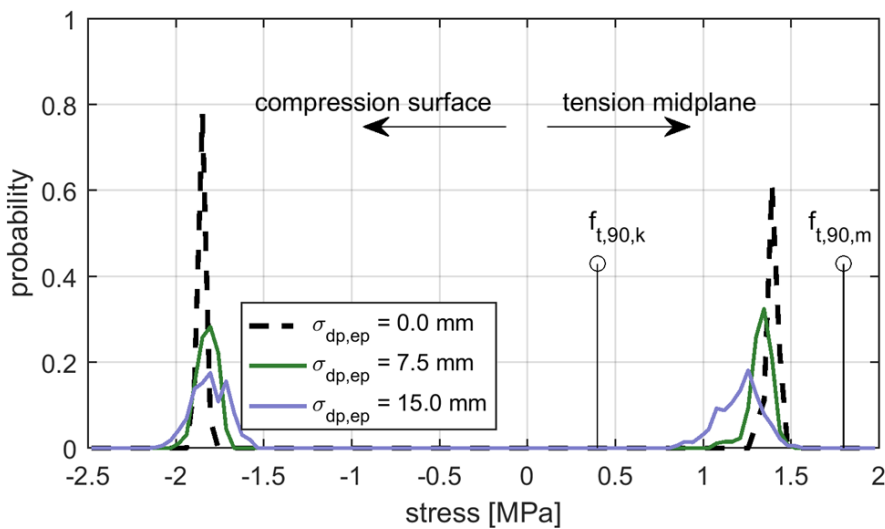
Figure 65: Effect of pith spread on minimum and maximum stresses occurring in the midplane and surface under wetting loads

7.6 Cross-section deformations due to moisture content variations

Deformations corresponding to the applied step loads are observed in Figure 66. The plotted deformations are obtained from the maximum duration of the simulations. This was set to 120 days on the smaller cross-sections and 360 days on the large cross-sections. The smaller cross-sections respond faster to moisture content increases, due to the smaller amount of constraint during swelling and the faster increase in moisture. The moisture content distribution is plotted on the upper diagram, the deformation in the lower diagram. It takes a long time until the moisture content reaches equilibrium in the centre of the cross-section. Hence, building with wider cross-sections most likely results in smaller deformations.
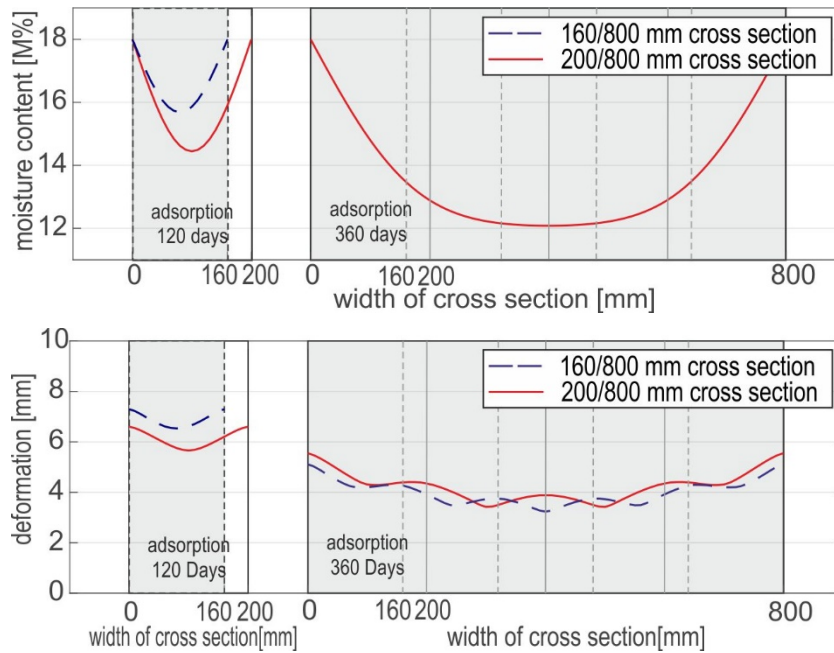
Figure 66: Deformation of timber beams of different widths subjected to step loads of 6 M% moisture content increase. All beams have a height of 800 mm and the duration of the simulations is indicated in the figures. The bottom plot shows the moisture content distributions.

8 Impact of Erection Time and Inspection of Timber Structures

8.1 Erection time

Drying or wetting of timber elements also takes place in insulated and heated buildings. The process of manufacturing, building period, until the intended operation during the «first winter» affects the moisture content distributions in the load bearing cross sections. It is believed to be best if timber elements are installed at equilibrium moisture content that is expected later in the finished building. Gentle pre-conditioning is to be recommended, especially where high-performance requirements are to be met. Deformations in connections are to be limited where visual aspects are important. Protection from precipitation must be used during transport and erection and elements are to be covered when possible, see Figure 68. Wetting at the surface results in high stresses perpendicular to the grain which can lead to cracks in later when surrounding relative humidities reduce again later. Difference should be made between cracks which only reduce the visual appeal and those that have structural relevance. The use of alternative surface treatments is to be checked individually, but too little experience has yet been gained on this matter.

Conditioning/weather protection

- The time of erection can reduce the expected moisture variations
- The pre-conditioning is possible during or after the manufacturing when properly planned
- Effective planning of protection against weather/precipitation

  - Protection during transport and storage
  - Although expensive, use of temporary roofs is recommended
  - Efficient sequential erection with direct implementation of the finishing façade and/or roof as weather protection

Figure 67: Efficient protection during evenings, nights and weekends or during rain; removing of the protection during the working times (Swatch building, Biel/Bienne)

8.2 Numerical parameter study to seasonal time

The season or period of construction affects the erected structures differently. As discussed in Chapter 5 already, spring and summers are generally dryer than autumns and winter. Figure 68 shows the moisture content variations, the dimensional changes, and the resulting moisture induced stresses in Service Classes 1 and 2 for structures erected either in January or June. The following conclusions can be drawn from the diagrams.

- Moisture induced stresses at the surface react quickly to both drying or wetting loads in the surrounding climate.
- The smallest generated stresses due to seasonal variations in ambient climate are expected when structures are erected in summer period.
- Larger moisture induced stresses are expected when structures are erected during winter season.
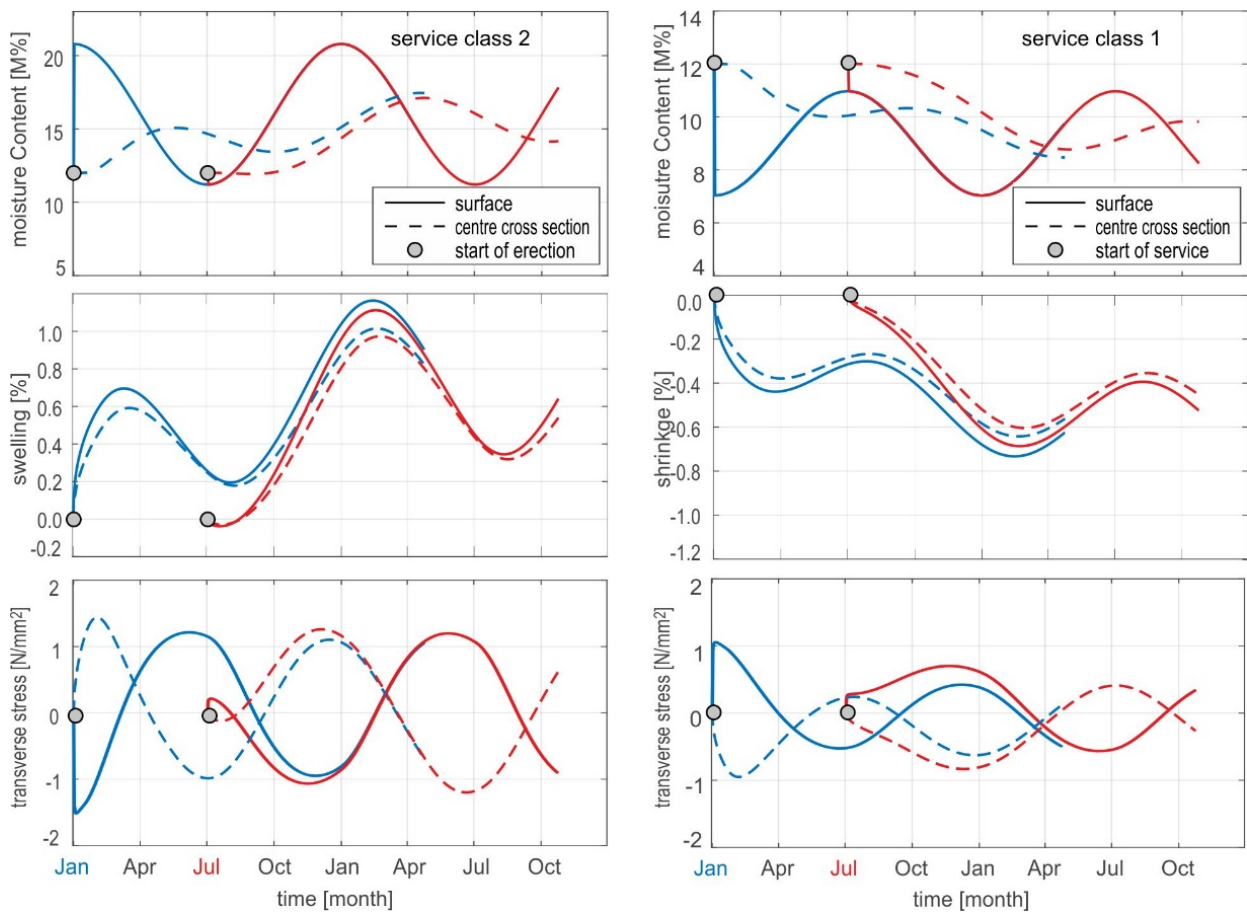
Figure 68: Results of the moisture content (left) and transverse stresses (right) for a cross section of 200/800 mm in Service Class 1 and 2 including seasonal changes of the ambient climate

- In erected structures the moisture induced stresses are expected to be lower in Service Class 1 operation than in Service Class 2 operation.
- The maximum tensile strength perpendicular to grain is expected to around 10 M%, which could be an explanation of the observed cracks perpendicular to the grain in dry structures.
- Moisture induced stresses in the midplane of the cross section take longer to develop. However, similar levels as achieved at the surface during drying are observed.
- Wood moisture content in the centre of cross sections of 200 mm require between one or two years to achieve the equilibrium moisture content due to their surrounding climates.
- Moisture diffusion in practice can be slower as expected from the simulations as slightly higher values were used than found in in-situ measurements.

8.3 Measurements of climate and moisture content inside the structure during construction

Two sets of data were obtained where climate and moisture were measured during building erection. The structures were intended to be for heated operation. The first set of data was obtained from the 'Quellgarten', the second for CC. An extract of the data measured at 'Quellgarten' is plotted in Figure 69. The figure shows measure humidity and temperature at four locations. The measurements span a period where the freshly poured screed was set to dry. It is noted that the relative humidities are around 80 %RH to 90 %RH for about a week and these drop afterwards to 30 %RH to 40 %RH as the temperature is increased to 30 °C and even 35 °C. for a period of almost three weeks. The data plotted in the figure is not raw data but obtained from plots itself and represent an estimated value. Delamination in cross laminated timber plates was observed after this drying operation.
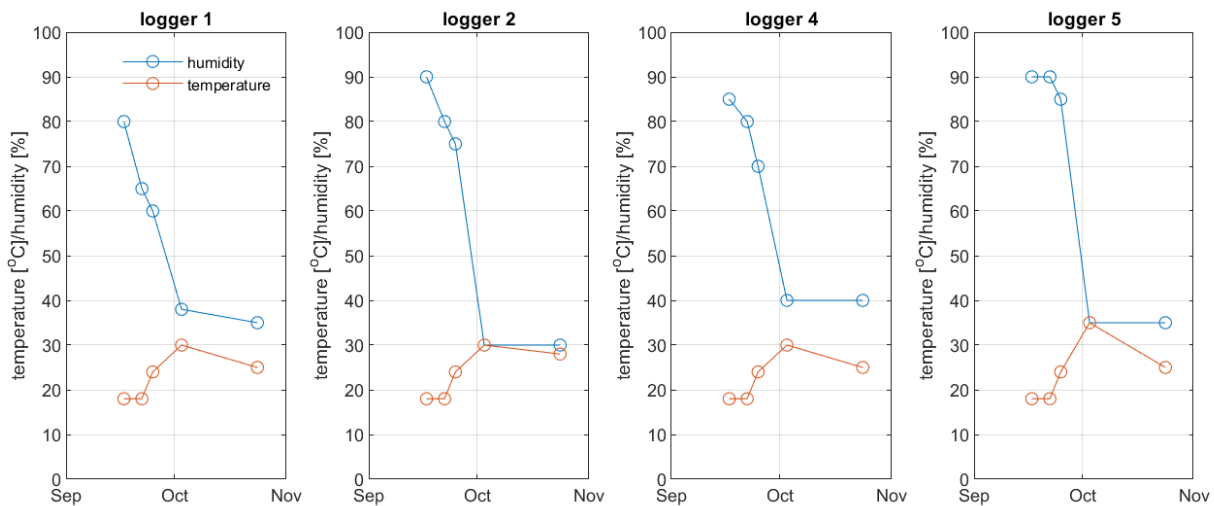
Figure 69: Summary of the measured humidity and temperature obtained from 'Quellgarten' on four out of six loggers (raw data not used)

8.4   Information on inspections, maintenance and monitoring of timber structures

Timber structures need to be monitored and assessed in regular intervals for quality assurance purposes according to standards:

▪ SIA 469 – "Erhaltung von Tragwerken",
▪ SIA 462 – «Beurteilung der Tragsicherheit bestehender Bauwerke»,
▪ SIA 269 – «Grundlagen der Erhaltung von Tragwerken»,
▪ SIA 269/5 – «Erhaltung von Tragwerken – Holzbau».

For timber bridges ASTRA 12002 (2005) «Überwachung und Unterhalt der Kunstbauten der Nationalstrassen» can be followed in addition to the listed standards. The most important rules for inspection are summarised:

▪ In general, all structures and members must be closely checked. Sheeting/cladding needs to be opened and scaffoldings or portable hoisting platforms should be used.
▪ Considering of days with rainfall for observation of leakages and water flow.
▪ For ice rinks two inspections moments necessary to obtain a total image of the condition:
  - During summer, it is the dryer season without ice, possible cracks at surface are opened and the total dimension can be measured
  - During winter, period of ice, checking the moisture content

Required service life of bridges is different in various countries according to Pousette et al. (2013). Finland requires a service life of 100 years, Sweden between 40 and 120 years, Norway 100 years, USA 75 years, and Switzerland between 80-100 years. Design of details, production quality, well set up maintenance and inspection programs, and planned repair efforts are key to fulfil this.

Pousette et al. (2013) mentions that preventive maintenance can already include regular cleaning of connections, cleaning clogged drains, etc. These tasks are easily performed and can significantly contribute to service life of a bridge. Checks could also include simple visual inspections for collision damages, vandalism, dirt, loose parts, vegetation close to the bridge, etc. Bachofer and Conzett (2013) mention that decay of single details can already lead to significant repair and maintenance costs.

For the design of details and inspection of timber bridges official standardized regulations or guides currently are missing in Switzerland. Main points for inspection are as following and can be found in international guides and recommendations:

▪ Inspection of timber bridges should occur at best during rainfall or at least shortly after. This is when clogged drains are quickly discovered, leaks are identified, etc. (Burkhart and Kleppe, 2017).

- There is no timber bridge inspection manual, separate versions have been issued in different countries. Very globally, the following three types of inspections are distinguished:
    1. The main inspection: planned long a forehand at a frequency of perhaps every five years that can be executed with simple tools (moisture content meter, a screwdriver, flashlight, etc.
    2. The intermediate inspection: planned after a main inspection to monitor development of damage.
    3. The special inspection: this needs to be done right after special occasions such as high water, landslides or earthquakes. Accidents can be considered as well.

- After each of these inspections, an evaluation of the state of the structure can be set up to evaluate if the measures need to be taken to take further action. Examples of how such report are set up can be found in Steiger (2000), ASTRA (2005), and ProHolz Austria (2006).

Further information regarding inspection of timber structures and timber bridges can be found in:

- Franke, B. Franke S. (eds.) (2014) Cost Workshop - Highly performing timber structures: Reliability, Assessment, Monitoring and Strengthening, Bern University of Applied Sciences, Biel, ISBN 978-3-9523787-3-1
- Steiger R. (2000) Kontrolle, Überwachung und Unterhalt von Holzbrücken, EMPA/HSR Fortbildungskurs
- Simon A., Arndt R. W., Jahreis M. G., Koch J. (2018) Muster-Prüfhandbuch für Holzbrücken, Forschungsprojekt ProTimB, Fachhochschule Erfurt.
- Simon A., Arndt R. W., Jahreis M. G., Koch J. (2018) Muster-Wartungshandbuch für Holzbrücken, Forschungsprojekt ProTimB, Fachhochschule Erfurt.
- Dietsch P., Köhler J. (Editors) (2010) Assessment of Timber Structures, COST Action E55 Modelling of the performance of timber structures, Shaker Verlag, ISBN 978-3-8322-9513-4
- Schickhofer G., Unterwieser H. (2005) Wartungsmanual für Holzbrücken – Ein Leitfaden zur Brückenüberwachung, Technische Universität Graz

Monitoring the moisture content is an appropriate early warning system. The measuring points should be placed at critical points/hot spots. This could be the bridge transition joint, bearing areas, passages or penetrations. To measure the moisture content as an early warning system, the electrical resistance method or the void method can be used (both explained in chapters 2.2 and 2.3). Table 12 gives an overview of the key characteristics of both methods. Measuring the moisture content is a non-destructive test method and can be applied for solid timber, glued laminated timber, and timber products. The measuring data can be online transferred and analyzed. Experts should be asked for the planning process, the service and analyses of the measuring results. The application of areal monitoring systems is currently mainly applied in geotechnical applications but is also recommended and available in civil structures like in flat roof constructions as well as timber road decks or wild animal crossing structures. However, application in timber bridges is still new and not much experience has been gained yet.

Table 12: Measuring methods of moisture content

	Electrical resistance method	**Void method**
Measuring values	Wood moisture content, temperature	Temperature and relative humidity
Measuring corrections	Temperature compensation	Calculation of moisture content according to sorption isotherms, Simpson (1973)
Measuring device	Measuring needles or screws (partly insulated and used as pair) Temperature sensor Climate sensor (optional)	Small void including a hygroscopic sensor Climate sensor (optional)
Data transfer	Remote	Remote
Application limits	Temperature > 5 ˚C	Temperature -20 ˚C < T < 50 ˚C
Accuracy	± 2 M%	± 2 M%

9 Conclusions and Outlook

The moisture content is one of the important indicators for the quality assurance of timber structures. Wood is a hygroscopic material and adapts its moisture content to the surrounding climate. The moisture content variations lead to shrinkage and swelling of timber and change of material properties. Humid or dry surrounding climate leads to an adsorption or desorption respectively. The change of the moisture content leads not only to deformations but can also lead to moisture induced stresses in addition to the stresses caused by dead and service loads such that cracks can develop. Cracks at the surface reduce the visual appeal but can also lead to a reduction of load-bearing capacity.

Several buildings and structures were monitored and analyzed to investigate and estimate the influence of the climate on the wood moisture content and the risk to crack initiation. The monitoring objects comprise riding halls, ice rinks, timber bridges and buildings in alpine regions. The results could be used to define standard climates depending on the operation. Bridges were handled separately.

Moisture content was measured through the electrical resistance method or the sorption method. Both methods are indirect methods. The methods are however non-destructive, making them suitable for monitoring applications. The reliability of both methods depends on the quality of the conversion data from either electrical resistance to moisture content or relative humidity to moisture content. Temperature effects should be accounted for in both methods. Whereas the electrical resistance method is not recommended below zero degrees Celsius, the sorption method can be used over a wide range of temperatures if sorption isotherms are representative. The sorption method does however not allow monitoring in the over-hygroscopic range but is recommended in chemically aggressive environments. The electrical resistance method can be applied in the over-hygroscopic range although the reliability of the method decreases drastically. Condensation or measurement of high humidities over extended periods of time should be considered when humidity sensors are selected for monitoring applications. The choice of conversion data is not large; however, choice of conversion data should be carefully made based upon used equipment. If possible, conversion data should be determined using the used electrodes, equipment, and gauge setup. Moisture content in high altitudes (above 1000 m a.s.l.) can best be monitored by using the sorption method. At lower altitudes, both the sorption and resistance method can be used. A careful choice should be made, or these conversion parameters can be determined like done for beech veneer. It does, in the end, assure large reliability of the measured data.

Moisture content monitoring methods should also focus on the effects of dynamic environments on moisture content measurements. Both the electrical resistance method and the method where climate is calibrated in static conditions, where application later is often in dynamic conditions. This is sufficient for moisture content monitoring applications but insufficient for the measurement of detailed dynamic effects in applied climate and response of timber structures. In addition, methods that allow fast determination of conversion data from either electrical resistance to moisture content or sorption isotherms should be developed. These are not necessarily labour intensive but are time intensive.

Monitoring results for timber structures and timber bridges are summarized through envelope diagrams that show the moisture content variation and the variation of the surrounding climate during service. Sport halls and production halls show very low moisture contents. The climate in riding halls presumably follows the climate around the building to a large extent. Ventilation should be allowed by small openings in the window area. Storage halls show also very low moisture contents, but this can depend on the stored material. Changes in the moisture content must be considered whenever stored material changes. A moisture content below 20 M% can be assumed for timber bridges if adequate constructive wood protection is met. The risk of fungi is avoided effectively.

Timber is often the material of choice for construction in alpine regions since the material itself is abundant and elements can be flown to the construction site without too much effort. Climate in the alpine regions is slightly dryer than in lower altitudes and is therefore beneficial to the timber. In winter, low relative humidities result in low moisture contents, being advantageous as load bearing properties are used to support snow loads. High moisture contents in alpine regions do not seem to be a point of concern. However, within heated structures very dry environments can be generated. Absolute moisture content outside is already low and temperature differences between outside and inside are large. This

means the low relative humidities can be found around the load bearing elements increasing the risk of initiation of drying cracks. First indications of these types of damages are known but the extent or severity of this problem needs to be quantified.

Ice rinks are a special case within timber structures. Problems with moisture have repeatedly been mentioned and observed. It is suggested that there are three possible options: (1) build open and well ventilated ice rinks but under Service Class 3 to account for condensation of water, (2) build open ice rinks but provide an extra lamella or two on the bottom face of each horizontally placed beam as a protection of the load bearing part, or (3) to close the entire perimeter and install a dehumidifier to reduce humidity levels when necessary.

Use of timber in bridges is not considered as a problem from the climate point of view, provided that enough ventilation is always available, also around structural details. Design of details, providing protection of structural elements against impact of rain and sun, and keeping a maintenance log is expected to more important to the durability of the bridge structure. Whether it crosses a water body or road is likely to have an impact, but this is for the moment considered unmeasurable with regards to at least average moisture content.

The Swiss climate is affected by the presence of the Alps, the Atlantic Ocean, and Mediterranean climate. For Switzerland, the biogeographical regions were used to assess the impact of meteorological climate on timber structures. The daily averages of temperature and relative humidity were used spanning up to 30 years on 110 weather stations. The corresponding equilibrium moisture content according to the meteorological climate values were plotted as average value and as possible annual variation on a map of Switzerland. The research results can be used for the approximation of the moisture content of newly planned timber structures or the effects during the periods of erection.

The research results are supported by numerical simulations. The numerical simulations include moisture transport and the resulting stress distributions over various cross sections. The numerical simulations allowed insight in the dependency of moisture load and geometry on the generated moisture induced stresses. The results showed that moisture induced stresses depend on board layup, moisture load amplitude, geometry and beam slenderness, and sideway joining into block-glulam members. Drying loads almost instantly lead to high tensile stresses at the surface (and visible cracks), whereas wetting loads lead to gradual increase of tensile stresses in the midplane of the cross section. Cracks generated in the midplane are not visible but have however been observed during the demolition and inspection of timber structures. High moisture induced stress levels during wetting are already found in beams with slenderness ratios (height over width) of two and more. Drying stresses are not affected by the geometry. Use of block-gluing shows a positive effect on the development of stresses in the cross-section.

The impact of the erection time on the moisture content, shrinkage and swelling as well as moisture induced stresses were investigated numerically too. It shows that moisture induced stresses at the surface react quickly to both drying or wetting loads in the surrounding climate. Moisture induced stresses in the midplane of the cross section take longer to develop. However, similar stress levels during both the wetting and drying are observed.

Results of numerical simulations have been used to calculate moisture effects in realistic beam layups. Methods to calculate damage initiation have not been used but are recommended for future work. The best methods go towards fracture energy and use of cohesive zones in FEM modelling techniques. Parameters that need to be determined are the fracture energy at different moisture contents. More generic methods should be based on experiments that for a statistical basis. Interesting aspects of moisture induced stresses also concern the restraint swelling and shrinkage within connections with slotted in steel plates and dowels, glued in rods, or screws. The research on moisture content needs to be extended on these details. Similar behaviours can occur by reinforcements with glued-in or drilled-in rods.

10 Indexes

10.1 Bibliography

Alghren, L. (1972) Moisture fixation in porous building materials, Division of Building Technology, Lund Institute of Technology, Report 36, Lund, Sweden

Angst-Nicollier V. (2012) Moisture induced stresses in glulam - effect of cross-section geometry and screw reinforcement, PhD thesis 2012:139, NTNU Trondheim, Norway

Angst V., Malo K. (2012) Effect of self-tapping screws on moisture induced stresses in glulam, Engineering Structures, Vol. 45, pp. 299–306

ASTRA (2005) Überwachung und Unterhalt der Kunstbauten der Nationalstrassen, Bern, Switzerland

Bachofer R., Conzett J. (2013), Brücken in Holz, Möglichkeiten und Grenzen, Forschungsprojekt AGB 2003/012 auf Antrag der Arbeitsgruppe Brückenforschung (AGB), Bundesamt für Strassen

Basellandschaftliche Zeitung (2012), Kunsteisbahn in Sissach wegen Einsturzgefahr geschlossen, 29 October 2012 (in German)

Berger U. (2014), Measuring Methods for Moisture Content of Wood, Cost Workshop FP 1101, Biel Switzerland

Birschke C., Rapp A.O., Bayerbach R., Morsing N., Fynholm P., Welzbacher C. (2008) Monitoring the ''material climate'' of wood to predict the potential for decay: Results from in situ measurements on buildings, Building and Environment 43, pp. 1575–1582

Björngrim N., Fjellström P.A., Hagman O. (2017) A Robust, Passive Resistance Sensor for Moisture Content Monitoring of Timber Bridges, Conference Proceedings International Conference of Timber Bridges ICTB, Skelleftea Sweden

Burkart H., Dyken T. (2017) Design flaws on Norwegian Timber Bridges, ICTB 2017 Conference Proceedings, Skelleftea, Sweden

Burkart H., Kleppe O. (2017) Learning Experiences from Norwegian Timber Bridge Inspections, ICTB 2017 Conference Proceedings, Skelleftea, Sweden

Cid Alfaro M., Suiker A., Borst R., Remmers J. (2009) Analysis of fracture and delamination in laminates using 3D numerical modelling, Engineering Fracture Mechanics 76, pp. 761–780

Crank J. (1975) Evaluation of wood sorption Models and Creation of Precision Diagrams for the Equilibrium Moisture Content, Oxford University Press, second edition, ISBN 0-19-853344-6

Cruz H., Custódio J. (2006) Durability and temperature effects on bond line, Presentation at COST Action FP 1101, Assessment, Reinforcement and Monitoring of Timber Structures, Trento, Italy

De Backer L., Laverge J., Janssens A., de Paepe M. (2018) Evaluation of the diffusion coefficient and sorption isotherm of different layers of early netherlandish wooden panel paintings, Wood Science and Technology (52), pp. 149-166

Dietsch P., Franke S., Franke B., Gamper A., Winter S. (2015) Methods to determine wood moisture content and their applicability in monitoring concepts, Journal of Civil Structural Health Monitoring 5 (2), pp. 115-127

Dietsch P. and Winter S. (2018) Structural failure in large-span timber structures: A comprehensive analysis of 230 cases, Journal of Structural Safety 71, pp. 41-46

Droin-Josserand A., Taverdet J.M., Vergnaud J.M. (1989), Modelling the process of moisture adsorption in three dimensions by wood samples of various shapes, Wood Science and Technology 23, pp. 259–271

Fortino S., Genoese A., Genoese A., Nunes L., Palma P. (2013), Numerical modelling of the hygro-thermal response of timber bridges during their service life: A monitoring case-study, Construction and Building Materials 47, pp. 1225-1234

Fortino S., Hradil P., Genoese A., Genoese A., Pousette A., Fjellström PA. (2016), A multi-Fickian hygro-thermal model for timber bridge elements under northern europe climates, WCTE 2016 conference proceedings, Vienna, Austria

Fragiacomo M., Fortino S., Tononic D., Usardi I., Toratti T. (2011), Moisture-induced stresses perpendicular to grain in cross-sections of timber members exposed to different climates, Engineering Structures 33 (11), pp. 3071–3078

Frandsen H., Damkilde L., Svensson S. (2007), A revised multi-Fickian moisture transport model to describe non Fickian effects in wood, Holzforschung 61, pp. 563-572

Franke B., Franke S., Müller A. (2014) Case studies: long-term monitoring of timber bridges, Journal of Civil Structural Health Monitoring 5 (2), pp. 195-202

Franke B. and Quenneville P. (2011) Numerical Modeling of the Failure Behavior of Dowel Connections in Wood, Journal of Engineering Mechanics 137(3), pp.186-195

Franke B., Müller A., Franke S., Magnière N. (2016), Langzeituntersuchung zu den Auswirkungen wechselnder Feuchtegradienten in blockverleimten Brettschichtholzträgern, Research Report Berner Fachhochschule, ISBN 978-3-9523787-7-9

Franke S., Schiere M. (2017) Development of FBGS-systems for Monitoring Purposes of large Timber Structures, SMAR conference proceedings, Zürich, Switzerland

Frese M., Blaß H.J. (2011) Statistics of damages to timber structures in Germany, Engineering Structures 33 (11), pp. 2969–2977

Frühwald E., Serrano E., Toratti T., Emilsson A., Thelandersson S. (2007), Design of safe timber structures – how can we learn from structural failures in concrete, steel, and timber?, Division of Structural Engineering, Lund University, Lund, Sweden.

Gamper A., Dietsch P., Merk M. (2012) Gebäudeklima – Langzeitmessung zur Bestimmung der Auswirkungen auf Feuchtegradienten in Holzbauteilen, Research Report, Technical University of Munich, Germany, ISBN 978-3-8167-9518-6

Gamper A., Dietsch P. (2015), Gebäudeklima - Langzeitmessung zur Bestimmung der Auswirkungen auf Feuchtegradienten in Holzbauteilen, Research Report, Technical University of Munich, Germany, Fraunhofer IRB Verlag 2015, ISBN 978-3-8167-9518-6

Gereke T. (2009) Moisture induced stresses in cross-laminated solid wood panels, PhD thesis, ETH Zurich, Switzerland, dissertation ETH no. 18427

Gereke T., Niemz P. (2010) Moisture-induced stresses in spruce cross-laminates, Engineering Structures, Vol. 32, pp. 600–606, 2010

Häglund M. (2010) Parameter influence on moisture induced eigen-stresses in timber, European Journal for Wood Products, Vol. 68, pp. 397–406

Hanhijärvi A. (2000) Advances in the knowledge of the influence of moisture changes on long-term mechanical performance of timber structures, Materials and Structures, Vol. 33, pp. 43-49

Hansen K.K. (1986) Sorption isotherms – A catalogue, Technical University of Denmark, Department of Civil Engineering, Building Materials Laboratory, Technical Report162/86

Hassani M. (2015) Adhesive Bonding of Structural Hardwood Elements, PhD thesis, ETH Zurich, Switzerland, dissertation ETH no. 20762

Hassani M., Wittel F., Ammann S., Niemz P., Herrmann H. (2016) Moisture induced damage in laminated beech, Wood Science and Technology, Vol. 50, pp. 917-940

Hedlin C.P. (1968) Sorption Isotherms of twelve species at subfreezing temperatures, Forest Products Journal, Vol. 17, p. 43-48

Hermann M (2009) Innovationen der Holzfeuchtemessung, Master Thesis 201, TUM Munich, Germany

Jönsson J. (2004) Internal stresses in the cross-grain direction in glulam induced by climate variations, Holzforschung, Vol. 58, pp. 154–159

Kanoopka D., Kaliske K. (2016) Hygro-mechanical FE-analysis of wooden structures: implementation and application or reliable moisture transport model, WCTE Conference Proceedings, Vienna, Austria

Kelsey K. (1957) Sorption of water vapour by wood, Australian Journal of Applied Sciences, Vol. 8, p. 42-54

Keylwerth R., Noack D. (1964) Kammertrocknung von Schnittholz, Holz als Roh- und Werkstoff 22, pp. 29-36

Koch J., Arndt R., Simon A., Jahreis M. (2017) Moisture monitoring of nine protected timber bridges in Germany, ICTB 2017 Conference Proceedings, Skelleftea, Sweden

Kottek M., Greiser J., Beck C., Rudelf B., Rubel F. (2006) World Map of the Köppen-Geiger Climate Classification Updated, Meteorologische Zeitschrift, pp. 259-263

Krabbenhoft K., Damkilde L. (2004) A model for non-fickian moisture transfer in wood, Materials and Structures 37, pp. 615–622

Li H., Perrin M., Eyma F., Jacob X., Gibiat V. (2018) Moisture content monitoring in glulam structures by embedded sensors via electrical methods, Wood Science and Technology (52), pp.733–752

Luimes R., Suiker A., Schellen H., Jorissen A. (2016) Fracture behavior of historic oak wood, WCTE Conference Proceedings, Vienna, Austria

Luimes R., Suiker A., Jorissen A., Schellen H., Duin P. van (2018) Climate-induced damage in historical cabinet doors, WCTE conference proceedings 2018, Seoul, South Korea

Melin C., Gebäck T., Heintz A., Bjurman J. (2016) Monitoring dynamic moisture gradients in wood using inserted relative humidity and temperature sensors, e-Preservation Science, 1581-9280 (eISSN), Vol. 13, p. 7-14

MeteoSchweiz[1] 2018, personal correspondance dwhservice@meteoschweiz.ch, october

MeteoSchweiz[2] 2018, www.meteoschweiz.admin.ch (Messinstrumente), website, November

MeteoSchweiz[3] 2018; www.meteoswiss.ch

Möhler K., Steck G. (1980) Untersuchungen über die Rissbildung in Brettschichtholz infolge Klimabeanspruchungen, Bauen mit Holz 4/80, pp. 194-200

Müller A., Franke B. (2015) Methoden der Zustandserfassung bei Holzbauwerken, 8. Europäischer Kongress (EBH) Bauen mit Holz im urbanen Raum, Gürzenich Köln, Deutschland

Müller A., Franke B., Schiere M., Franke S. (2017) Advantages of moisture content monitoring in timber bridges, ICTB 2017 Conference Proceedings, Skelleftea, Sweden

Niklewski J., Isaksson T., Frühwald Hansson E., Thelandersson S. (2017) Moisture conditions of rain-exposed glue-laminated timber members: the effect of different detailing, Wood Material Science & Engineering, Vol. 13, p. 129-140

Niklewski J. (2018) Durability of timber members: moisture conditions and service life assessment of bridge detailing, Dissertation Lund University, Sweden

Norsk Treteknisk Institut (2013) Monitoring five timber bridges in Norway - results 2012, Report no. 310332, Oslo, Norway

Olek W., Perré P., and Weres J. (2005) Inverse analysis of the transient bound water diffusion in wood, Holzforschung, Vol. 59, pp. 38–45

Ormarsson S., Dahlblom O., Petersson H. (1999) A numerical study of the shape stability of sawn timber subjected to moisture variation Part 2: Simulation of drying board, Wood Science and Technology, Vol. 33, pp. 407-423

Patera A., Derluyn H., Derome D., Carmeliet J. (2016), Influence of moisture hysteresis on moisture transport in wood, Wood Science and Technology (50), pp 259-283

Pollmeier (2018), Structural physics 03, Structural physics 10-18-EN

Pousette A., Malo K.A., Thelandersson S., Fortino S., Salokangas L., Wacker J. (Editors) (2013) Durable Timber Bridges, Final report and guidelines, RISE Research Institutes of Sweden, SP Rapport 2017:25, ISSN 0284-5172, Skellefteå, Sweden

ProHolz Austria (2006) Brücken aus Holz - für einen standardisierten Holzbrückenbau, Salzburg Austria

Rijsdijk J.F., Laming B.L. (1994) Physical and Related Properties of 145 Timbers; Information for practice. Kluwer Academic Publishers, Dordrecht, The Netherlands, ISBN 0-7923-2875-2.

Rode C., Clorius C. (2004) Modeling of Moisture Transport in Wood with Hysteresis and Temperature Dependent Sorption Characteristics, Performance of Exterior Envelopes of Whole Buildings IX: International Conference, Oak Ridge, TN, USA

Rugenstein J. (2016) Delaminierungsverhalten von Brettschichtholz in trockener Luft in Abhängigkeit der Oberflächenbehandlung, Diplomarbeit, TU Dresden, Germany

Saft S., Kaliske M. (2013) A hybrid interface-element for the simulation of moisture-induced cracks in wood, Engineering Fracture Mechanics, Vol. 102, pp. 32–50

Schickhofer G., Unterwieser H. (2005) Wartungsmanual für Holzbrücken – ein Leitfaden zur Brückenüberwachung, Bautechnikzentrum der TU Graz, Graz

Schiere M. (2016) Moisture diffusion and moisture induced stresses in glulam cross-sections, MSc Thesis, BFH Bern, Switzerland, thesis no. MHT/PA/MA/045/16/00

Schiere M. (2018), Moisture content of Timber Structures in Varying Ambient Climates, STSM report, COST Action FP1402

Siau J. (1971) Flow in Wood, Syracuse University Press, Syracuse, New York, U.S.A., first edition

Sigrist C. (2013) Dachkonstruktion Eishalle Kandersteg, Interner Bericht Nr. 9385-ZB-01, Berner Fachhochschule 2013

Simon A., Jahreis M., Koch J., Arndt R. (2017) New design guidelines for structural protected timber bridges, International Conference on Timber Bridges conference proceedings, Skellefteå, Sweden

Simpson W. (1973) Predicting equilibrium moisture content of wood by mathematical models, Wood and Fiber, 5 (1), 41-49.

Simpson W. (1998) Equilibrium Moisture Content of Wood in Outdoor Locations in the United States and Worldwide. Research Note FPL-RN-0268, Madison, WI: U.S. Department of Agriculture, Forest Service, Forest Products Laboratory

Skaar C. (1988), Wood-water relations, Springer Verlag, Germany, ISBN 3-540-19258-1

Steiger R. (2000) Kontrolle, Überwachung und Unterhalt von Holzbrücken, EMPA/HSR Fortbildungskurs 2000, EMPA, Switzerland

Toratti T. (1992) Modelling the creep of timber beams, Journal of Structural Mechanics, Vol. 25, pp. 12-35

Toratti T., Svensson S. (2000) Mechano-sorptive experiments perpendicular to the grain under tensile and compressive loads, Wood and Science Technology, Vol. 34, pp. 317–326

Tschuck P., Schmid E.L. (2012) Holzfeuchtemessung mittels Widerstandsmethode, Projektarbeit 5. Semester, Berner Fachhochschule Biel, Projektarbeit Nr. H/M12/759/12/0

Wadsö L. (1994), Describing non-Fickian water-vapour sorption in wood, Journal of Materials Science 29, pp. 2367–2372

Wenker J. and Welling J. (2017), Klimaversuche für den Baustelleneinsatz, Bauen mit Holz, November 2017

Wimmer R., Kläusler O., und Niemz P. (2013), Water sorption mechanisms of commercial wood adhesive films, Wood Science and Technology, Vol.47, pp. 763-775

Yiang J., Dietsch P., Oberhardt J., Simon J. (2017) Landwirtschaftliche Nutzgebäude in Holzbauweise ohne vorgebenden chemischen Holzschutz (gebrauchsklasse 0 (GK 0)) – Besondere bauliche Massnahmen in Anlehnung and DIN 68800, Intermediate Research Report, Technical University of Munich, Germany

10.2 Index of Tables

10.3 Index of Figures

Appendix A   Monitoring objects

A.1 Cable car stations in Andermatt, Nätschen and Schneehüenerstock

A.1.1 Meteorological data

The meteorological station Andermatt ANT (1438 m a.s.l.) and Gütsch ob Andermatt GUE (2283 m a.s.l.) were used for a comparison of the temperature and relative humidity of the last three years (2014-2017). The average values of the temperature are lower at station GUE whereas the extrema show a wider spread at station ANT. The relative humidity reaches values down to 20 %RH at station GUE, whereas the relative humidity did not reach values below 40 %RH at station ANT. The observed variations show that 21 % and 26 % of the values are higher than 90 %RH (20 M% moisture content) at both meteorological stations. The sunshine duration is in average 5 hours per day in GUE and 4.2 hours per day in ANT. The reason could be shadow from the mountains or clouds in the valley.
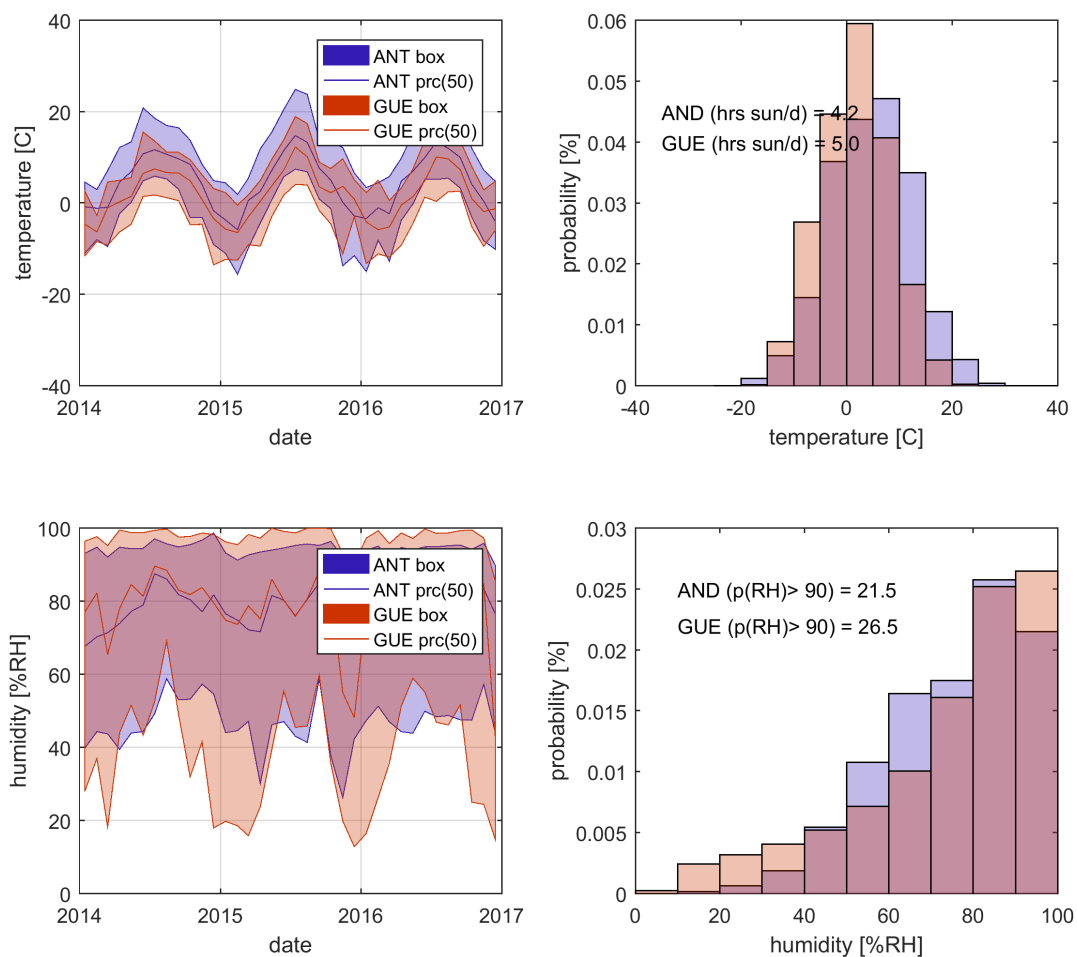
Figure 1: Climate data of meteo station Andermatt ANT and Gütsch ob Andermatt GUE between 2014 and 2017

A.1.2 Structures and measured data

Table 1: Fact sheet – Andermatt

Address	Talstation Seilbahn Andermatt
	Gotthardstrasse 2, 6490 Andermatt
Building information	▪ Cable car station ▪ Altitude 1500 m a.s.l. ▪ Building volume: 9.3 m in width, 31.9 m in length and 8 to 9 m in height ▪ Unheated and uncontrolled climate ▪ Large openings to outside, in winter period two sides are open during operation hours
Structure/Material	▪ Spruce Glulam ▪ Dimension of member b/h = 480/840mm (M1) 480/926 mm (M2) ▪ Surface protection – None
Erection	Summer 2017
Measuring period	Start: August 2017, for up to 3 years
Measuring values	▪ Measuring frequency of 3 hours

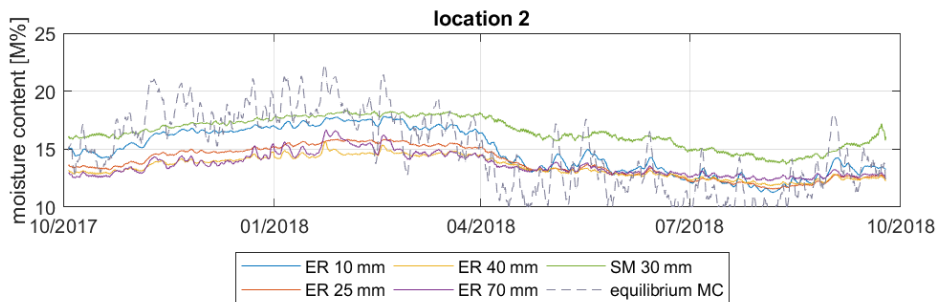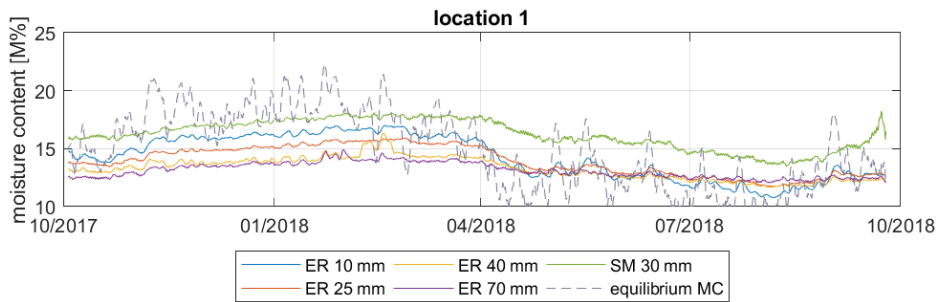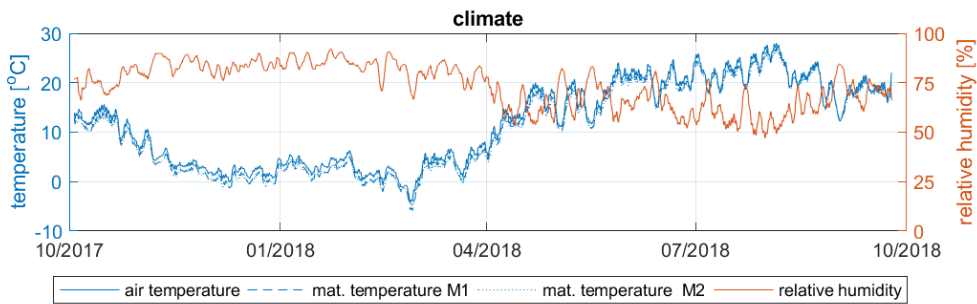| Measuring point 1	Measuring point 2
Climate (%RH/T) 30 mm	Climate (%RH/T) 30 mm
Temperature 25 mm	Temperature 25 mm
Electrical resistance 7 mm	Electrical resistance 7 mm
Electrical resistance 25 mm	Electrical resistance 25 mm
Electrical resistance 50 mm	Electrical resistance 50 mm
Electrical resistance 75 mm	Electrical resistance 75 mm

Floor plan and sectional views

Picture of measuring devices
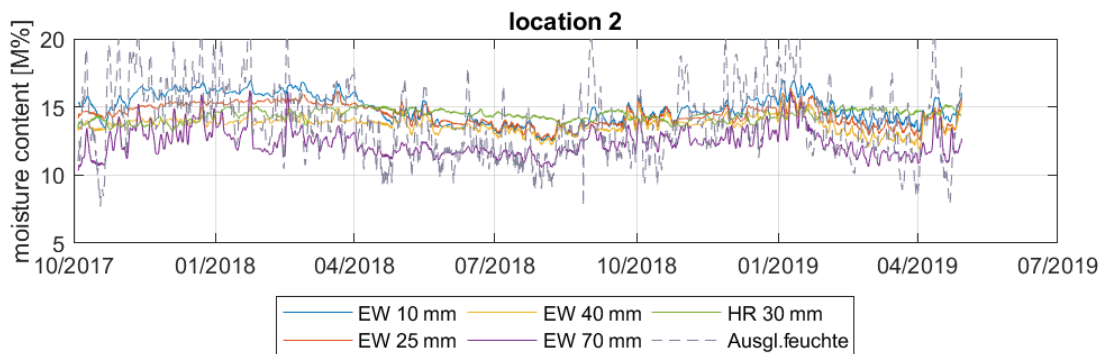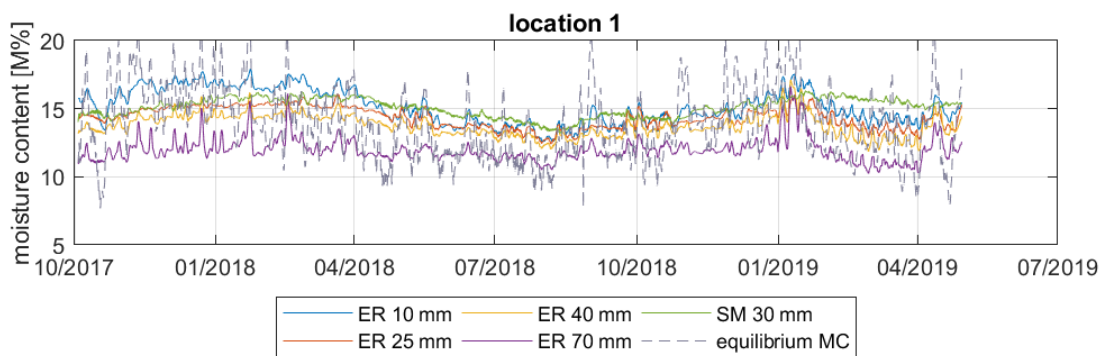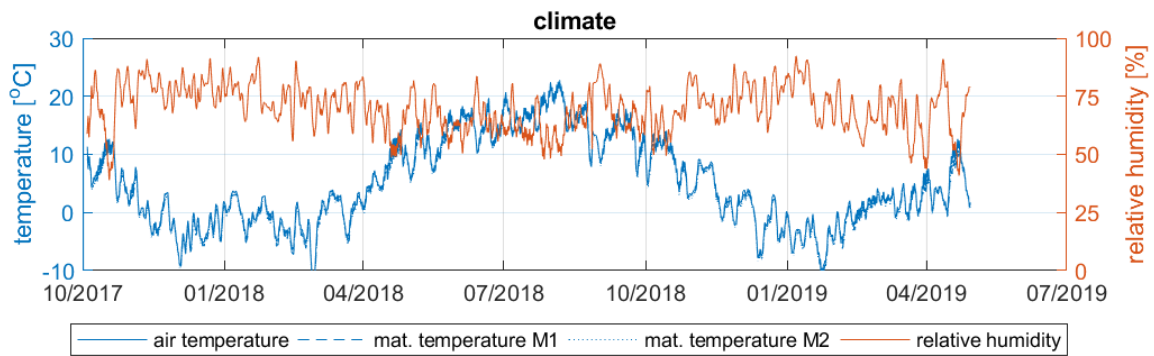
Figure 2: Measured climate and moisture content in the cable car station of Andermatt

Table 2: Fact sheet – Andermatt-Nätschen

Address	Mittelstation Seilbahn Andermatt-Nätschen
	Nätschen 1, 6490 Andermatt
Building information	▪ Cable car station
	▪ Altitude 1900 m a.s.l.
	▪ Building volume: 32 m in width, 35 m in length and up to 8 m in height
	▪ Unheated and uncontrolled climate
	▪ Two openings at south side and complete open on north side
Structure/Material	▪ Spruce Glulam
	▪ Dimension of member b/h = 280 mm/920 mm (M1) and 200 mm/560 mm (M2)
	▪ Surface protection – None
Erection	Summer 2017
Measuring period	Start: 4. October 2017, for up to 3 years
Measuring values	▪ Measuring frequency of 3 hours

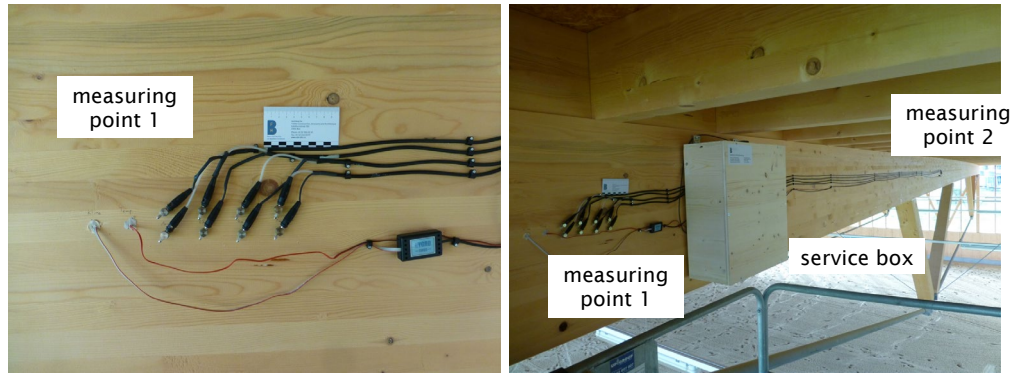| Measuring point 1	Measuring point 2
Climate (%RH/T) 40 mm	Climate (%RH/T) 40 mm
Temperature 30 mm	Temperature 30 mm
Electrical resistance 10 mm	Electrical resistance 10 mm
Electrical resistance 25 mm	Electrical resistance 25 mm
Electrical resistance 40 mm	Electrical resistance 40 mm
Electrical resistance 70 mm	Electrical resistance 70 mm

Floor plan and sectional views

Measuring
devices

Figure 3: Measured climate and moisture content in the cable car station of Nätschen

Table 3: Fact sheet – Schneehüenerstock

Address	Schneehüenerstock 6490 Andermatt
Building information	▪ Cable car station ▪ altitude 2600 m.a.s.l. ▪ Building volume chair lift: approximately 17.8 m wide, 16.9 m long and 9 m high ▪ Unheated and uncontrolled climate ▪ Large openings to outside, in winter period two sides are open during operation time
Structure/Material	▪ Spruce Glulam ▪ Dimension of instrumented member b/h = 360 mm/560 mm (M1) und 160 mm/200 mm (M2) ▪ Surface protection – None
Erection	Autum 2017
Measuring period	Start: December 2017, for up to 2 years
Measuring values	▪ Measuring frequency of 3 hours

Measuring point 1	Measuring point 2
Climate (%RH/T) 40 mm	Climate (%RH/T) 40 mm
Temperature 30 mm	Temperature 30 mm
Electrical resistance 7 mm	Electrical resistance 7 mm
Electrical resistance 25 mm	Electrical resistance 25 mm
Electrical resistance 50 mm	Electrical resistance 50 mm
Electrical resistance 75 mm	Electrical resistance 75 mm

Floor plan and sectional views

Measuring
devices

Figure 4: Measured climate and moisture content in the cable car station of Schneehüenerstock

A.2 Riding rink Kobiboden in Einsiedeln

A.2.1 Meteorological data

The meterological data shows that Einsiedeln (EIN) is a very wet region. The relative humidity exceeded 90 %RH (20 M% moisture content) for 45 % during the last 3 years, especially during the winter in 2016. The temperatures were below 30 °C due to the greater altitude. The sunshine duration was 4.5 h per day in average over the last 3 years.
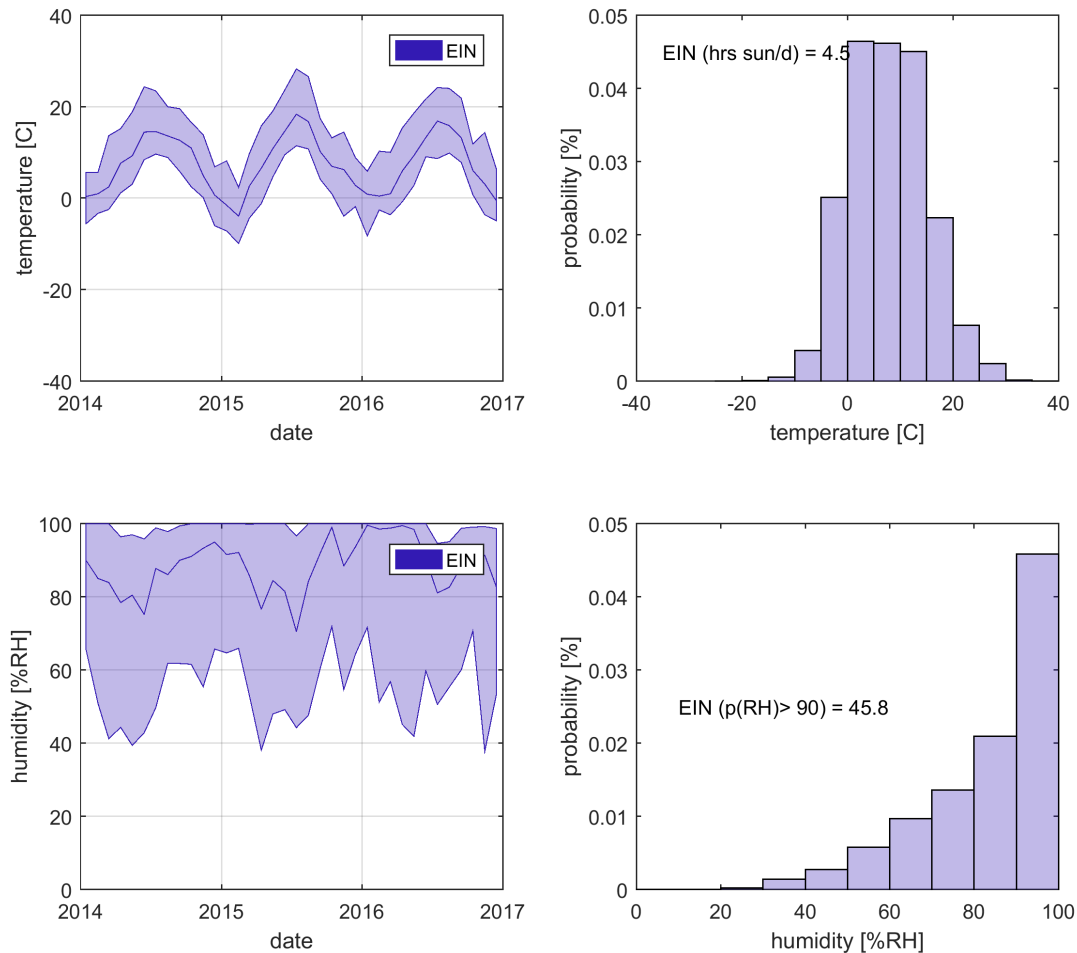
Figure 5: Climate data of meteo station Einsiedeln between 2014 and 2017

A.2.2 Facts and Data

Table 4: Fact sheet – Riding rink Kobiboden in Einsiedeln

Address	Riding rink Kobiboden in Einsiedeln
	Steig, 8840 Einsiedeln
Building information	▪ Riding rink ▪ altitude 880 m a.s.l. ▪ Building volume: 36 m in width, 90 m in length and 7.30 m in height ▪ Unheated and uncontrolled climate ▪ Wet floor of loamy soil ▪ Opening gap over complete between window panel and wooden structure
Structure/Material	▪ Trussed beam system ▪ Spruce Glulam ▪ Dimension of member b/h = 400/960 mm ▪ Surface protection – None
Erection	Summer 2017
Measuring period	Start: August 2017, for 1 up to 3 years
Measuring values	▪ 2 Measuring points, measuring frequency of 3 hours ▪ Electrical resistance: 7 / 25 / 50 / 70 mm ▪ Temperature: 25 ▪ Climate: 30 mm
Measuring values	▪ Measuring frequency of 3 hours

Measuring point 1	Measuring point 2
Climate (%RH/T) 30 mm	Climate (%RH/T) 30 mm
Temperature 25 mm	Temperature 25 mm
Electrical resistance 7 mm	Electrical resistance 7 mm
Electrical resistance 25 mm	Electrical resistance 25 mm
Electrical resistance 50 mm	Electrical resistance 50 mm
Electrical resistance 75 mm	Electrical resistance 75 mm

Floor plan and sectional views

Measuring
devices

Figure 6: Measured climate and moisture content in the riding hall in Einsiedeln

A.3 Open Ice rinks

A.3.1 Meteorological data

Delémont DLM (439 m.a.s.l.) + la Chaux-de-Fonds CDF (1017 m.a.s.l.)

The temperatures in DLM are slightly higher as in CDF during the last 3 years. The relative humidities in DLM are above 90 %RH (20 M% moisture content) during 45 % of the last 3 years. The sunshine duration is 10 % longer in CDF compared to DLM. The reason could be a cloud layer quite often in the DLM region.
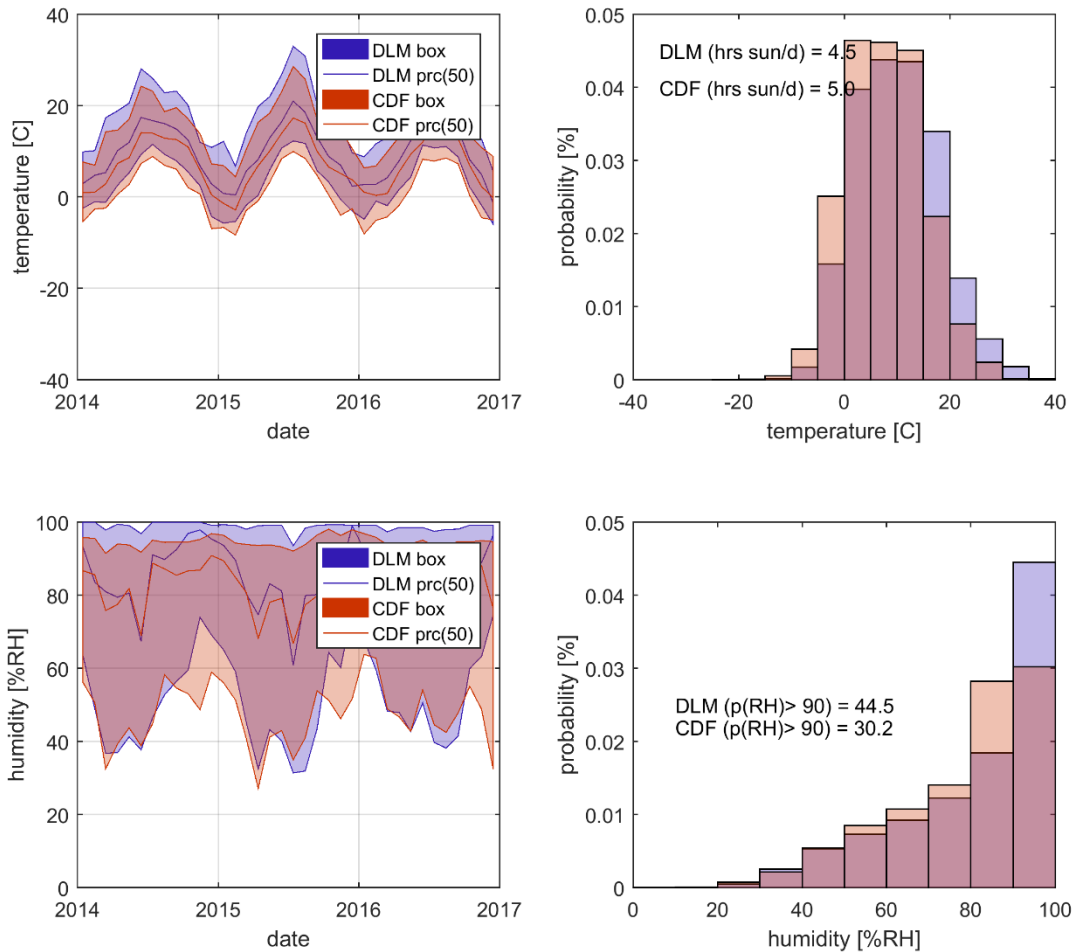
Figure 7: Climate data of meteo station Delémont and la Chaux-de-Fonds between 2014 and 2017

A.3.2 Facts and Data

Table 5: Fact sheet – Ice rink Delémont

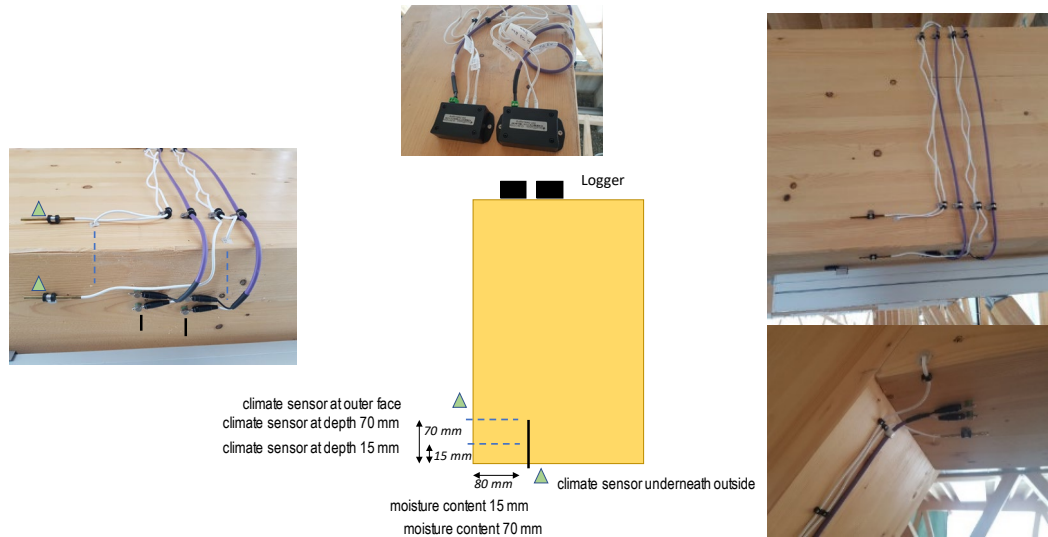|	
Address	Delémont
	Rue de la Blancherie 4, 2800 Delémont
Building information	▪ Ice rink, open ▪ Altitude 420 m a.s.l. ▪ Building volume: 60 m in length, 45 m in width ▪ Two sites are closed, south side tribune installed ▪ Unheated and uncontrolled climate
Structure/Material	▪ Truss System ▪ Structure made of spruce and larch (partial) glulam ▪ Dimension of member b/h = 320 mm/660 mm ▪ Surface protection – Unknown
Erection	2011
Measuring period	Start: August 2017, for 1 up to 3 years
Measuring values	▪ Measuring frequency of 3 hours

Measuring point 1	Measuring point 2
Climate (%RH/T) Temperature 20 mm Electrical resistance 15 mm	Electrical resistance 15 mm

Floor plan and sectional views

cross section

climate
measuring point 1 (15 mm)
temperature (20 mm)

66 cm
31 cm

measuring point 2 (15 mm)

15 cm
32 cm

side view

Logger

moisutre content
handheld device

40 cm
20 cm
20 cm
70 cm

Measuring devices

logger (2x)

measuring point 1
temperature/climate

measuring point 2
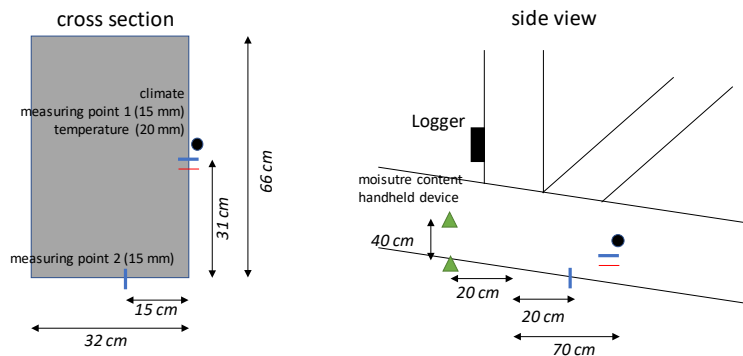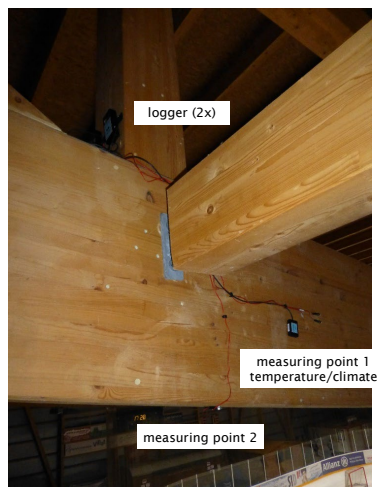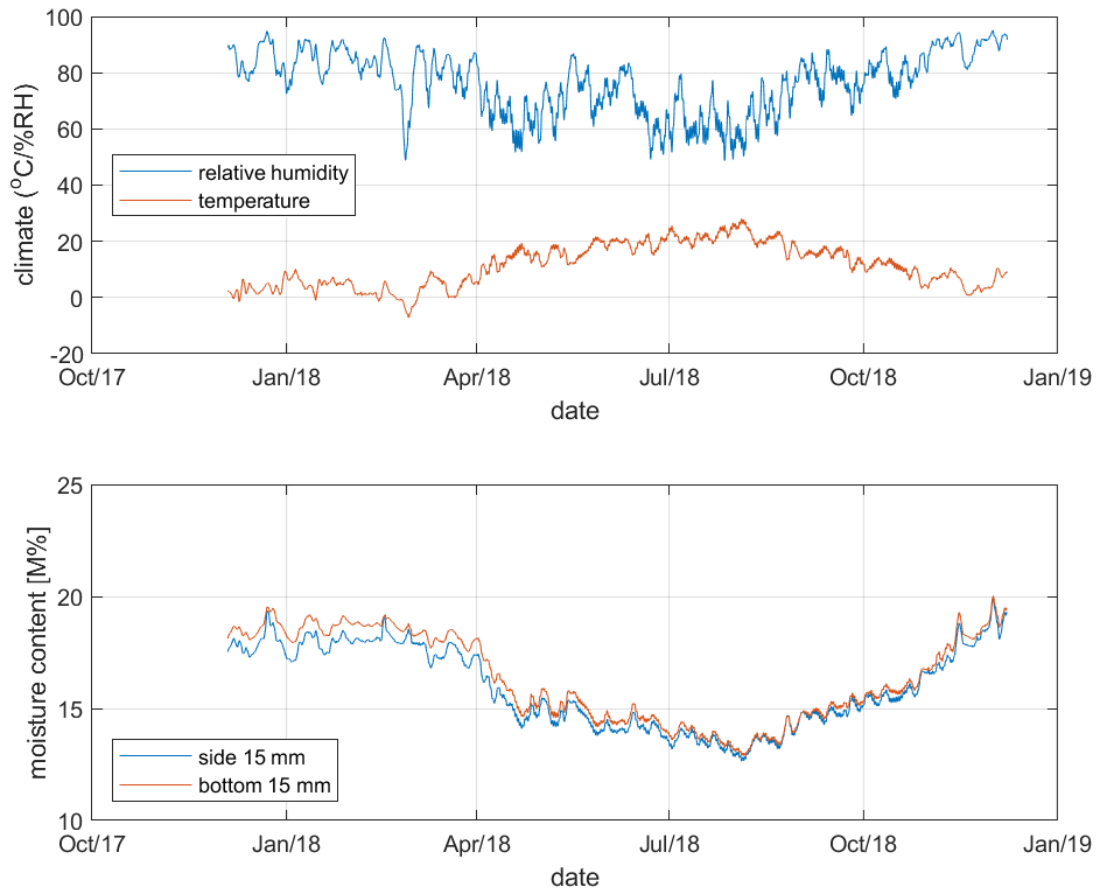
Figure 8: Measured climate and moisture content in the ice rink of Delémont

Table 6: Fact sheet – Ice rink Le Locle

Address	Le Locle
	Route du Communal 5, 2400 Le Locle
Building information	▪ Ice rink, open ▪ Altitude 1030 m a.s.l. ▪ Building volume: 60 m in length, 45 m in width ▪ West side closed, north and south side half closed, east side open, façade ends 60-80 cm before roof, relative good ventilation through opening gap ▪ Unheated and uncontrolled climate
Structure/Material	▪ Truss System ▪ Structure made of spruce glulam ▪ Dimension of member b/h = 360 mm/700 mm ▪ Surface protection – Unknown
Erection	2004
Measuring period	Start: August 2017, for 1 up to 3 years
Measuring values	▪ Measuring frequency of 3 hours

Measuring point 1	Measuring point 2
Climate (%RH/T) Temperature 20 mm Electrical resistance 15 mm	Electrical resistance 15 mm

Plans and sectional views

cross section

climate
measuring point 1 (15 mm)
temperature (20 mm)
70 cm
32 cm
measuring point 2 (15 mm)
15 cm
36 cm

side view

moisture content
handheld device
400 cm
110 cm
Logger

Measuring devices

measuring point 1
temperature / climate

measuring point 2
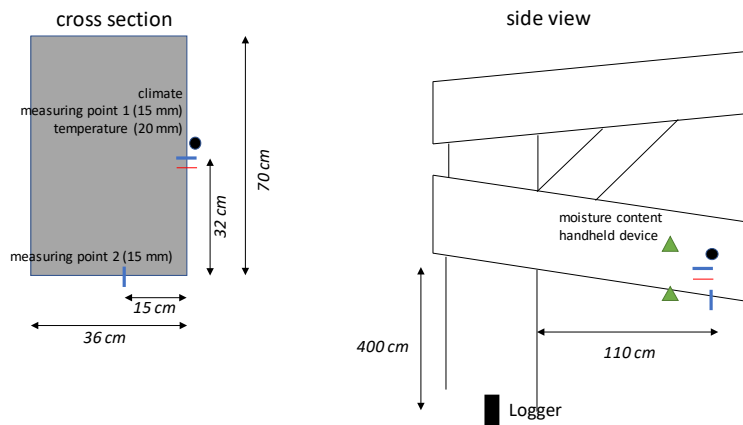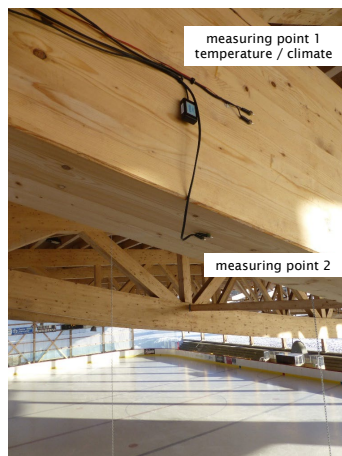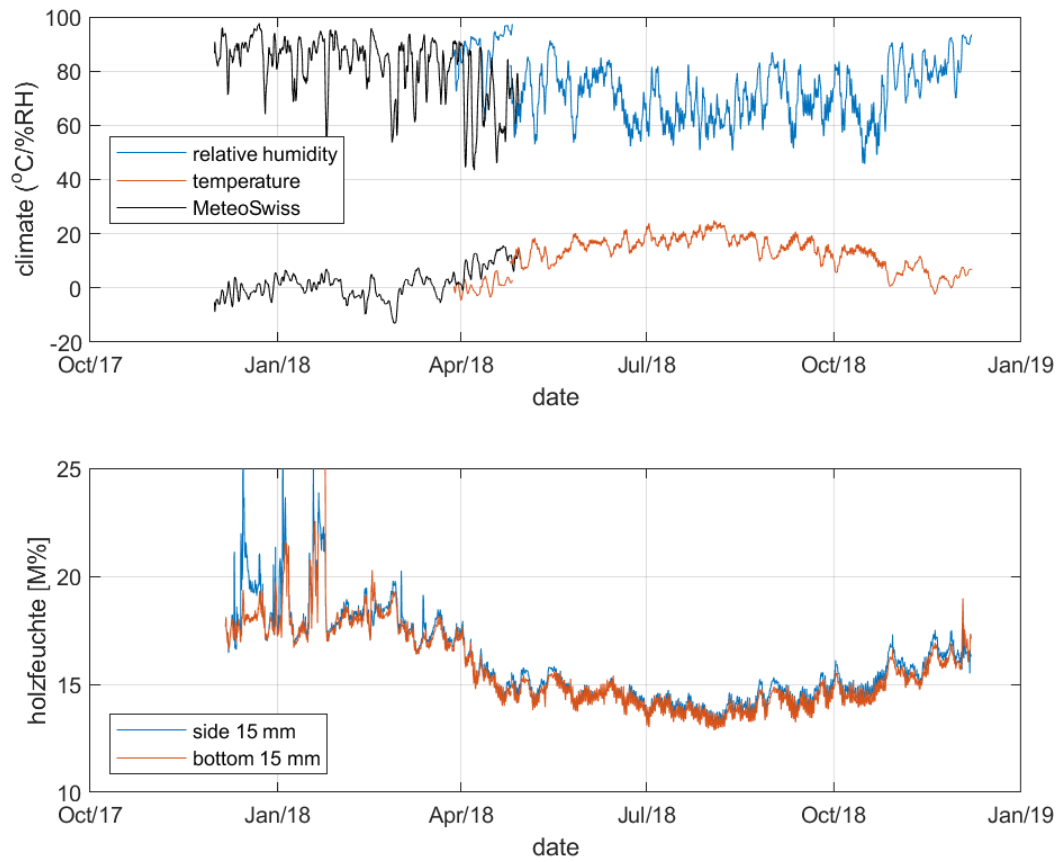
Figure 9: Measured climate and moisture content in the ice rink of Le Locle

A.4 Ice rink closed

A.4.1 Meteorological data of Davos

Davos DAV (1594 m.a.s.l.)

Most of the temperatures in DAV are found between 0˚C and 10˚C between 2014 and 2017. The relative humidities in DAV are over 90 %RH (20 M% moisture content) for only 23 % of the time. The average relative humidity is found around 80 %RH.
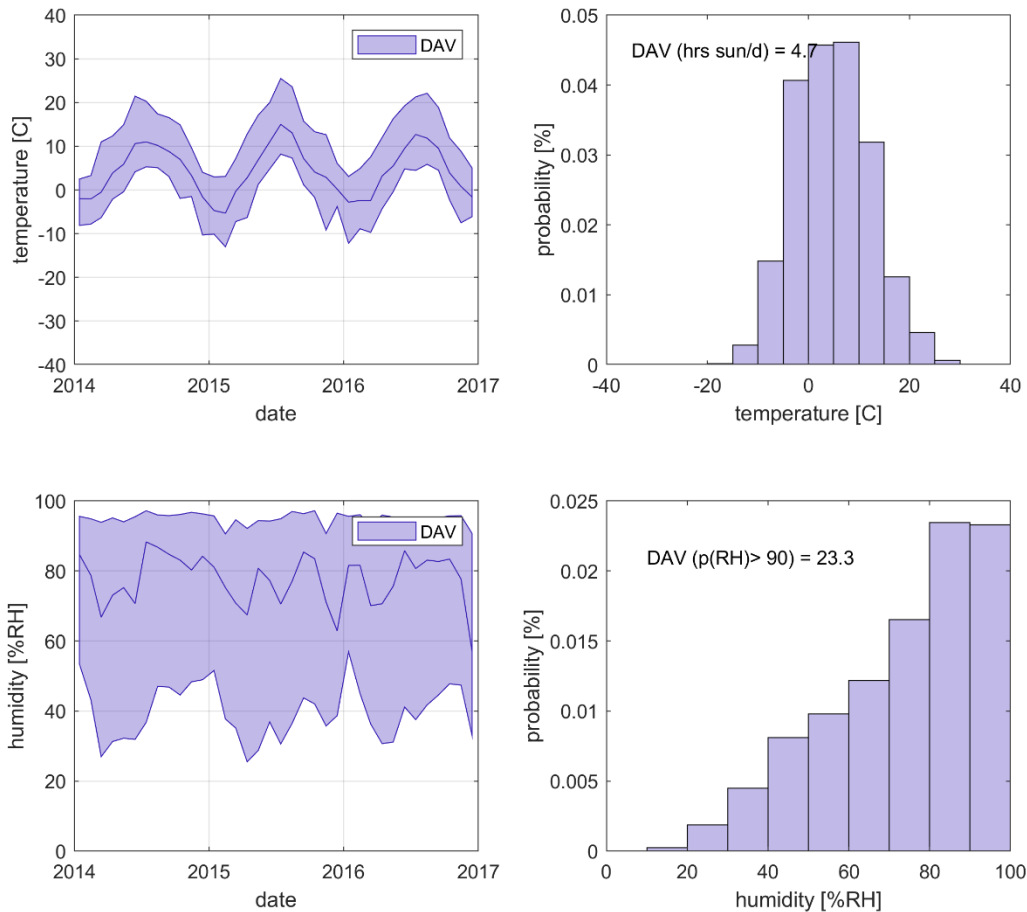
Figure 10: Climate data of meteo station Davos between 2014 and 2017

A.4.2 Building and Measurements

Table 7: Fact sheet – Ice rink Davos

Address	Davos
	Eisbahnstrasse, 7270 Davos
Building information	▪ Ice rink, closed building envelope ▪ Altitude 1560 m a.s.l. ▪ Building volume: 66 m long, 47 m wide and 11m high ▪ Heated gym rooms above ice rink on galleries ▪ Controlled climate, dehumidifier for ice rink area
Structure/Material	▪ Truss System ▪ Structure made of spruce glulam ▪ Dimension of member b/h = 480 /680 mm ▪ Surface protection – unknown
Erection	2018
Measuring period	Start: 28. August 2018, for 1 up to 3 years

Measuring values	▪ Measuring frequency of 1 hours			
	Axis I – End grain	**Axis I** – Mid span	**Axis K** – End grain	**Axis K** – Mid span
	<u>Underneath</u> Climate (%RH/T) surface Climate (%RH/T) 15 mm Moisture content 15 mm	<u>Underneath</u> Climate (%RH/T) surface Climate (%RH/T) 15 mm Moisture content 15 mm	<u>Underneath</u> Climate (%RH/T) surface Climate (%RH/T) 15 mm Moisture content 15 mm	<u>Underneath</u> Climate (%RH/T) surface Climate (%RH/T) 15 mm Moisture content 15 mm
	<u>Side surface</u> Climate (%RH/T) surface Climate (%RH/T) 70 mm Moisture content 70 mm	<u>Side surface</u> Climate (%RH/T) surface Climate (%RH/T) 70 mm Moisture content 70 mm	<u>Gallery</u> Climate (%RH/T) surface Climate (%RH/T) 15 mm Moisture content 15 mm	<u>Side surface</u> Climate (%RH/T) surface Climate (%RH/T) 70 mm Moisture content 70 mm

Floor plan and sectional views

axis K

axis I   axis K

side

centre

North

Measuring devices

Logger

climate sensor at outer face
climate sensor at depth 70 mm
climate sensor at depth 15 mm

70 mm
15 mm

80 mm

climate sensor underneath outside

moisture content 15 mm
moisture content 70 mm
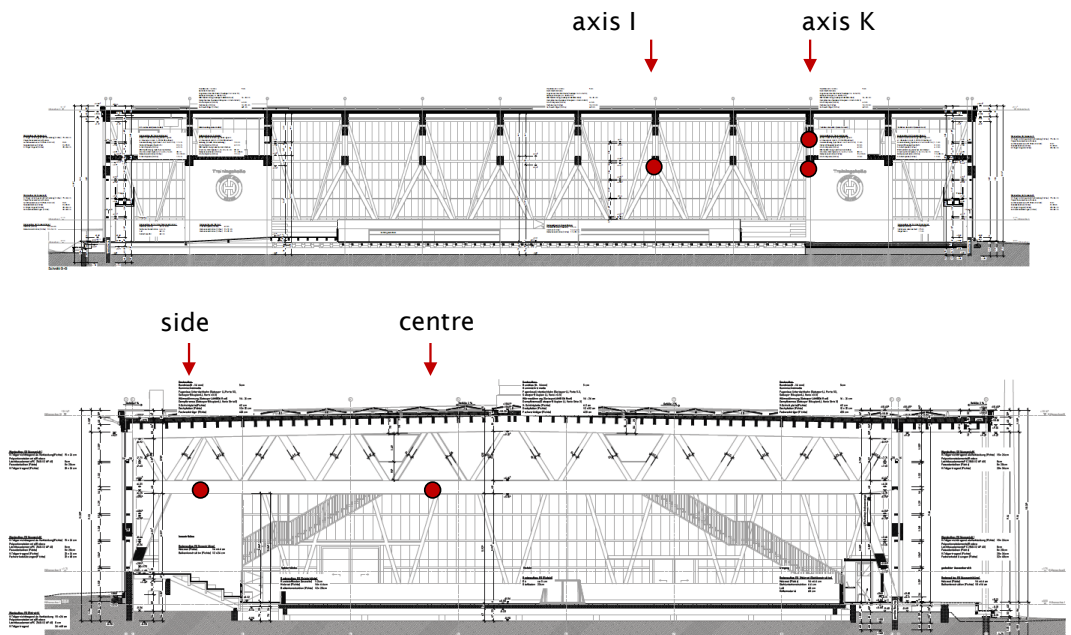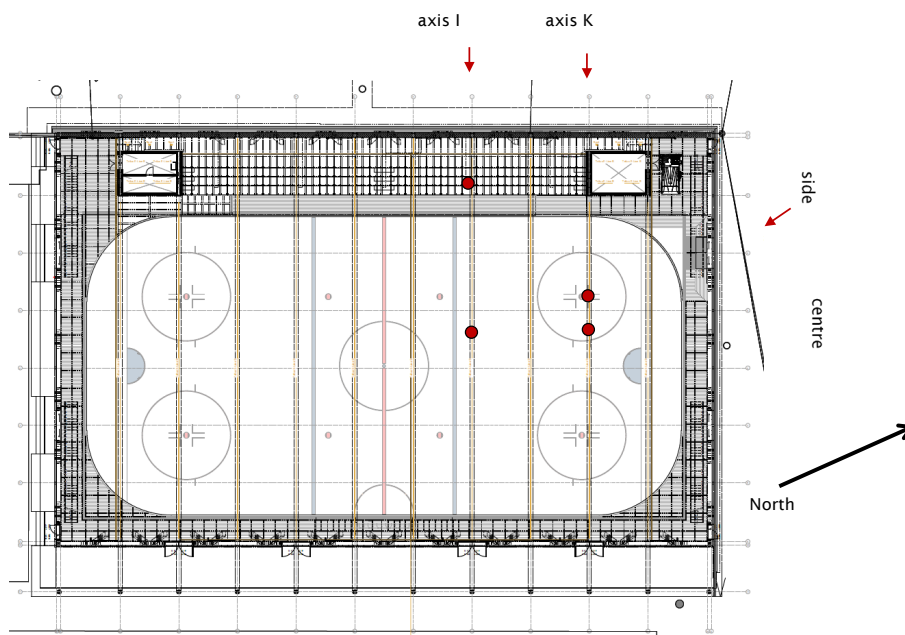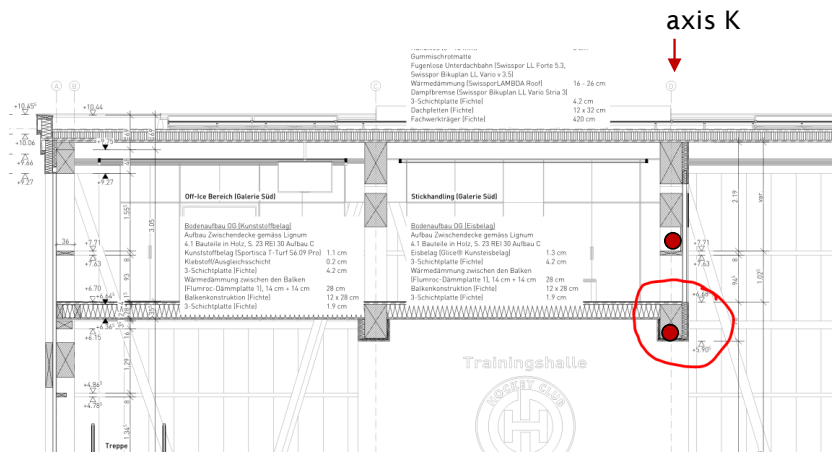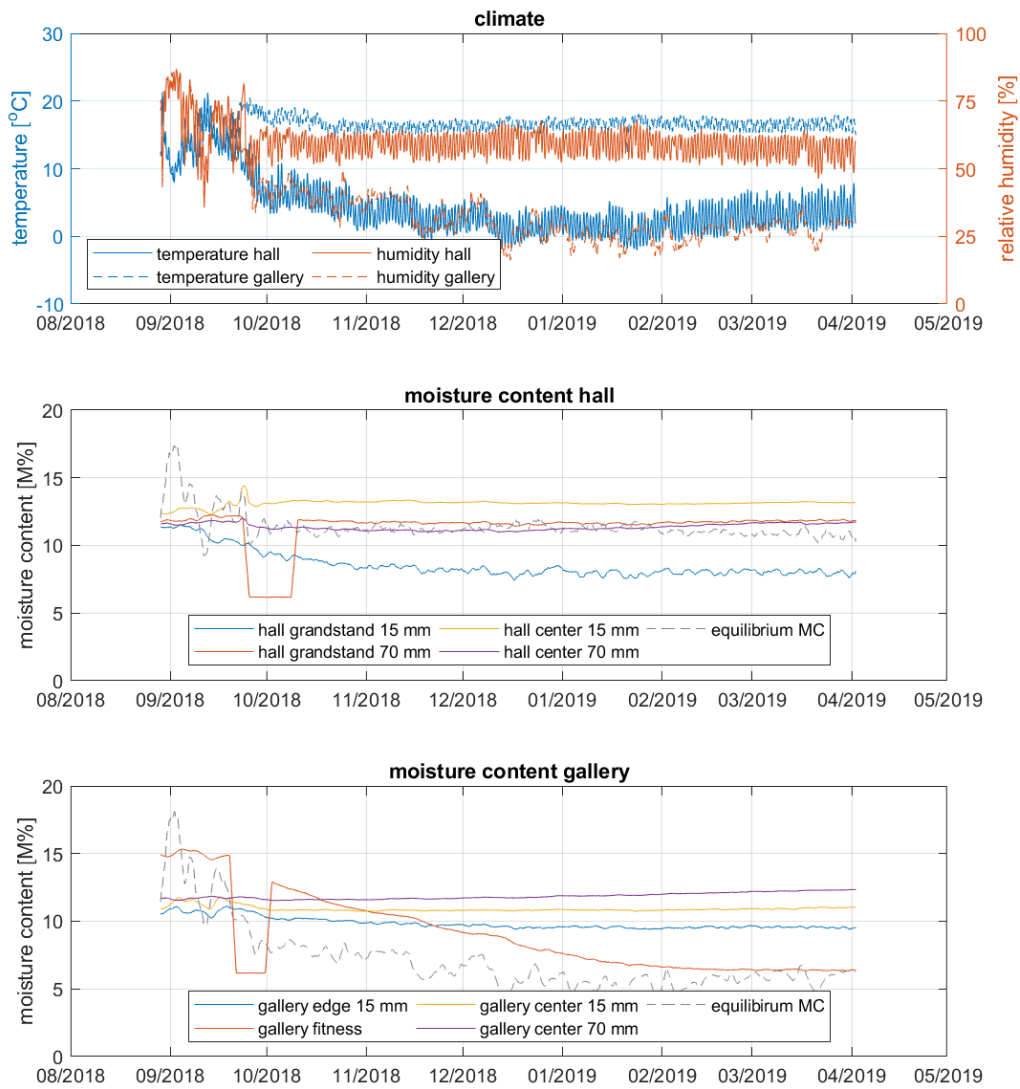
Figure 11: Measured climate and moisture content in the ice rink in Davos

A.5 Bridge - Andelfingen

Table 8: Fact sheet – Bridge Andelfingen

Address	Bridge Andelfingen
	Schaffhauserstrasse, 8451 Andelfingen
Building information	▪ Bridge, crossing water, covered
	▪ Altitude 370 m.a.s.l.
	▪ Total span of 71 m with two sections
Structure/Material	▪ Covered bridge, reinforced 2018
	▪ Reinforced with LVL of Beech
	▪ Dimension of member b/h = 300 mm/600 mm and 300 mm/500 mm
	▪ Surface protection – paint
Erection	1814
Restoration	Spring/Summer 2018
Measuring period	Start: June 2017, for 1 up to 3 years
Measuring values	▪ Measuring frequency of 1 hours
	▪ Climate sensor

Measuring point 1	Measuring point 1	Block 1	Block 2
Electrical resistance 15 mm	Electrical resistance 15 mm	Electrical resistance 15 mm	Electrical resistance 15 mm
Electrical resistance 40 mm	Electrical resistance 40 mm	Electrical resistance 40 mm	Electrical resistance 40 mm
Temperature 50 mm	Temperature 50 mm	Climate 30 mm	Climate 30 mm

Floor plan and sectional views

Measuring devices

measuring point 1

measuring point 2
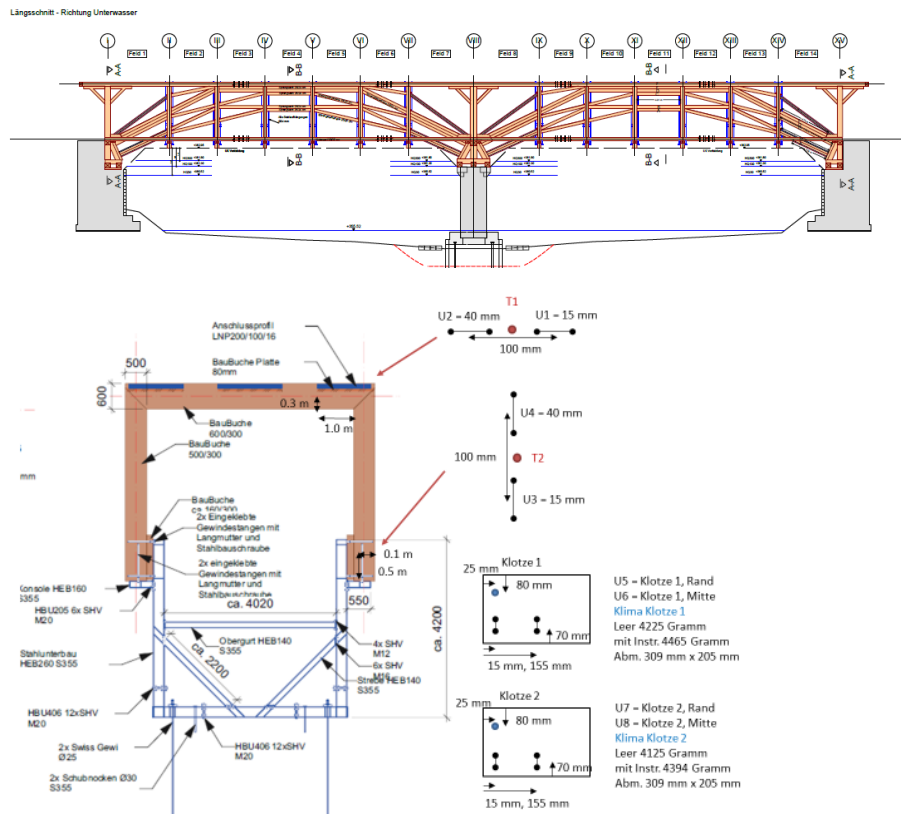
measuring point - blocks
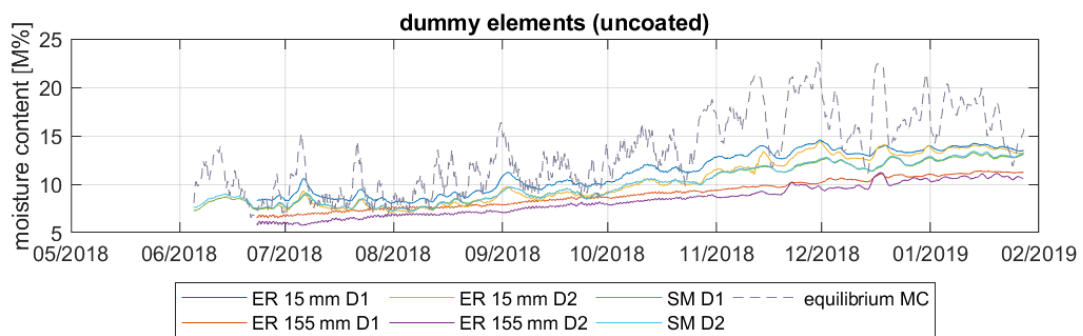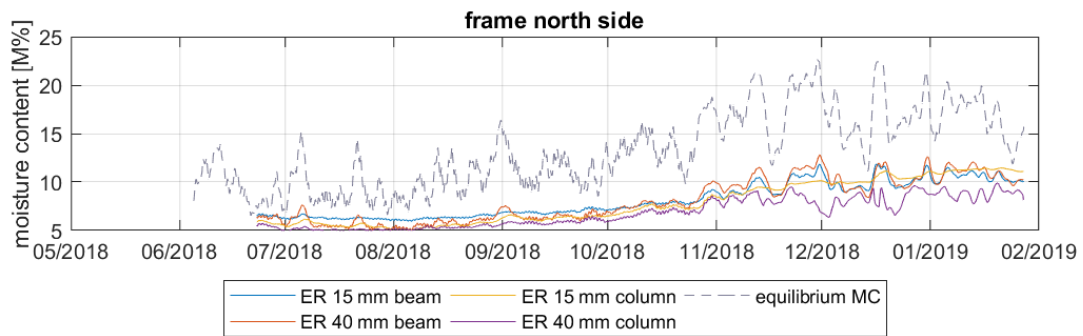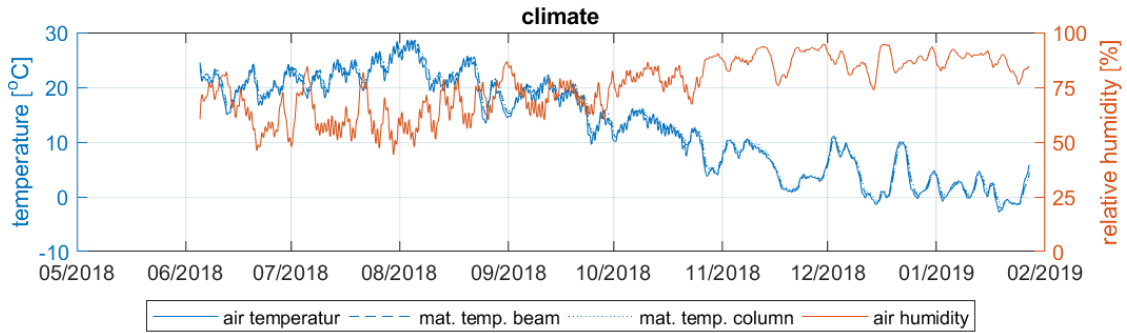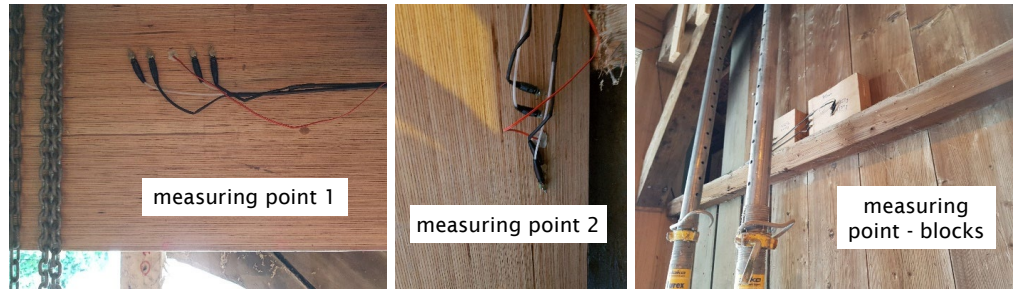
Figure 12: Measured climate and moisture content on the bridge in Andelfingen

A.6 Bridge - Bubenei

Table 9: Fact sheet – Bridge Bubenei

Address	Bridge Bubenei
	Bubenei, 3535 Signau
Building information	▪ Bridge, crossing water, covered ▪ Altitude 680 m.a.s.l. ▪ Total span of 45 m ▪ Traffic load 40 tons
Structure/Material	▪ Main load bearing system are two arches ▪ Original structure made from Spruce solid wood ▪ Dimension of member b/h = various ▪ Surface protection – None
Erection	1814
Restoration	Spring/Summer 2018
Measuring period	Start: July 2012
Measuring values	▪ 24 Measuring points (8 at the transition of the road to the bridge on west side 8 along the span 8 at the transition of the road to the bridge on east side) ▪ Measuring frequency of 3 hours ▪ Temperature, Climate
Floor plan and sectional views	
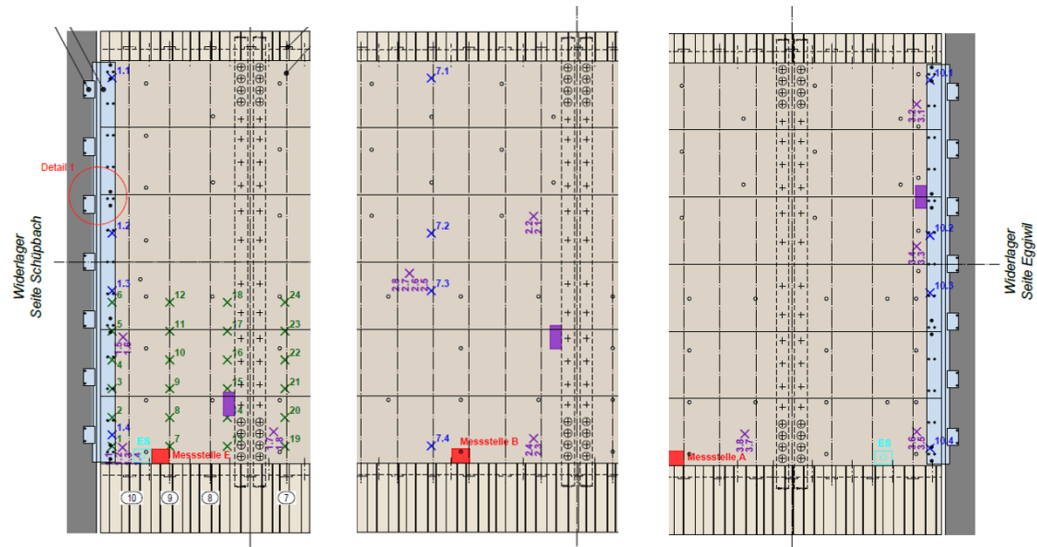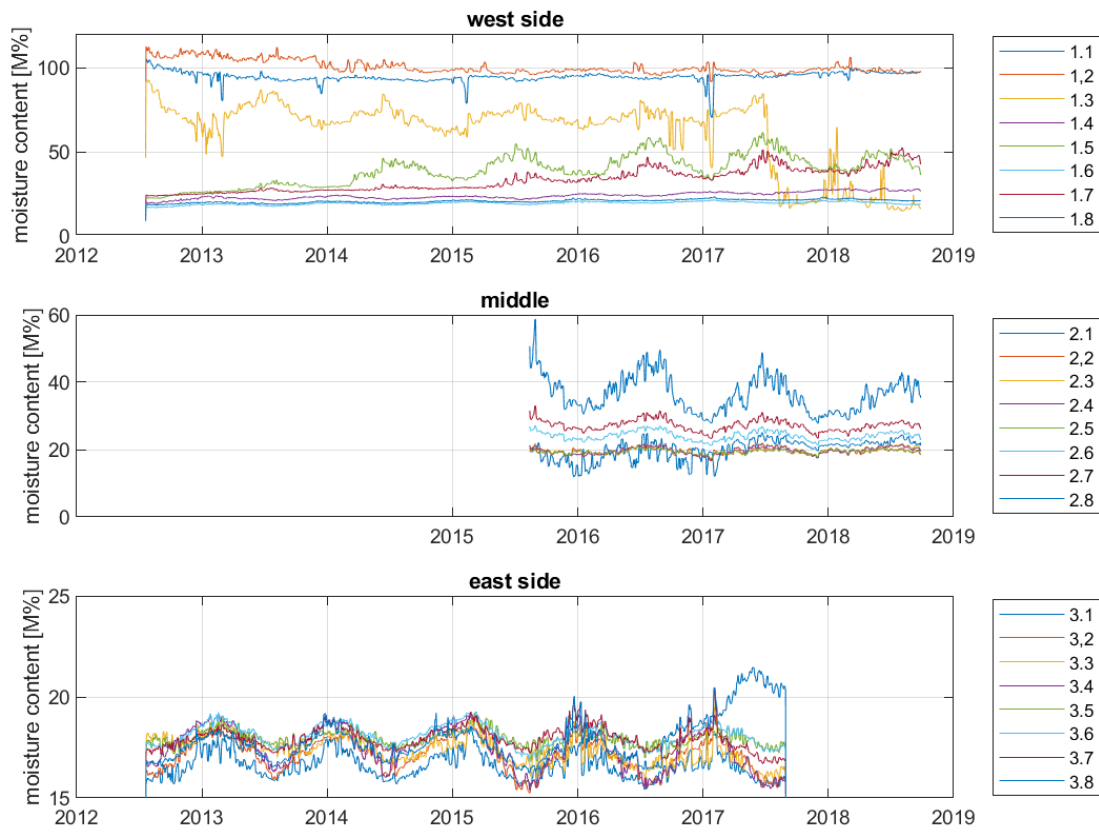
Figure 13: Moisture content measurements made on the Bubenei bridge during about six years

A.7 Bridge - Obermatt

Table 10: Fact sheet – Bridge Obermatt

Address	Bridge Obermatt
	Obermattweg, 3543 Lauperswil
Building information	▪ Bridge, crossing water ▪ Altitude 648 m a.s.l. ▪ Total span of 32 m ▪ Traffic load 40 tons
Structure/Material	▪ Main load bearing system are two beams ▪ Main members made of spruce solid wood ▪ Cross members made from Kerto ▪ Dimension of main member b/h = various
Erection	2007
Measuring period	▪ Start: December 2010 ▪ Measuring frequency of 3 hours

Measuring values	▪ 16 Measuring points
	  (8 at the transition of the road to the bridge on north side
	  8 at the transition of the road to the bridge on south side,
	  4 from this in Kerto material)
	▪ Temperature, Climate

Floor plan and sectional views

Layout of measuring points incl. sensor names

Sensornames XX_S/N_OF/T_#

HF = wood moisture content
HT = wood temperature
LF = air humidity
LT = air temperature
S = southern end of bridge
N = northern end of bridge
OF = measurement at surface
T = measurement in depth (10.5cm)
# = number
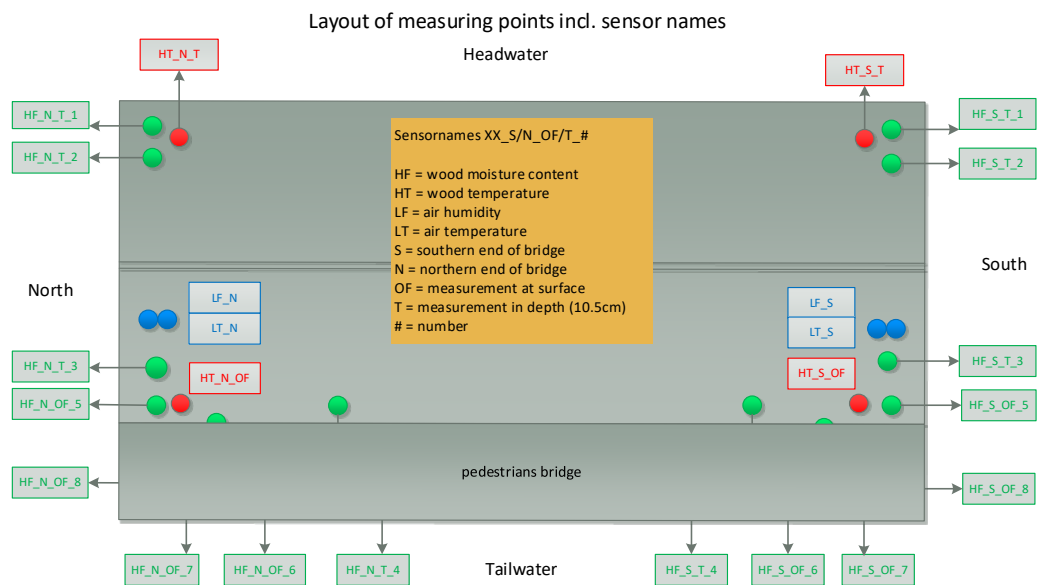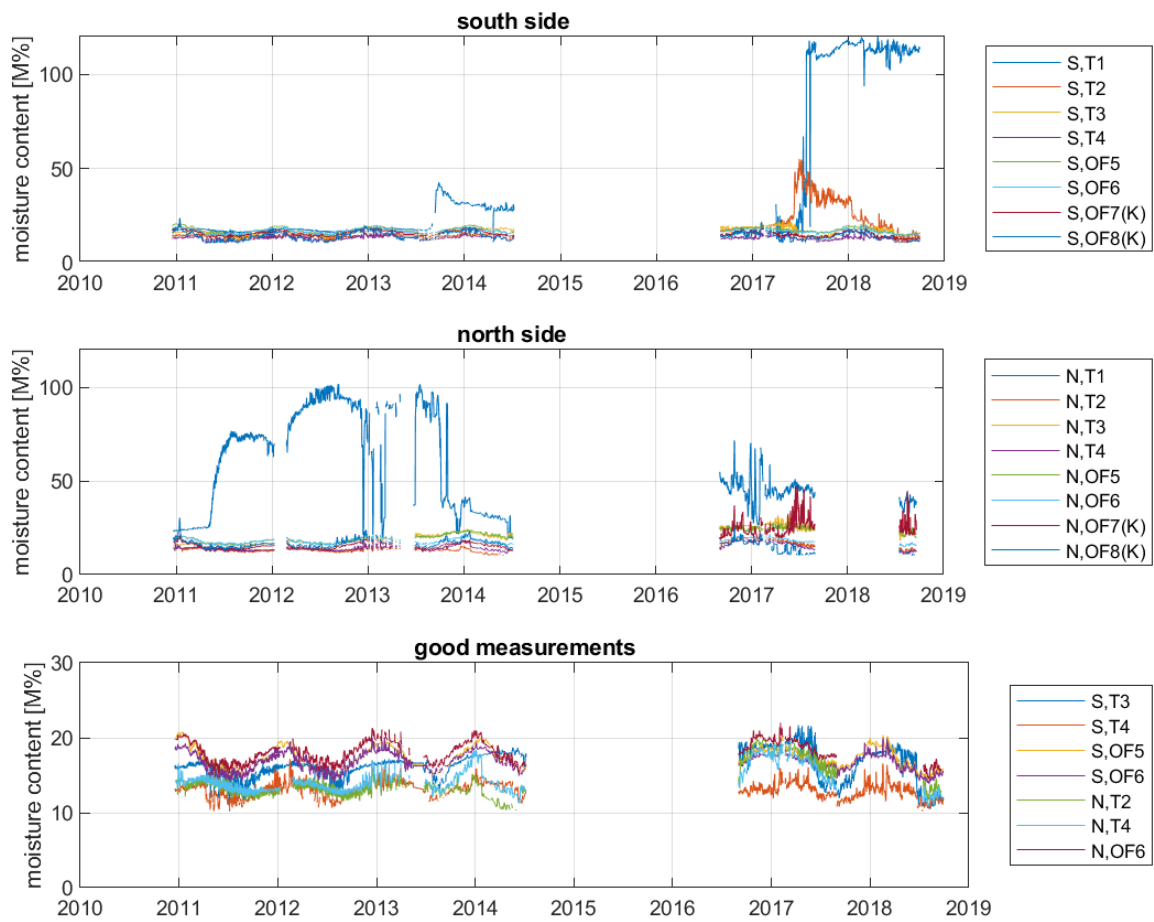
Figure 14: Measured moisture content made on the Obermatt bridge during almost eight years including a gap of two years

A.8 Bridge - Horen

Table 11: Fact sheet – Bridge Horen

Address	Bridge Horen	
Building information	▪ Open Bridge, crossing road ▪ Altitude 420 m a.s.l. ▪ Total span of 31 m ▪ Traffic load 40 tons	
Structure/Material	▪ Main load bearing system are two beams ▪ Origin structure made from Spruce block glued glulam ▪ Dimension of member b/h = 1680/500 mm end grain, b/h = 1680/1100 mm at midspan ▪ Surface protection – Yes	
Erection	2008	
Measuring period	Start: October 2009	
Measuring values	▪ 20 Measuring points (10 at the end grain of the member, west side, and 10 at the midspan of the member) ▪ Measuring frequency of 3 hours ▪ Electrical resistance: 210 /930 mm ▪ Temperature, Climate	
Floor plan and sectional views		
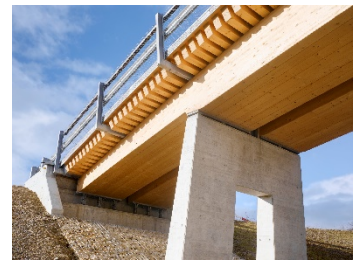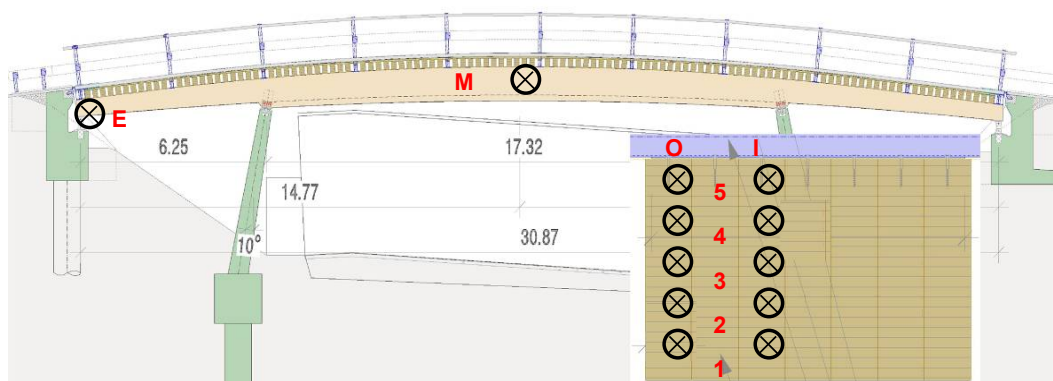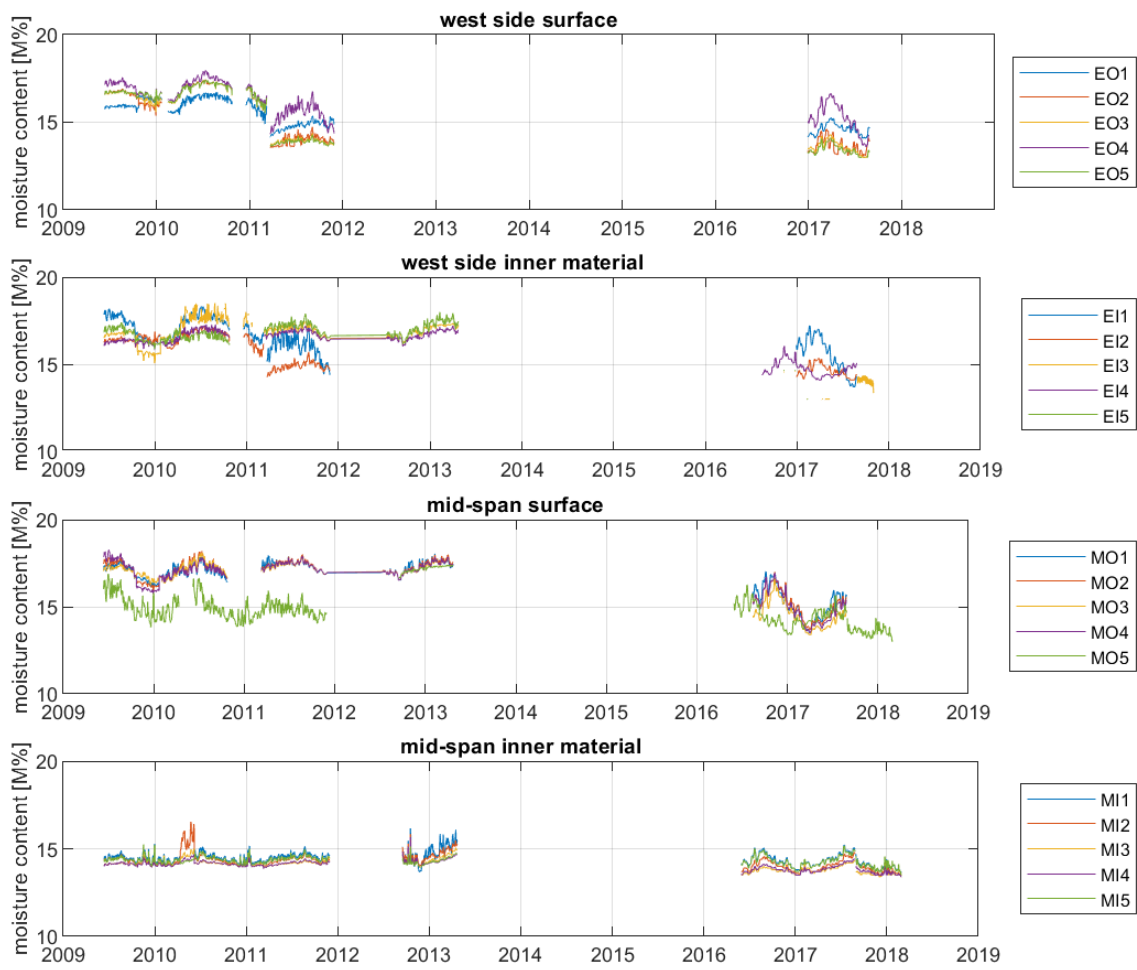
Figure 15: Measured moisture content at the Horen Bridge during almost ten years with a gap of four years

A.9 Bridge - Schachenhaus

Table 12: Fact sheet – Bridge Schachenhaus

Address	Bridge Schachenhaus
	Schachenhaus, 3555 Trubschachen
Building information	▪ Bridge, crossing water ▪ Altitude 731 m a.s.l. ▪ Total span of 20.4 m ▪ Traffic load 40 tons
Structure/Material	▪ Timber concrete composite bridge ▪ Original structure made from Spruce solid wood
Erection	2000
Measuring period	Start: March 2011- July 2014
Measuring values	▪ 8 Measuring points (at the transition of the road to the bridge on north east side) Measuring frequency of 3 hours ▪ Temperature, Climate sensor

Floor plan and sectional views

Layout of measuring points incl. sensor names
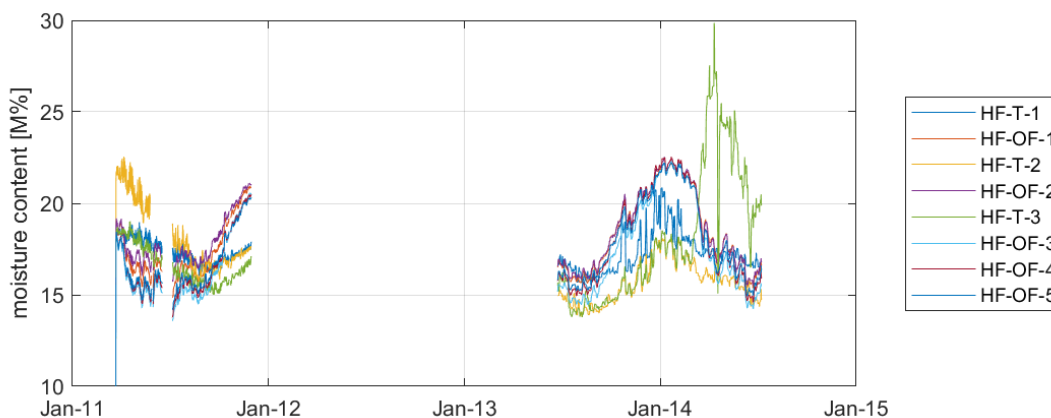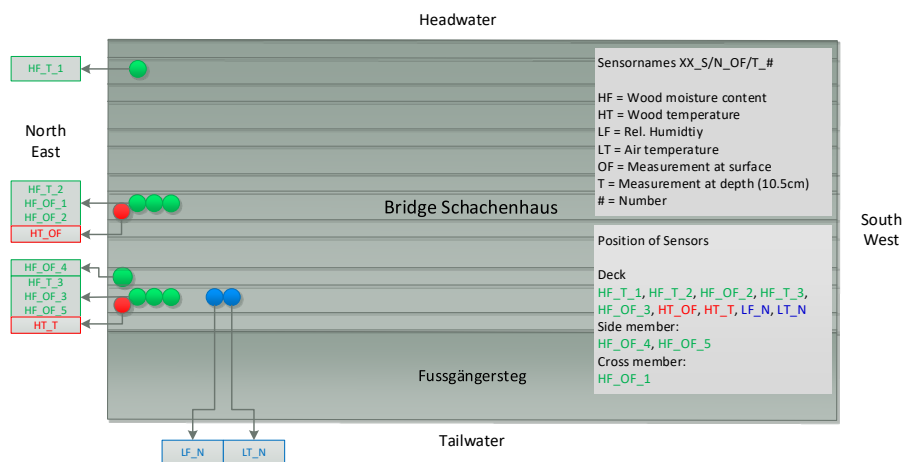
Figure 16: Measured moisture content on the Schachenhaus bridge

A.10 Bridge - Muotathal

Table 13: Fact sheet – Bridge Muotathal

Address	Bridge Muotathal
	Hundenengässli, 6436 Muotathal
Building information	• Bridge, crossing water • Altitude 615 m.a.s.l. • Total span of 33.4 m • Traffic load 40 tons
Structure/Material	• Arch bridge • Original structure made of spruce solid wood • Dimension of member b/h = 1200/900 mm
Erection	2009
Measuring period	Start: October 2009 – Dec 2011

Measuring values	• 20 Measuring points
	  (10 at 800 mm distance from end grain
	   10 at 2000 mm distance from end grain)
	• Measuring frequency of 3 hours
	• Temperature, Climate

Floor plan and sectional views	
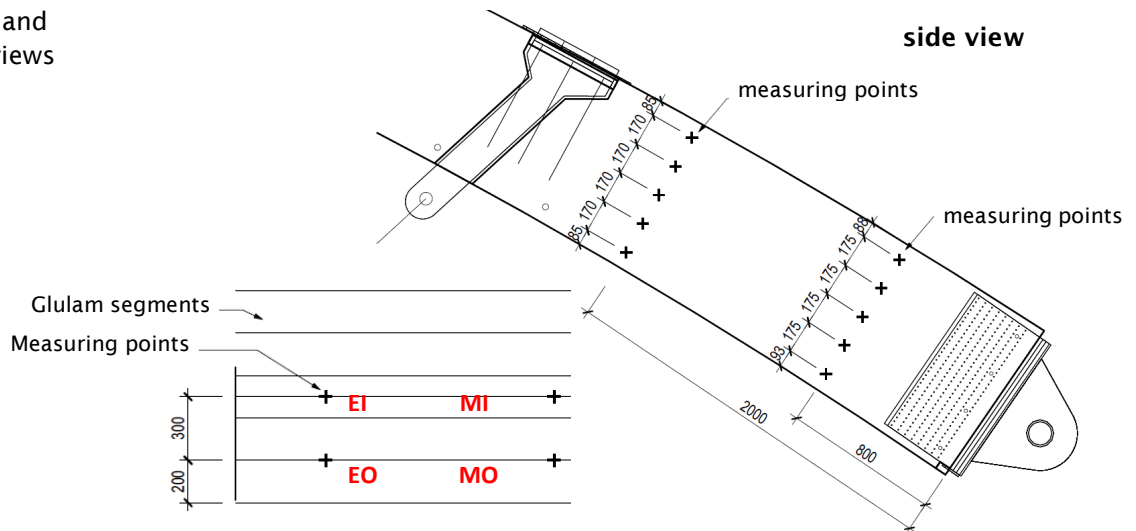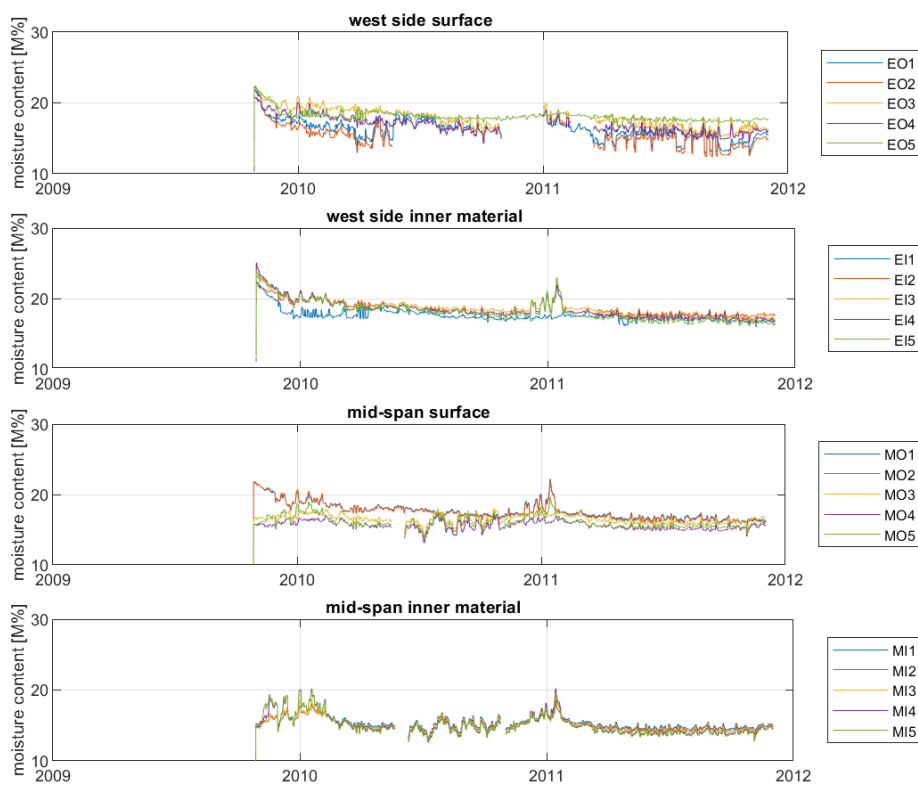
Figure 17: Measured moisture content on the bridge of Muotathal made on two different depths from the end grain of the arches

A.12 Bridge - Hoengesberg (DE) monitored by Fachhochschule Erfurt

Table 14: Fact sheet – Bridge Hoengesberg

Address	Bridge Hoengesberg (DE)

Source: FH Erfurt

Building information	▪ Bridge, crossing water and land ▪ Altitude 110 m a.s.l. ▪ Total span of 66.5 m ▪ Traffic
Structure/Material	▪ Bridge of three spans, middle span is an arch ▪ Structure made from Spruce glulam GL 28h, arch made of Spruce Glulam GL 32c ▪ Dimension of member b/h = unknown ▪ Surface protection – unknown/cladded
Erection	2014
Measuring period	Start: August 2015
Measuring values	▪ Measuring frequency of 1 hours

Measuring point 1	Measuring point 2	Measuring point 3
<u>Midspan, Side member, underneath</u>	<u>Midspan, deck, underneath</u>	<u>North side intermediate bearing, End wood</u>
Moisture content 20 mm	Moisture content 20 mm	Moisture content 20 mm
Moisture content 100 mm	Moisture content 100 mm	Moisture content 60 mm
Temperature 20 mm		Moisture content 100 mm
Climate (%RH/T) surface		Moisture content 135 mm
		Temperature 60 mm
		Climate (%RH/T) surface

Figure 18: Measured moisture content on the Hoengesberg bridge (DE) over a river (above) and over land (below)

A.13 Bridge - Schwäbis Gmünd (DE) monitored by Fachhochschule Erfurt

Table 15: Fact sheet – Bridge Schwäbis Gmünd (DE) monitored by Fachhochschule Erfurt

Address	Bridge Schwäbis Gmünd (DE)
Building information	▪ Bridge, crossing water and land ▪ Altitude 321 m a.s.l. ▪ Total span of 25.3 m ▪ Slow traffic, Pedestrian
Structure/Material	▪ Timber concrete composite bridge ▪ Structure made from Spruce glulam GL32c ▪ Dimension of member b/h =unknown mm ▪ Surface protection – unknown
Erection	2012
Measuring period	Start: 27.10.2016
Measuring values	▪ Measuring frequency of 1 hours

Source: FH Erfurt

| Measuring point 1	Measuring point 2
North side	Midspan
Moisture content 20 mm	Moisture content 20 mm
Moisture content 40 mm	Moisture content 40 mm
Moisture content 60 mm	Moisture content 60 mm
Moisture content 80 mm	Moisture content 80 mm
Temperature 60 mm	Temperature 60 mm
Climate (%RH/T) surface	Climate (%RH/T) surface

Figure 19: Measured moisture content made on the bridge of Schwäbis Gmünd (DE) for nearly two years

A.14 Bridge Werdau - (DE) monitored by Fachhochschule Erfurt

Table 16: Fact sheet – Bridge Werdau (DE) monitored by Fachhochschule Erfurt

Address	Bridge Werdau (DE)	
Building information	▪ Bridge, crossing water and land ▪ Altitude 334 m a.s.l. ▪ Total span of 15.4 m ▪ Slow traffic, Pedestrian	
Structure/Material	▪ Single span member ▪ Structure made from Spruce glulam GL 28c (Larch) ▪ Dimension of member b/h = unknown ▪ Surface protection – unknown	Source: FH Erfurt
Erection	2011	
Measuring period	Start: 23.11.2016	
Measuring values	▪ Measuring frequency of 1 hours	

Measuring point 1	Measuring point 2	Measuring point 3
<u>Bearing west side, main member</u>	<u>Bearing west side, side member</u>	<u>Midspan, main member</u>
Moisture content 20 mm	Moisture content 20 mm	Moisture content 20 mm
Moisture content 40 mm	Moisture content 40 mm	Moisture content 40 mm
Moisture content 70 mm	Temperature 40 mm	Moisture content 70 mm
Temperature 40 mm		Temperature 40 mm
Climate (%RH/T) surface		Climate (%RH/T) surface
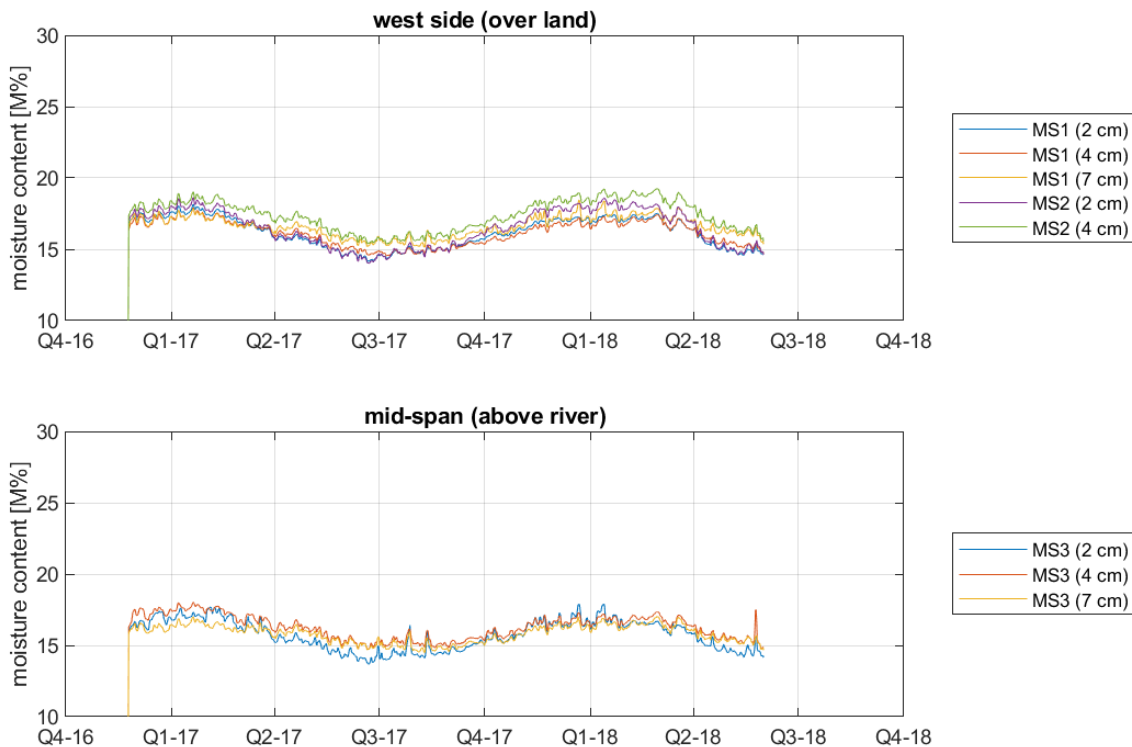
Figure 20: Measured moisture content on the bridge Werdau (DE) for nearly two years

A.15 Elephant house monitored by MAGEBA

Table 17: Fact sheet – Elephant house, Zoo Zürich, monitored by MAGEBA

Address	Zoo Zürich
Building information	▪ Hall ▪ Altitude 408 m.a.s.l. ▪ Agricultural use for Elephants
Structure/Material	▪ Main roof structure of wood, free forming shell ▪ Diameter of 85 meters, height from 1.5 – 18 m ▪ Structure made from Spruce CLT ▪ Dimension: 3 layers of 80 mm thick CLT plates ▪ Surface protection – unknown
Erection	2013/14
Measuring period	September 2014 – June 2017
Measuring values	▪ 14 Measuring points ▪ Measuring frequency various for all sensors ▪ Moisture content: Humimeter (Schaller GmbH)

Source: https://www.waltgalmarini.ch/
portfolio/elefantenanlage-zoo-zuerich/
(13.02.2019)

Floor plan and
sectional views
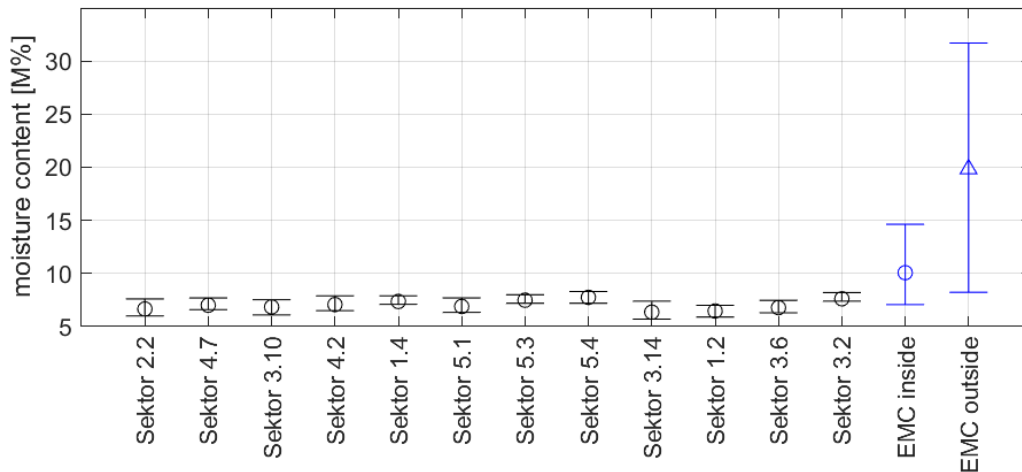
Figure 21: Box plots of wood moisture contents measured in the roof structure. The data was measured from September 2014 to June 2017. The theoretical equilibrium moisture content was calculated using data from the climate loggers in the building.

A.16 House of Natural Resources Hönggerberg Campus ETH Zurich, monitored by ETH

Table 18: Fact sheet – A.16 House of Natural Resources Hönggerberg Campus ETH Zurich, monitored by ETH

Address	House of Natural Resources
	Hönggerberg Campus ETH Zurich
Building information	▪ Office Building with three floors, ground floor made of reinforced concrete, upper floors made of timber
	▪ Altitude 525 m.a.s.l.
Structure/Material	▪ Post-tensioned timber frame and composite slabs
	▪ Timber-concrete composite slab made of a 40 mm thick LVL beech wood plate (BauBuche) and a 160mm thick concrete layer
	▪ Post-tensioned beam-column timber joint made of glued laminated timber (spruce) and local strengthening of the joint with hardwood (ash)
Erection	2014
Measuring period	September 2014 – June 2017
Measuring values	▪ 5 gages (Beech CLT)
	▪ 23 gauges façade floor C
	▪ 20 gauges façade floor D
	▪ post-processed data used (daily averages)

Source: http://www.honr.ethz.ch/fotogalerie.html (13.02.2019)
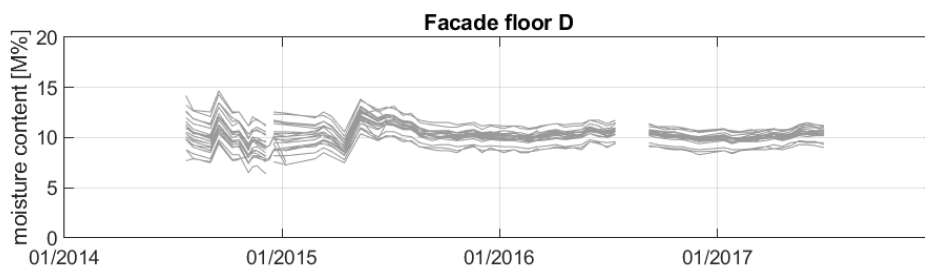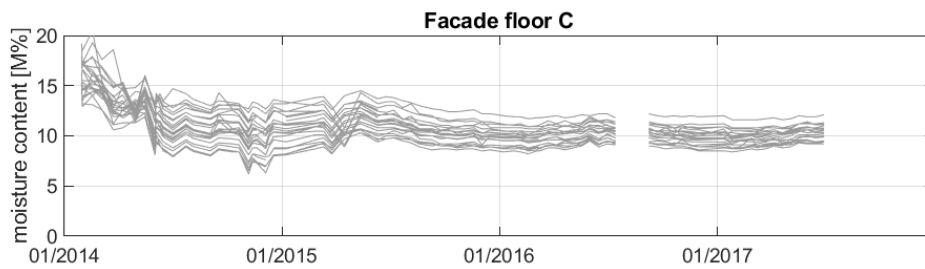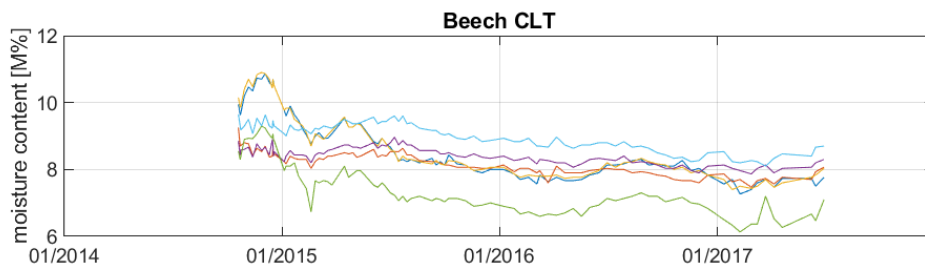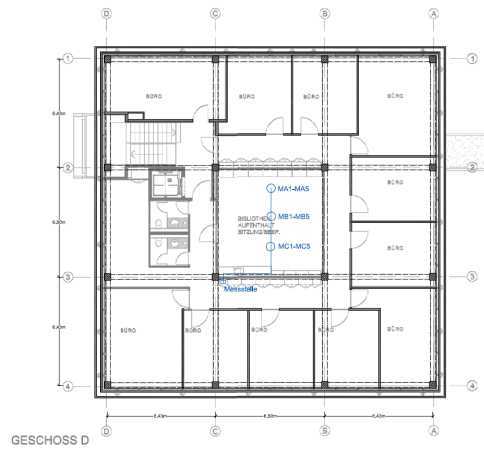
Floor plan and sectional views
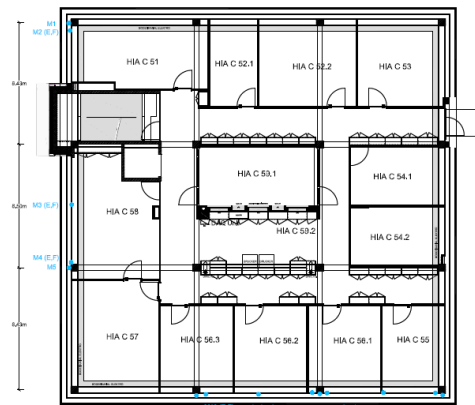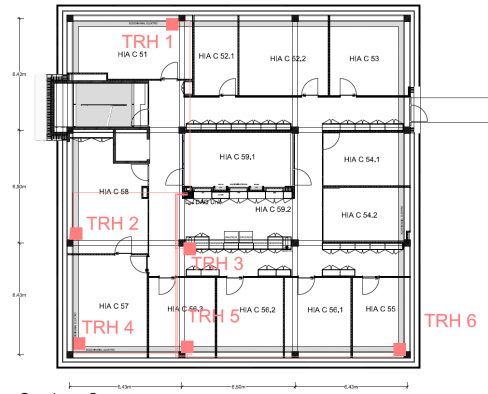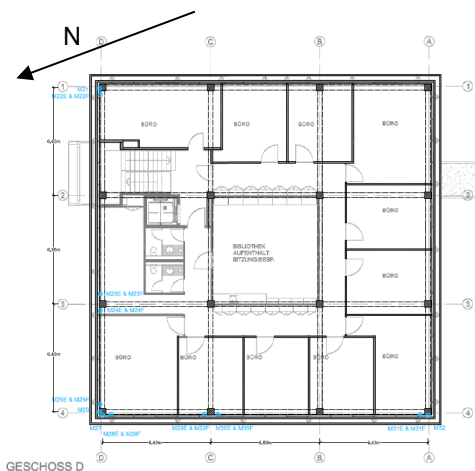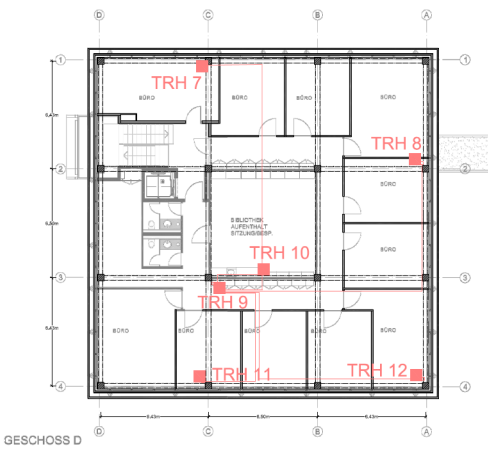
Figure 22: Measured moisture contents in the beech CLT floor and façade (Beech, Spruce and Ash) of the House of Natural Resources in Zürich

9 783906 878041 >